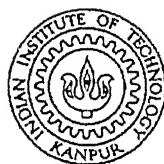


INVESTIGATION OF IS CODE PROVISIONS ON SEISMIC DESIGN OF REINFORCED CONCRETE STRUCTURAL WALLS

A Thesis Submitted
in Partial Fulfillment of the Requirements
for the Degree of

MASTER OF TECHNOLOGY

by
Kaustubh Dasgupta
Y010321



**Department of Civil Engineering
Indian Institute of Technology Kanpur**
August 2002

4 JUN 2003

सुखवासम
भारतीय प्र.
व्यापि क्र० A 14304



CERTIFICATE

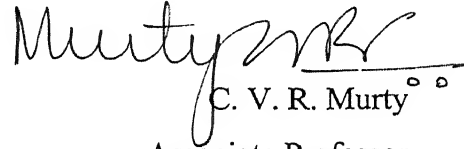
It is certified that the work contained in this thesis entitled "*Investigation of IS Code Provisions on Seismic Design of Reinforced Concrete Structural Walls*" by Mr. Kaustubh Dasgupta (Roll No. Y010321) has been carried out under our supervision and this work has not been submitted elsewhere for a degree.

Shailesh Kr. Agrawal

Scientist
Structural Engineering Division
Central Building Research Institute
Roorkee-247667



August 2002


C. V. R. Murty

Associate Professor
Department of Civil Engineering
Indian Institute of Technology
Kanpur-208016



Abstract

The compliance of wall sections, designed as per the current Indian Standard, with the capacity design philosophy is investigated. For this, the material characteristics during overstrength conditions are used for concrete and steel. The overstrength axial force-bending moment interaction curves are used to determine the flexural plastic hinge based overstrength shear demand that is compared with the design shear capacity. Structural walls of multistoreyed-framed buildings, designed as per the Indian Standard, are analysed to identify the possible modes of shear failure during flexural overstrength conditions. The top storeys of all the buildings and some storeys of the midrise buildings show vulnerability to shear failure. However no particular trend in the exceedance of shear demand over the design shear force is observed.

Acknowledgments

First of all, I am grateful to C.V.R.Murty for guiding me in my first venture in engineering research. Our technical and non-technical discussions kept the spirits high, thus making the stay at I.I.T. Kanpur enjoyable and motivating. Moreover his guidance has helped me to develop the various facets of my personality and own self. He reinforced my belief that anything is do-able and any goal is achievable through focus and sincere efforts.

I am indebted to Professor Sudhir K. Jain, for his invaluable advices and suggestions that not only helped in my thesis work but also in shaping my career. The resources and the materials in his office have helped a lot in this work. I thank all the faculty members of the institute who helped me learn the basics and guided me to face the various challenges of engineering problems. Special thanks to Dr. K.K. Bajpai for giving suggestions and advice.

I am grateful to Dr. Shailesh K. Agarwal for his sincere help and invaluable suggestions on my thesis. I thank all the CBRI people for their whole-hearted support.

Words are insufficient to describe my indebtedness to my parents whose encouragement and guidance have helped me strive forward throughout the Masters program. Special thanks to my father for enlightening me on some mathematical aspects of my thesis work.

Special thanks to Rupen, Goutam, Ms. T. Parvati and Ms. Priyam Verma for helping me write the Appendices of the thesis. I am grateful to Mr. Jitendra Bothara of University of Canterbury, Mr. Deepankar Choudhury of I.I.Sc. Bangalore and Mr. Qian Jiaru of Tsinghua University, Beijing for sending important journal papers.

The list of people whom I befriended is too long and the memorable experiences that I shared are too many. Still great injustice will be done if some of the names are not mentioned. My Structure-mates Sona, Rupen, Ajeet, *Sant-osh*, *Ani-rudh*, Chotu, Krishnamurthy, Murugan, Raghu, Major-saab and Colonel-saab, my Lab-mates Jas, Prabuddha, Hemant, Snehal, Ashu, Puneet, my hall-mates Balu, Mesho, Nano, Bhaipo, Shakila, Hulo, Bsuman, Malay-da, all made my stay enjoyable. Among my seniors Jayanta, Gupi, Roma, Rajrup, Ram-da, Bhuto are some of the names I'd like to add here. I thank Samit from the bottom of my heart, my batchmate in B.E. College, for guiding me throughout the M.Tech. program. Special thanks to Prabuddha, Diptesh-da and Jas for the help in technical matters.

I thank Motilal and Malkhan for all the cups of teas and other stationary they have supplied to me whenever I needed them.

I acknowledge gratefully the contribution of Kanpur city restaurants, e.g. *Semfex*, *Tandoori Nights*, *Baba*, *Anaicha*, *Host*, *Chung Fa*, *Mehfil*, *Kandhar* in my thesis for their stimulating cuisines.

Kaustubh

Table of Contents

	<i>Page</i>
Certificate	i
Abstract	ii
Acknowledgements	iii
Table of Contents	iv
List of Tables	vi
List of Figures	vii
List of Symbols	x
Chapter 1:: Literature Survey	
1.0 Introduction	1
1.1 Classification of Walls	1
1.2 Strength of RC Structural Walls	2
1.2.1 Flexural Strength	2
1.2.2 Shear Strength	2
1.3 Failure Modes of RC Structural Walls	3
1.4 Performance of RC Structural Walls	4
1.5 Experimental Studies	4
1.5.1 ATC 11 Studies	4
1.5.2 Slender Walls	5
1.5.3 Squat Walls	6
1.6 Analytical Studies	7
1.7 Current Code Provisions	9
1.7.1 Indian Concrete Code IS 456:2000	9
1.7.1.1 Limit State Design Philosophy	9
1.7.1.2 Flexural Design	10
1.7.1.3 Shear Design	10
1.7.2 Indian RC Ductile Detailing Code IS 13920:1993	12
1.7.2.1 General Requirements	12
1.7.2.2 Flexural Design	12
1.7.2.3 Shear Design	14
1.7.2.4 Design of Boundary Elements	15
1.7.3 ACI 318-1999	16
1.7.3.1 Flexural Design	17
1.7.3.2 Shear Design	17
1.7.3.3 Walls with Boundary Elements	17
1.7.3.4 Walls without Boundary Elements	18
1.7.4 New Zealand Concrete Structures Code NZS 3101 Part 1-1995	19
1.7.4.1 Shear Design	20
1.7.5 Japanese Standard AIJ	22
1.7.5.1 Structural Planning	22
1.7.5.2 Design Methods	22
1.7.5.2.1 Design Philosophies	22
1.7.5.2.2 Deformation Levels	23
1.7.5.2.3 Flexural Strength	23
1.7.5.2.4 Axial Load Limitation	24
1.7.4.2.5 Shear Design	24
1.7.4.2.6 Confinement	26

1.7.4.2.7 General Requirements	26
1.7.6 European Standard Eurocode 8	26
1.7.7 Swiss Standard SIA 160	27
1.7.8 Balkan Codes	28
1.7.8.1 Turkish National Code 1975	28
1.7.7.2 Bulletin d'Information No. 160	29
1.8 Miscellaneous Design Methods	30
1.8.1 Miscellaneous Design Methods	30
1.8.2 Displacement-Based Design	32
1.9 Capacity Design	36
1.10 Scope of Present Study	37
Figures	38
 Chapter 2:: Capacity Design of RC Structural Walls	
2.1 Introduction	50
2.2 Overstrength Plastic Moment Capacity	50
2.2.1 Expressions for P and M_{Ω} for Rectangular Wall Sections	51
2.2.1.1 Two Curtains of Vertical Reinforcement	52
2.2.1.2 One Curtain of Vertical Reinforcement	56
2.2.2 Step-wise Procedure for Obtaining $P - M_{\Omega}$ curves	57
2.3 Proposed Capacity Design Method	58
2.4 Numerical Study	60
2.4.1 Three Storeyed Building	61
2.4.2 Eleven Storeyed Building	62
2.4.3 Other Wall Buildings	63
2.5 Conclusions	63
Tables	65
Figures	68
 Chapter 3:: Summary and Conclusions	
3.1 Introduction	79
3.2 Summary	79
3.3 Conclusions	80
3.5 Proposed Changes in IS 13920:1993 Provisions	81
3.6 Scope of Future Work	82
 References	83
Appendix A	88
Appendix B	117

List of Tables

<i>Table</i>	<i>Title</i>	<i>Page</i>
1.1	Variation of dynamic shear magnification factor	20
1.2	Stiffness Reduction factors for walls	23
2.1	Geometric and Reinforcement details of building wall sections.	65
2.2	Shear Demands for building walls.	66
2.3	Demand Capacity Ratios for building walls.	67

List of Figures

<i>Figure Title</i>	<i>Page</i>
1.1 Possible modes of failure of slender walls, (a) flexural failure, (b) flexural-shear failure, (c) sliding failure, and (d) overturning failure [Paulay <i>et. al.</i> , 1982].	38
1.2 Possible nodes of failure of squat walls, (a) levels of diagonal tension failure depending on amount of reinforcement, (b) diagonal compression failure, and (c) sliding shear failure [Wakabayashi, 1986].	38
1.3 (a) Sliding at construction joint, spalled concrete and buckled edge reinforcement at Canal Beagle [Chile, 1985], Crushing of concrete and buckling of reinforcement in sixteen-storey building [Armenia, 1988], and (c) Diagonal cracking in walls	39
1.4 Slender RC wall subjected to quasi-static reversed cyclic loading, (a) Load-deformation curve, and (b) Cracking sustained in the lower portion of the wall [ATC 11, 1983].	40
1.5 Slender RC wall subjected to quasi-static reversed cyclic loading, (a) Load-deformation curve, (b) Cracking sustained in the bottom part of wall [ATC 11, 1983].	41
1.6 Moment curvature diagram of wall with concentrated steel at the ends [Cardenas and Magura, 1973].	42
1.7 Flexure-dominated failure modes, (a) Buckling of vertical steel, (b) Fracture of vertical steel, and (c) Crushing of concrete [ATC 11, 1983].	43
1.8 Shear-dominated failure modes, (a) Web Crushing, and (b) Sliding shear [ATC 11, 1983].	44
1.9 Wall specimens with bidiagonal reinforcement [Salonikios, 1999].	44
1.10 (a) Moment curvature diagram for walls, (b) Variation of ductility with load ratio, and (c) Variation of ductility with flange area ratio [Allen <i>et. al.</i> , 1973].	45
1.11 Code-specified stress-strain properties for obtaining the design flexural strength of RC wall section, (a) concrete, and (b) steel as per IS 456:2000 [IS 456, 2000].	46
1.12 Concrete contribution factor for slender and squat walls [ACI 318, 1999].	46
1.13 Bending moment envelope for design [NZS 3101, 1995].	47
1.14 (a) Schematic Relation between moment and curvature, and (b) Flexural strengths and Deformations of a wall section with distributed steel [AIJ, 1994].	47
1.15 Strain and Stress distributions in concrete and steel [ATC 11, 1983].	48
1.16 Curvature and deformation diagrams for wall [Wallace, 1994].	48
1.17 Strain and Stress distributions in the proposed design method [Wallace, 1994].	49
1.18 Steps in Displacement-Based Design method of walls [Kowalsky, 2001].	49
2.1 Stress-strain curves for $P - M_{\Omega}$ diagrams: (a) for unconfined concrete (<i>A</i>) and confined concrete (<i>B</i>), and (c) for HYSD bars.	68
2.2 General states of a RC cross section and strain distributions under combined <i>axial load</i> and <i>bending moment</i> during overstrength condition.	68
2.3 General sectional view of wall without boundary elements	69

2.4	Progressive movement of NA into the section and associated strain and stress variations in concrete as per capacity design philosophy: (a) to (d) for confined concrete, and (e) to (j) for unconfined concrete.	70
2.5	Unconfined and confined concrete areas in RC wall sections with (a) two curtains of vertical reinforcement in the web, and (b) one curtain of vertical reinforcement in the web.	71
2.6	Frame-wall building for numerical study: (a) elevation for the three-storeyed building, and (b) typical plan showing frame members.	72
2.7	Isolated wall section: (a) elevation and sectional plan, and (b) reinforcement details [Medhekar and Jain, 1993].	73
2.8	Idealized curves and parameters of hinges for pushover analysis, (a) P-M hinge, (b) M- θ hinge, and (c) V- Δ curve.	74
2.9	Design and Overstrength moment capacities of the third storey in the 3-storey building (Section 3W3 in <i>Building C</i>), by the Indian code and the proposed methods respectively.	75
2.10	P – M_{Ω} and $P_u - M_u$ [IS 456, 2000] curves for wall sections in (a) <i>Building C</i> , (b) <i>Building E</i> , (c) <i>Building F</i> , and (d) <i>Building H</i> .	76
2.11	Deviation of overstrength moment capacity from the code-specified [IS 456, 2000] flexural capacity for wall sections in (a) <i>Building C</i> , (b) <i>Building E</i> , (c) <i>Building F</i> , and (d) <i>Building H</i> .	77
2.12	Dimensional and stress-strain notations for wall section with boundary elements	78

List of Symbols

<i>Symbol</i>	<i>Description</i>
A	Ratio of moments due to axial load couple and overturning due to lateral loads [NZS 3101, 1995]
A_c	Cross sectional area of compressive side boundary column [AIJ, 1994]
A_{ce}	Effective area of boundary columns [AIJ, 1994]
A_{core}	Core area of boundary column on compression side [AIJ, 1994]
A_{cv}	Total concrete area in the direction of shear force (in in^2) [ACI 318, 1999]
A_f	1. Total area of flanges 2. Floor plan area of a building [Wallace, 1994]
A_g	Gross cross sectional area of wall (in mm^2) [IS 456, 2000]
A_h	Total area of horizontal shear reinforcement [IS 13920, 1993]
A_s	1. Total area of uniformly distributed vertical steel [Park and Paulay, 1975] 2. Area of tension steel [Wallace, 1994] 3. Area of longitudinal tension reinforcement [IS 456, 2000]
A_{sb}	Total area of steel in boundary element
A_{si}	Area of i -th layer of steel bar in RC section.
A_{st}	Area of vertical steel [IS 13920, 1993]
A_{sv}	Total cross sectional area of shear reinforcement [IS 456, 2000]
A'_s	Area of compression steel [Wallace, 1994]
A''_s	Area of distribution steel [Wallace, 1994]
A_w	Cross sectional area of the wall [Wallace, 1994]
A_{ws}	Area of vertical steel in wall panel [AIJ, 1994]
C	Distance between adjacent longitudinal bars (in mm).
C_d	Overstrength reduction factor
C_w	Horizontal centre to centre distance between boundary elements [IS 13920, 1993]
D	Total depth of section
D_c	Width of boundary column [AIJ, 1994]
E_c	Young's modulus of concrete [Wallace, 1994]
E_s	Young's modulus of steel
F_s	Factor of safety for moments [Allen <i>et. al.</i> , 1973]
M	Moment on the wall section
M_{bbc}	Contribution of bottom boundary element in the moment capacity of wall section with boundary elements.
M_{bc}	Contribution of boundary elements in the moment capacity of wall section with boundary elements.
M_c	Moment in concrete for the axial load capacity in RC section.

Symbol	Description
M_{cal}	Calculated bending moment capacity of a section for a given curvature
M_{code}	Moment resulting from code loading [NZS 3101, 1995, and Paulay and Williams, 1980]
M_{cr}	1. Cracking moment i.e. the moment at which the extreme tension fibre of concrete attains a stress of $7.5\sqrt{f'_c}$ (psi) [Allen <i>et. al.</i> , 1973] 2. Moment contribution of confined concrete in rectangular wall $P - M_{\Omega}$
M_{crt}	Moment contribution of confined concrete
M_{cvt}	Moment contribution of unconfined concrete
M_d	Design moment obtained from analysis
M_D	Design moment in RC sections
M_f	1. Failure moment of a wall section 2. Design moment from analysis [Allen <i>et. al.</i> , 1973]
M_E	Bending moment by static analysis from codal distribution of forces
M_i	Overstrength moment demand
M_l	Maximum moment [Allen <i>et. al.</i> , 1973]
M_n	Nominal flexural strength of wall [ATC 11, 1983]
M_o	Overturning moment at the base of the wall [NZS 3101, 1995] Overstrength moment capacity [NZS 3101, 1995]
M^o	Overstrength moment capacity [Paulay and Williams, 1980].
M_{tbc}	Contribution of top boundary element in the moment capacity of wall section with boundary elements.
M_u	Flexural moment capacity of a RC section for a given axial load
$(M_{\Omega})_{AB}$	Overstrength flexural capacity of a RC section at any point on segment AB of $P - M_{\Omega}$ interaction curve
$(M_{\Omega})_{BCD}$	Overstrength flexural capacity of a RC section at any point on segment BCD of $P - M_{\Omega}$ interaction curve
$(M_{\Omega})_{DE}$	Overstrength flexural capacity of a RC section at any point on segment DE of $P - M_{\Omega}$ interaction curve
M_{ud}	Ultimate design moment [Wallace, 1994]
$M_{u,d}$	Flexural strength of section under actual axial load
M_{uv}	Moment of resistance provided by distributed vertical reinforcement in the web [IS 13920, 1993]
M_u	Factored bending moment in wall section [ACI 318, 1999]
M_{uc}	Flexural capacity of slender wall section [Park and Paulay, 1975]
M_{wc}	Contribution of web in the moment capacity of wall section with boundary elements
M'_{bbc}	Partial contribution of bottom boundary element in the moment capacity of wall section with boundary elements
M_{Ω}	Overstrength moment capacity of RC section
N	Number of storeys of shear wall building [NZS 3101, 1995]

<i>Symbol</i>	<i>Description</i>
N_{cc}	Axial load on compressive side boundary column [AIJ, 1994]
N_u	Axial compressive load [Park and Paulay, 1975, and ATC 11, 1983]
N_w	Axial load on wall in yield mechanism assurance design [AIJ, 1994]
P	Applied axial load
P_b	Axial load for the balanced section
P_{bal}	1. Axial load for the balanced section [Cardenas and Magura, 1973] 2. Balanced axial load [ATC 11, 1983]
P_{bbc}	Design axial compression capacity of bottom boundary element
P_c	Force in concrete for the axial load capacity in RC section.
P_{cal}	Calculated axial strength of a section for a given curvature
P_{cr}	Axial compression contribution of confined concrete for rectangular walls
P_{crt}	Axial compression contribution of confined concrete for walls with boundary elements
P_{cv}^w	Axial compression contribution of unconfined concrete in wall
P_{cv}^{pw}	Axial compression contribution of parabolic stress block of unconfined concrete in wall
P_{cv}^{tw}	Axial compression contribution of trapezoidal stress block of unconfined concrete in wall
P_{cv}^1	Axial compression contribution of unconfined concrete in zone 1
P_{cv}^{1p}	Axial compression contribution of parabolic stress block of unconfined concrete in zone 1
P_{cv}^{1t}	Axial compression contribution of trapezoidal stress block of unconfined concrete in zone 1
P_{cv}^2	Axial compression contribution of unconfined concrete in zone 2
P_{cvt}	Axial compression contribution of unconfined concrete.
P_e	1. Compressive force induced by seismic action 2. Design axial load [NZS 3101, 1995]
P_g	Factored axial force in wall section due to gravity
P_{tbc}	Design axial compression capacity of top boundary element
P_u	Design axial load capacity of a RC section (in N) [IS 456, 2000]
P_{wc}	Design axial load capacity of web portion of wall
P'_{bbc}	Partial design axial compression capacity of bottom boundary element.
$(P)_{AB}$	Axial load capacity of a RC section at any point on segment AB of $P - M_{\Omega}$ interaction curve
$(P)_{BCD}$	Axial load capacity of a RC section at any point on segment BCD of $P - M_{\Omega}$ interaction curve.
$(P)_{DE}$	Axial load capacity of a RC section at any point on segment DE of $P - M_{\Omega}$ interaction curve.
R_d	Design limit deformation [AIJ, 1994]

Symbol	Description
R_w	UBC factor [Wallace, 1994]
S	Structural type factor [NZS 3101, 1995]
S_d	Spectral displacement [Wallace, 1994].
T	1. Axial load at the base of the coupled shear wall due to design earthquake loading [NZS 3101, 1995] 2. Natural time period of wall [Wallace, 1994].
V	Shear force on the section
$(V_c)_{max}$	Maximum shear capacity of concrete.
V_{cap}	Design shear capacity of RC section.
V_{cd}	Resistance of concrete against diagonal tension [EC 8, 1994]
V_{code}	Shear force resulting from design lateral loading [NZS 3101, 1995, and Paulay and Williams, 1980]
V_D	Design shear force in RC section
V_E	Shear force by static analysis from codal distribution of forces
V_{max}	Maximum shear capacity of RC section.
V_{min}	Shear strength of nonductile region [Paulay and Williams, 1980]
V_n	Nominal shear strength of wall section [ACI 318, 1999]
$(V_s)_{max}$	Maximum shear capacity of reinforcement.
V_u	1. Design shear capacity of RC section [IS 456, 2000] 2. Factored shear force in wall section [ACI 318, 1999] 3. Reliable shear strength of wall section [AIJ, 1994] 4. Design shear force [Allen <i>et. al.</i> , 1973]
V_{uc}	Design shear capacity of concrete [IS 456, 2000]
V_{ud}	Ultimate design shear [Allen <i>et. al.</i> , 1973]
V_{us}	Design shear capacity of steel [IS 456, 2000]
V_{uw}	Design shear capacity of wall section
V_w	Overstrength shear demand
V_{wall}	Shear force in wall during actual earthquake [NZS 3101, 1995]
V_{wd}	Shear resistance of web reinforcement [EC8, 1994]
V_{Ω}	Shear demand in RC section during flexural overstrength.
V_{Ω}^c	Shear demand from code approach.
V_p^c	Inelastic shear demand from pushover analysis.
Z	1. Factor depending on the aspect ratio of wall [NZS 3101, 1995] 2. Factor for calculating cracking moment [Allen <i>et. al.</i> , 1973]
a	1. Thickness of boundary element [Wallace, 1994] 2. Length of boundary element
a_o	Length of core concrete in boundary element (Figure 2.12)
b	1. Breadth of rectangular RC section [IS 456, 2000] 2. Length of boundary element [Wallace, 1994] 3. Length of web (Figure 2.12)

Symbol	Description
b_w	Thickness of web [EC8, 1994]
b_o	Length of core concrete in web (Figure)
c	1. Depth of compression zone [Park and Paulay, 1975, ACI 318, 1999, and Wallace, 1994] 2. Length of boundary element (Figure)
c_o	Length of core concrete in boundary element (Figure)
cov	Cover in the wall section (Figure)
d	Effective depth of a section.
d_b	Diameter of reinforcement (Mau, 1990)
d_s	Distance from centroid of total vertical reinforcement to extreme compression fibre of wall section [NZS 3101, 1995]
d_w	Effective depth for shear stress in wall section [IS 13920, 1993]
f'_c	Characteristic cylinder strength of concrete (in <i>psi</i>)
f_c	Average stress in concrete stress block.
f_{cc}	Ultimate stress of confined concrete [Razvi and Saatcioglu, 1999a]
f_{ck}	Characteristic compressive strength of concrete [IS 456, 2000]
f_{co}	Ultimate stress of unconfined concrete ($= 0.68 f_{ck}$)
f_{cr}^P	Axial compression from curved stress block of confined concrete
f_{cr}^{PP}	Axial compression from curved stress block of confined concrete
f_{cr}^t	Axial compression from trapezoidal stress block of confined concrete
f_{f1}	Axial compression from <i>zone 1con</i>
f_{f2}	Axial compression from <i>zone 2con</i>
f_{fp1}	Axial compression from parabolic stress block of <i>zone 1con</i>
f_{fp2}	Axial compression from parabolic stress block of <i>zone 2con</i>
f_{ft1}	Axial compression from trapezoidal stress block of <i>zone 1con</i>
f_{ft2}	Axial compression from trapezoidal stress block of <i>zone 2con</i>
f_{mw}	Moment from unconfined concrete in wall
f_{mwc}	Moment from confined concrete in wall
f_s	Stress in reinforcement [Wallace, 1994]
f_{su}	Ultimate stress of steel
f'_s	Stress in compression steel [Wallace, 1994]
f_w	Axial compression from unconfined concrete in wall
f_{wc}	Axial compression from confined concrete in wall
f_{wp}	Axial compression from parabolic stress block in wall
f_{wpc}	Axial compression from curved stress block of confined concrete
f_{wt}	Axial compression from trapezoidal stress block of unconfined concrete in wall

Symbol	Description
f_{wtc}	Axial compression from trapezoidal stress block of confined concrete in wall
f_y	Characteristic yield strength of steel [Park and Paulay, 1975]
f_{yd}	Design strength of reinforcement [EC8, 1994]
f_{yh}	Yield stress of horizontal shear reinforcement [NZS 3101, 1995]
f_{yn}	Yield stress of vertical shear reinforcement [NZS 3101, 1995]
f_{yt}	0.2% proof stress of transverse reinforcement
f_1	Axial compression contribution of <i>zone 1</i> .
f_{1a}	Stress in unconfined concrete (Figure C.1)
f_{1c}	Stress in confined concrete (Figure C.1)
f_2	Axial compression contribution of <i>zone 2</i> .
f_{2a}	Stress in unconfined concrete (Figure C.1)
f_{2c}	Stress in confined concrete (Figure C.1)
f_3	Axial compression contribution of <i>zone 3</i> .
f_{3a}	Stress in unconfined concrete (Figure C.1)
f_{3c}	Stress in confined concrete (Figure C.1)
f_4	Axial compression contribution of <i>zone 4</i> .
f_{4a}	Stress in unconfined concrete (Figure C.1)
f_{4c}	Stress in confined concrete (Figure C.1)
f_{5a}	Stress in unconfined concrete (Figure C.1)
f_{6a}	Stress in unconfined concrete (Figure C.1)
f_{6c}	Stress in confined concrete (Figure C.1)
f_{7a}	Stress in unconfined concrete (Figure C.1)
f_{7c}	Stress in confined concrete (Figure C.1)
f_{8a}	Stress in unconfined concrete (Figure C.1)
f_{1p}	Axial compression contribution of parabolic stress block of <i>zone 1</i> .
f_{1t}	Axial compression contribution of trapezoidal stress block of <i>zone 1</i> .
f_{2p}	Axial compression contribution of parabolic stress block of <i>zone 2</i> .
f_{2t}	Axial compression contribution of trapezoidal stress block of <i>zone 2</i> .
f_{3p}	Axial compression contribution of parabolic stress block of <i>zone 3</i> .
f_{3t}	Axial compression contribution of trapezoidal stress block of <i>zone 3</i> .
f_{4p}	Axial compression contribution of parabolic stress block of <i>zone 4</i> .
f_{4t}	Axial compression contribution of trapezoidal stress block of <i>zone 4</i> .
h_{cr}^p	Lever arm of axial compression from curved stress block of confined concrete
h_{cr}^t	Lever arm of axial compression from trapezoidal stress block of

Symbol	Description
	confined concrete
h_{cv}^w	Lever arm of force of unconfined concrete in wall.
h_{cv}^{pw}	Lever arm of axial compression of parabolic stress block of unconfined concrete in wall
h_{cv}^{tw}	Lever arm of axial compression of trapezoidal stress block of unconfined concrete in wall
h_{cv}^1	Lever arm of force of unconfined concrete in <i>zone 1 con.</i>
h_{cv}^{p1}	Lever arm of axial compression of parabolic stress block of unconfined concrete in zone 1
h_{cv}^{t1}	Lever arm of axial compression of trapezoidal stress block of unconfined concrete in zone 1
h_{cv}^2	Lever arm of force of unconfined concrete in <i>zone 2</i>
h_{f1}	Lever arm of force in <i>zone 1 con.</i>
h_{f2}	Lever arm of force in <i>zone 2 con.</i>
h_{fp1}	Lever arm of force of parabolic stress block in <i>zone 1 con.</i>
h_{fp2}	Lever arm of force of parabolic stress block in <i>zone 2 con.</i>
h_{ft1}	Lever arm of force of trapezoidal stress block in <i>zone 1 con.</i>
h_{ft2}	Lever arm of force of trapezoidal stress block in <i>zone 2 con.</i>
h_s	Height of wall [Wallace, 1994]
h_w	1. Height of wall panel. 2. Lever arm of force in unconfined concrete of wall.
h_{wc}	Lever arm of force in confined concrete of wall.
h_{wp}	Lever arm of force of parabolic stress block in unconfined concrete of wall.
h_{wpc}	Lever arm of force of parabolic stress block in in confined concrete of wall.
h_{wt}	Lever arm of force of trapezoidal stress block in unconfined concrete of wall.
h_{wtc}	Lever arm of force of trapezoidal stress block in confined concrete of wall.
h_1	Lever arm of force in <i>zone 1</i> .
h_2	Lever arm of force in <i>zone 2</i> .
h_3	Lever arm of force in <i>zone 3</i> .
h_4	Lever arm of force in <i>zone 4</i> .
h_{1p}	Lever arm of force of parabolic stress block in <i>zone 1</i> .
h_{1t}	Lever arm of force of trapezoidal stress block in <i>zone 1</i> .
h_{2p}	Lever arm of force of parabolic stress block in <i>zone 2</i> .
h_{2t}	Lever arm of force of trapezoidal stress block in <i>zone 2</i> .
h_{3p}	Lever arm of force of parabolic stress block in <i>zone 3</i> .
h_{3t}	Lever arm of force of trapezoidal stress block in <i>zone 3</i> .

Symbol	Description
h_{4p}	Lever arm of force of parabolic stress block in zone 4.
h_{4t}	Lever arm of force of trapezoidal stress block in zone 4.
k_3	Confinement coefficient [AIJ, 1994]
l	1. Distance between vertical reference axes of coupled shear walls [NZS 3101, 1995] 2. Length of rectangular wall section without boundary elements
l_e	Effective length of transverse reinforcement.
l_p	Plastic hinge length [Wallace, 1994]
l_w	1. Length of rectangular wall section [Park and Paulay, 1975] 2. Horizontal length of wall [IS 13920, 1993]
l_{wa}	Equivalent width of wall panel in arch mechanism [AIJ, 1994]
l_{wb}	Equivalent width of wall panel in truss mechanism [AIJ, 1994]
l'_w	Clear span of wall panel [AIJ, 1994]
n	1. Number of storeys of wall [Wallace, 1994] 2. Number of layers of bars in wall section with boundary elements.
nw	Number of layers of bars in web portion.
P	Ratio of wall area to floor plan area for the walls aligned in the direction in which the time period is calculated [Wallace, 1994]
p_l	Lever arm notation for curved stress block in confined concrete stress-strain curve.
p_t	Percentage of longitudinal tension reinforcement [IS 456, 2000]
p_s	Shear reinforcement ratio in wall panel [AIJ, 1994]
r	Width of boundary element (Figure).
r_o	Width of core concrete in boundary element (Figure).
s	Width of boundary element (Figure)
s_o	Width of core concrete in boundary element (Figure).
s_v	Spacing of stirrups in a rectangular section [IS 456, 2000]
s_{vw}	Spacing of horizontal steel in walls
t	Thickness of rectangular wall section without boundary elements.
t_w	Thickness of web [IS 13920, 1993].
t_o	Thickness of core concrete in wall section (Figure).
w	Unit floor weight including tributary wall height [Wallace, 1994]
x	Distance of neutral axis from the geometric centroidal axis of a RC section.
x_b	Distance of neutral axis from the geometric centroidal axis of a balanced RC section.
x_p	Lever arm distance of parabolic stress block of unconfined concrete from its origin.
x_u	Depth of neutral axis [IS 13920, 1993]
x_u^*	Balanced depth of neutral axis [IS 13920, 1993]
y	Distance of 0.002 compressive strain line from neutral axis.
y_a	Distance of 0.002 compressive strain line from neutral axis

<i>Symbol</i>	<i>Description</i>
y_c	Distance of ε_{lc} strain line from neutral axis in the strain diagram for confined concrete
y_d	Distance of 0.0035 compressive strain line from neutral axis.
y_{si}	Distance of i -th layer of reinforcement from the edge of compression face of the section.
z	Effective internal lever arm [EC8, 1994]
$\Phi_{o,w}$	Flexural overstrength factor for wall
α_c	Coefficient defining the relative contribution of concrete strength to wall strength [ACI 318, 1999]
α_2	Factor for flexural capacity of wall sections [IS 13920, 1993]
α_3	Factor for flexural capacity of wall sections [IS 13920, 1993]
β	1. Factor for shear strength of RC sections [SP:24-1983] 2. Factor for flexural capacity of walls [IS 13920, 1993] 3. Coefficient giving the ratio of capacity of shear reinforcement and shear capacity of concrete [AIJ, 1994]
β_1	Factor for maximum compressive strain in concrete [Wallace, 1994]
δ	Factor for effect of compression on shear strength [IS 456, 2000]
δ_c	Displacement capacity at the top of wall [Wallace, 1994]
δ_u	(i) Design displacement (in <i>in</i>) [ACI 318, 1999] (ii) Roof displacement [Wallace, 1994]
δ_y	Displacement from elastic deformation [Wallace, 1994]
$\varepsilon_{c \max}$	Maximum compressive strain of concrete [Wallace, 1994]
ε_{cu}	Ultimate longitudinal compressive strain of unconfined concrete
ε_s	Strain in steel.
ε_{si}	Strain in i -th layer of reinforcement from the edge of compression face of the section.
$(\varepsilon_c)_m$	Concrete strain value [Priestley and Kowalsky, 1998]
$(\varepsilon_c)_{\max}$	Maximum compressive strain in concrete in Limit State Flexural Design [IS 456, 2000]
$(\varepsilon_c)_{\min}$	Minimum compressive strain in concrete in Limit State Flexural Design [IS 456, 2000]
$(\varepsilon_{cc})_{\max}$	Maximum compressive strain in confined concrete (Figure 2.1a)
$(\varepsilon_s)_m$	Steel strain value [Priestley and Kowalsky, 1998]
$(\varepsilon_s)_{\max}$	Maximum tensile (rupture) strain in HYSD bars (Figure 2.1b)
ε_{01}	Strain value = 0.002.
ε_{02}	Strain value = 0.0035.
ε_l	Strain at extreme edge on tension face.
ε_{lc}	Strain corresponding to stress f_{cc} in confined concrete with negative sign.
$\varepsilon_2, \varepsilon_3, \varepsilon_4,$ $\varepsilon_5, \varepsilon_6, \varepsilon_7$	Strain values (Figure 3.3)

<i>Symbol</i>	<i>Description</i>
ε_8	Strain at the edge of the compression face
γ_m	Partial Safety Factor for material in Limit State Design [IS 456, 2000]
γ_n	Shear force amplification factor
γ_r	Resistance factor
γ_o	Overstrength factor for reinforcing steel
λ	Nondimensional factor for flexural capacity of walls [IS 13920, 1993]
ϕ_u	Ultimate curvature at a section
ϕ_y	Yield curvature at a section
μ_Δ	Displacement ductility factor
μ_δ	Ductility factor [Wallace, 1994]
θ_p	Plastic rotation [Wallace, 1994]
ϕ	1. Angle of compression strut in truss mechanism [AIJ, 1994] 2. Strength Reduction factor [ATC 11, 1983] 3. Factor for calculation of flexural capacity of walls [IS 13920, 1993]
ϕ_{\max}	Curvature capacity of a RC section under axial load.
$(\phi_{\max})_{AB}$	Curvature capacity of a RC section at any point on segment AB of $P - M_\Omega$ interaction curve.
$(\phi_{\max})_{BCD}$	Curvature capacity of a RC section at any point on segment BCD of $P - M_\Omega$ interaction curve.
$(\phi_{\max})_{DE}$	Curvature capacity of a RC section at any point on segment DE of $P - M_\Omega$ interaction curve.
ϕ_o	Flexural overstrength factor [NZS 3101, 1995, and Paulay and Williams, 1980]
ϕ_u	Ultimate curvature [Wallace, 1994]
ϕ_y	Curvature at first yield [Priestley and Kowalsky, 1998, and Wallace, 1994]
ν	Effectiveness factor for compressive strength of concrete [AIJ, 1994]
ν_c	Shear strength of concrete [NZS 3101, 1995]
ν_i	Shear stress along any horizontal plane [NZS 3101, 1995]
σ_E	Compressive strength of concrete [AIJ, 1994]
σ_{si}	Stress in the i -th layer of reinforcement from the edge of compression face of the section.
σ_{sy}	Strength of shear reinforcement in wall panel [AIJ, 1994].
σ_{wyu}	Material strength of vertical steel in wall panel for upper bound flexural strength [AIJ, 1994].
ρ	1. Ratio of vertical reinforcement [IS 13920, 1993] 2. Tension steel ratio [Wallace, 1994]

<i>Symbol</i>	<i>Description</i>
ρ'	Compression steel ratio [Wallace, 1994]
ρ''	Distribution steel ratio [Wallace, 1994]
ρ_h	Ratio of horizontal steel area to the gross sectional area [NZS 3101, 1995, and EC8, 1994]
ρ_n	Ratio of area of distributed steel parallel to the plane of A_{cv} to gross concrete area perpendicular to that reinforcement [ACI 318, 1999 and NZS 3101, 1995]
ρ_v	Vertical steel ratio in wall section [ACI 318, 1999, and EC8, 1994)
ρ_l	Ratio of tension reinforcement [EC8, 1994]
$\tau_{c,max}$	Maximum allowable shear stress (in MPa) [IS 456, 2000]
τ_v	Nominal shear stress in a RC rectangular section [IS 456, 2000]
τ_{vw}	Nominal shear stress in RC wall
ω	Amplification factor (SIA 160)
ω_v	Dynamic shear magnification factor [NZS 3101, 1995, and SIA 160)
Δl_{wa}	Incremental wall width in arch mechanism [AIJ, 1994]
Δl_{wb}	Incremental wall width in truss mechanism [AIJ, 1994]

Chapter 1

Literature Review

1.0 INTRODUCTION

Reinforced concrete structural walls are important components of lateral load resisting systems in multistoreyed buildings. Due to their high lateral stiffness, the walls restrict the deformation response of buildings under lateral loads, thereby reducing the nonstructural damage of the building at the same time. Wall sections, which are designed and detailed for seismic forces, can achieve sufficient ductility and ensure good hysteretic response of the building system during earthquakes.

1.1 CLASSIFICATION OF RC STRUCTURAL WALLS

Based on their geometry, structural walls are grouped into two types [Penelis and Kappos, 1997], namely (a) Slender walls, whose aspect ratio h_w / l_w is more than 2.0, and (b) Squat walls, whose aspect ratio h_w / l_w is less than 0.5 where h_w is the height of the wall and l_w is the total length of the wall. Structural walls are also classified based on their behaviour [Allen *et. al.*, 1973] into three types, namely: (a) *Shear* shear wall whose shear deformation exceeds or equals 10% of the total deformation under lateral forces, (b) *Moment* shear wall, whose shear deformation is less than 10% of the total deformation, and (c) *Ductile-Moment* shear wall, which is also a *Moment* shear wall but having ductility capacity factor of more than 3.0. In general, since structural walls are relatively very stiff compared to the frame columns and draw most of the shear forces, they are often simply called “shear walls” irrespective of the above behavioural classification.

1.2 STRENGTH OF RC STRUCTURAL WALLS

1.2.1 Flexural Strength

Flexural strength (*i.e.*, bending moment capacity) of a wall depends on the axial force level and the section properties, namely dimensions, material properties, and amount of vertical and horizontal reinforcements. At each floor level of a multistoreyed building, the axial force P -bending moment M interaction curve gives the flexural capacity of the wall section based on the axial force coming on the wall at that level.

In slender walls with flanges or with boundary elements, an increase in longitudinal (vertical) steel in the flange of boundary region enhances the bending moment and curvature ductility capacities of the sections. But increasing the vertical steel in the boundary region can result in high shear demand on the wall when the overstrength flexural capacity is mobilized. The flexural capacity M_{uc} of a rectangular slender wall section of length l_w with uniformly distributed vertical steel of area A_s can be written as [Park and Paulay, 1975]

$$M_{uc} = 0.5A_s f_y l_w \left(I + \frac{N_u}{A_s f_y} \right) \left(I - \frac{c}{l_w} \right), \quad (1.1)$$

where N_u is the axial compressive force on the wall, c is the depth of neutral axis from the edge of maximum compression and f_y is the characteristic yield strength of steel. Here the confining effect of concrete by transverse reinforcement is not accounted for in the estimation of M_{uc} .

The flexural demand on a squat wall is less than that on a slender wall of the same section properties. This is because the lateral forces are resisted by a dominant diagonal strut action.

1.2.2 Shear Strength

The shear strength of slender walls can be determined using the same approach as

that employed in beams [Park and Paulay, 1975]. The enhancement of shear resistance offered by concrete due to presence of axial compression can be considered when the axial compressive stress exceeds $0.2f'_c$. A minimum recommended effective depth for calculation of shear capacity of slender wall sections is $0.8l_w$. In the seismic design of a multistoreyed building wall, the code-specified minimum horizontal steel may suffice in the upper storeys where the shear demand is less. But, in the lower storeys with high shear demand, design of horizontal reinforcement larger than the code-specified value may be required.

For squat walls, the shear strength can be obtained using deep beam theory [Park and Paulay, 1975]. Diagonal compressive struts and tension ties are formed in the wall at approximately 45 degrees orientation to the horizontal. Equal horizontal and vertical reinforcement is recommended for squat walls against diagonal tension. Unlike in slender walls, the contribution of vertical reinforcement to shear strength is critical in squat walls.

1.3 FAILURE MODES OF RC STRUCTURAL WALLS

In general slender and squat structural walls have different modes of failure. Slender walls have four basic failure modes, namely (a) ductile flexural failure with yielding of vertical steel (Figure 1.1a), (b) flexural shear failure with flexural cracks extending as diagonal shear cracks (Figure 1.1b), (c) horizontal sliding failure between the wall and its foundation or at construction joints (Figure 1.1c), and (d) overturning failure due to partial uplift at the foundation of the wall (Figure 1.1d). At high ductility levels, the sliding shear deformation tends to increase along the extensive flexural cracks [Salonikios, 2002].

Squat walls have three prominent failure modes namely, (a) diagonal tension failure (Figure 1.2a) with tensile cracks normal to the tension diagonal, (b) diagonal

compression failure with crushing of concrete along the compression diagonal, when adequate reinforcement is provided to take care of the diagonal tension (Figure 1.2b), and (c) horizontal sliding shear failure due to crushing of concrete at both the bottom edges and along the length of the wall under reversed loading action. When the axial stresses are small and shear stresses are high (Figure 1.2c), sliding failure may occur along a horizontal plane along the wall length. Squat walls can also fail in ductile flexural mode when the wall section is designed for the maximum shear demand generated under flexural overstrength conditions [Park and Paulay, 1975].

1.4 PERFORMANCE OF RC STRUCTURAL WALLS

The most common failure modes of RC structural walls observed in past earthquakes are: (a) Sliding failure at construction joint (Figure 1.3a) [Chile, 1995], (b) Buckling of vertical steel in the boundary region (Figure 1.3b) [Chile, 1995; San Salvador, 1986, and Armenia, 1988], and (c) Diagonal shear cracking with spalling of concrete (Figures 1.3c). The structural walls proved to be effective in collapse prevention of RC frame buildings. Thus the code provisions need to be reviewed for proper design and detailing of the walls.

1.5 EXPERIMENTAL STUDIES

1.5.1 ATC 11 Studies

The experiments carried out on RC structural walls [ATC 11, 1983] consisted of three types of tests, namely (a) Static monotonic load tests, (b) Quasi-static reversed cyclic load tests, and (c) Dynamic shake-table tests using past earthquake records as input ground motions. Walls of different aspect ratios were studied under reversed cyclic loading. In slender walls designed to fail in flexure, the shear stresses generated at ultimate stage were small.

The lateral load-deformation curve of the wall under a maximum shear stress of $3.1\sqrt{f'_c}$ is shown in Figure 1.4a. Although the ductility capacities of the walls were high, the strength deterioration and stiffness degradation were higher in the larger displacement excursion cycles. In the initial stages, the damage was in the form of horizontal cracks at the lower portion of the wall (Figure 1.4b). After the formation of flexural hinge (*i.e.*, yielding of vertical reinforcement), shear was transferred through friction at interface cracks and dowel action of bars. Some horizontal flexural cracks bent downwards and resulted in flexural-shear cracking in the central web of the wall section.

In another wall under a higher ultimate shear stress of about $8.8\sqrt{f'_c}$, the damage was of different type. The load-deformation curve is shown in Figure 1.5a. There is significant strain hardening of the member, with relatively less strength deterioration. While horizontal cracking was initiated by flexure, at higher levels of cyclic lateral displacement the shear was resisted predominantly by truss mechanism, resulting in symmetric inclined cracks throughout the height of the wall (Figures 1.5a and 1.5b).

Slender and squat walls sustained different failure modes. The damage type in the former depended on the relative flexural and shear strengths of the section; shear damage increased with increase in the flexural strength. Shear sliding and web crushing were also observed in squat walls.

1.5.2 Slender Walls

The experiments conducted on slender walls [Cardenas and Magura, 1973; ATC 11, 1983; Lefas *et. al.*, 1990; Tasnimi, 2000, and Oh *et. al.*, 2002] showed the following salient behavioural features:

1. Wall sections having concentrated vertical steel in the boundary region show higher ductility capacity and ultimate curvature (Figure 1.6) than the wall having distributed steel. Higher percentage of steel increases the moment capacity but does not affect the

yield curvature (Figure 1.6).

2. The drift capacity and displacement ductility capacity of the wall section increase with confinement of vertical reinforcement in the boundary region.
3. Under reversed cyclic loadings, slender wall sections showed deteriorations in strength and stiffness.
4. Under repeated inelastic load reversals, vertical reinforcement is subjected to alternate tensile yielding and compressive buckling (Figure 1.7a); this may lead to fracture of vertical steel (Figure 1.7b).
5. For over-reinforced wall sections with high percentage of vertical reinforcement, failure occurs through crushing of concrete (Figure 1.7c) in boundary elements.
6. The failure mode of wall sections can be either flexural or shear depending on the amount of vertical steel in the boundary regions. For higher amount of steel in the boundary region, flexural overstrength may cause brittle shear failure.

1.5.3 Squat Walls

The experimental studies [Corley *et. al.*, 1981; Elnashai *et. al.*, 1990; Lefas *et. al.*, 1990; Cheng *et. al.*, 1993; Salonikios *et. al.*, 1999; Salonikios, 2002, and Hidalgo *et. al.*, 2002] on squat walls showed the following salient behavioural features:

1. Ductile shear behaviour of squat wall is observed under both monotonic and cyclic loadings.
2. Under large inelastic compressive strains, crushing of web concrete (Figure 1.8a) is a common mode of failure in squat walls with the formation of diagonal struts.
3. Vertical steel contributes substantially to the shear strength of squat wall sections along with the horizontal steel. Bi-diagonal reinforcement is effective in resisting shear under reversed cyclic loading.
4. Lower portions of squat walls are vulnerable to sliding failure (Figure 1.8b) along

increasing horizontal cracks under reversed cyclic loading. Under monotonic loading, the squat walls are less vulnerable to sliding shear failure than under reversed cyclic loading.

5. Placement of extra vertical reinforcement at the base of the wall over a specified height at the middle region of the section increases the sliding shear strength. Properly detailed bidiagonal reinforcement (Figure 1.9) is more effective in resisting sliding than orthogonal grids of vertical and horizontal reinforcement.
6. For properly designed walls, even with low aspect ratio of 1.0, the principal failure mechanisms were the crushing of web and the buckling of vertical steel. Thus, the behaviour of walls, categorized as “squat” in design codes, can fail in flexural mode if properly detailed.

1.6 ANALYTICAL STUDIES

The analytical studies [Allen *et. al.*, 1973; Bachmann and Linde, 1995; Wood *et. al.*, 1995; Priestley and Kowalsky, 1998; Kwak and Kim, 1999; Wang, 1999, and Hidalgo *et. al.*, 2002] on structural walls with or without boundary elements, showed the following salient behavioural features:

1. For a given axial load and A_f / A_g ratio, the yield curvature and the ultimate curvature remain almost constant irrespective of the percentage of vertical steel. However the moment capacity increased with increase in percentage of steel (Figure 1.10a). The curvature ductility decreases with increase in axial load for a given percentage of steel and A_f / A_g ratio (Figure 1.10b) but increases with increase in A_f / A_g ratio (Figure 1.10c).
2. The beneficial effects of diagonal reinforcement at the base of a wall section under cyclic loading, are shown by finite element analysis of walls with material

nonlinearity. Also reduction factors need to be applied on compressive strength of walls under reversed cyclic loadings.

3. The distributions of dynamic curvature ductility demand and dynamic moment demand along the height of a wall, may be different from the demands obtained from static analysis. Higher moment demand may also increase the dynamic shear demand.
4. Elastic behaviour above the plastic hinge region is ensured by applying a modified distribution of flexural strength.
6. The displacement ductility capacity of a wall decreases with the aspect ratio of wall.
7. The tension-stiffening effect needs to be considered in the concrete stress-strain property during nonlinear analysis of structural walls. The increase of lateral stiffness and ultimate compressive load with increase in vertical compressive load is also demonstrated from nonlinear analysis.

The influence of axial load ratio, ratio of vertical steel and distribution of vertical steel on three curvature quantities, was addressed in a moment-curvature analysis of rectangular walls [Priestley and Kowalsky, 1998]. These quantities are, (a) *yield curvature*: 5 times the curvature ϕ_y at first yield (the lower of the curvatures on the section corresponding to $(\varepsilon_s)_m = f_y / E_s$ and $(\varepsilon_c)_m = 0.002$); (b) *serviceability curvature*: the lower of the curvatures on the section corresponding to $(\varepsilon_c)_m = 0.004$ and $(\varepsilon_s)_m = 0.015$, and (c) *ultimate curvature*: the lower of the curvatures on the section corresponding to $(\varepsilon_c)_m = 0.018$ and $(\varepsilon_s)_m = 0.06$. Moment-curvature analysis was carried out for 4m long and 250mm thick wall section with $f'_c = 27.5 \text{ MPa}$ and $f_y = 415 \text{ MPa}$. The axial load ratio was varied between 0 and 0.11, and the vertical steel between 0.25% and 2.0%. The study concluded that:

1. The yield curvature is a function of wall length alone, and not of the axial load ratio

and vertical steel. Thus, since yield displacements of walls with different lengths in the same direction in a building are different, the design assumption of their simultaneous yielding is not valid.

2. The design flexural strength of walls is proportional to l_w^2 instead of l_w^3 as specified in the New Zealand code design procedure.
3. The displacement ductility capacity of walls decreases with aspect ratio.

Moment-curvature analysis [Jogala, 1999] of rectangular walls with boundary elements, designed for multistoreyed buildings in seismic zones IV and V, showed the values of yield curvature and ultimate curvatures in the order of 10^{-7} and 10^{-6} respectively with the resulting curvature ductility in the range of 3-12.

1.7 CURRENT CODE PROVISIONS

The current code provisions of various countries for flexural and shear design of structural walls have been reviewed here, and the issues relevant to capacity design philosophy discussed.

1.7.1 Indian Concrete Code IS 456:2000

1.7.1.1 Limit State Design Philosophy

The philosophy of limit state method of design of RC structures proposes that the structure should withstand safely all possible loads throughout its design life by satisfying certain specified acceptable limit states of collapse and serviceability. The possibility of a structure attaining one of its limit states is determined using inputs from probabilistic studies. The probable variations in material properties and loads are accounted for through appropriate partial safety factors based on inputs from statistical analysis.

Sections 35 and 36 of the Indian Standard [IS 456, 2000] discuss the limit states of collapse and serviceability for the design of reinforced concrete structures. The limit

states of collapse include the limits for flexure, compression, torsion and shear, and the limit states of serviceability include the limits for deflection and cracking.

1.7.1.2 Flexural Design

The assumptions for flexural limit state design, as in Section 38, specify the limit states in terms of the maximum compressive strain in the extreme layer of concrete in bending and the minimum tensile strain in the extreme layer of steel in bending. While the limit states are sufficient for over-reinforced RC sections, the limit states for under-reinforced designed sections are not addressed to.

1.7.1.3 Shear Design

Section 40 discusses the shear design provisions for RC sections. The nominal shear stress τ_v in a RC rectangular section of uniform depth is defined as

$$\tau_v = \frac{V_D}{bd} \quad (1.2)$$

where V_D is the factored design shear force, b is the breadth, and d is the effective depth of the section. This nominal shear stress τ_v is required to be less than the maximum allowable shear stress $\tau_{c,max}$ (in MPa) in concrete given by [SP:24-1983]

$$\tau_{c,max} = 0.83\sqrt{f'_c}, \quad (1.3)$$

where f'_c is the cylinder strength of concrete.

The design shear strength V_u of an RC section is contributed by both concrete and the shear reinforcement, and is given as

$$V_u = V_{uc} + V_{us}, \quad (1.4)$$

where the shear strengths V_{uc} and V_{us} are contributed by concrete and steel respectively

$$V_{uc} = \tau_c bd, \text{ and} \quad (1.5)$$

$$V_{us} = 0.87f_y A_{sv} \left(\frac{d}{s_v} \right), \quad (1.6)$$

in which

$$\tau_c = \frac{0.85\sqrt{0.8f_{ck}}(\sqrt{1+5\beta}-1)}{6\beta}, \text{ and} \quad (1.7)$$

$$\beta = \frac{0.8f_{ck}}{6.89p_t} \geq 1. \quad (1.8)$$

Further τ_c is the design shear strength of concrete, f_y is the characteristic strength of stirrup not to be greater than 415 MPa , A_{sv} is the total cross sectional area of shear reinforcement, s_v is the spacing of the stirrups along the length of the member, f_{ck} is the characteristic compressive strength of concrete, and p_t is the percentage of longitudinal tension reinforcement $\left(= 100 \frac{A_s}{bd} \right)$.

For sections under axial compression, the design shear strength of concrete is $\delta\tau_c$, where

$$\delta = 1 + \frac{3P_u}{A_g f_{ck}} \leq 1.5, \quad (1.9)$$

where P_u is the axial compressive force (in N), and A_g is the gross area of the concrete section (in mm^2). The minimum shear reinforcement specified is,

$$\frac{A_{sv}}{bs_v} \geq \frac{0.4}{0.87f_y}. \quad (1.10)$$

For RC walls with boundary elements as in buildings, the contribution of boundary elements in the total shear capacity of the wall section needs to be calculated as per Eq.(1.4).

1.7.2 Indian RC Ductile Detailing Code IS 13920:1993

Section 9 specifies the design provisions of RC structural walls that are part of the lateral force resisting system of the structure.

1.7.2.1 General Requirements

The general requirements of RC structural walls of Section 9.1 pertain to the dimensional constraints and the sectional characteristics. A few of the salient clauses therein are:

1. A minimum thickness of wall of $150mm$ is specified to ensure stability of the web under compressive load.
2. A minimum reinforcement is specified along both vertical and horizontal directions as 0.25% of the gross area of cross section. This reinforcement is required to be distributed uniformly in the plane of the wall.
3. Two curtains of reinforcement are to be provided along each of the horizontal and transverse directions in the web of the wall when the factored shear stress in the wall exceeds $0.25\sqrt{f_{ck}}$ or when the wall thickness exceeds $200mm$.
4. A maximum diameter of reinforcement is specified at any location of the wall is one-tenth of the thickness at that location.
5. A maximum spacing of reinforcement in either direction is specified as the smaller of $\frac{l_w}{5}$, $3t_w$ and $450mm$, where l_w is the horizontal length of the wall and t_w is the thickness of the web.

1.7.2.2 Flexural Design

Section 9.3 recommends the moment of resistance M_{uv} of RC walls with uniformly distributed vertical steel to be calculated in the same way as is done for RC sections subjected to combined uniaxial bending M_u and axial compression P_u as per

Indian Concrete Code, and provides the following expressions in terms of the length l_w and thickness t_w of the wall, material properties E_s , f_y and f_{ck} , and the percentage of vertical steel $\rho \left(= \frac{A_{st}}{t_w l_w} \right)$.

To begin with the parameters, ϕ , λ and β are calculated as

$$\phi = \frac{0.87f_y \rho}{f_{ck}}, \quad (1.11)$$

$$\lambda = \frac{P_u}{f_{ck} t_w l_w}, \text{ and} \quad (1.12)$$

$$\beta = \frac{0.87f_y}{0.0035E_s}. \quad (1.13)$$

When the depth of neutral axis is above the balanced depth of neutral axis, i.e., $\frac{x_u}{l_w} \leq \frac{x_u^*}{l_w}$,

then

$$\frac{M_{uv}}{f_{ck} t_w l_w^2} = \phi \left[\left(1 + \frac{\lambda}{\phi} \right) \left(\frac{l}{2} - 0.416 \frac{x_u}{l_w} \right) - \left(\frac{x_u}{l_w} \right)^2 \left(0.168 + \frac{\beta^2}{3} \right) \right], \quad (1.14)$$

where

$$\frac{x_u}{l_w} = \frac{\phi + \lambda}{2\phi + 0.36}, \text{ and} \quad (1.15)$$

$$\frac{x_u^*}{l_w} = \frac{0.0035}{0.0035 + \frac{0.87f_y}{E_s}}. \quad (1.16)$$

When the depth of neutral axis is below the balanced depth of neutral axis, i.e.,

$$\frac{x_u^*}{l_w} < \frac{x_u}{l_w} < 1.0, \text{ then}$$

$$\frac{M_{uv}}{f_{ck}t_w l_w^2} = \left[0.36 + \phi \left(1 - \frac{\beta}{2} - \frac{1}{2\beta} \right) \right] \left(\frac{x_u}{l_w} \right) - \alpha_2 \left(\frac{x_u}{l_w} \right)^2 - \alpha_3 - \frac{\lambda}{2}, \quad (1.17)$$

$$\alpha_2 = 0.15 + \frac{\phi}{2} \left(1 - \beta - \frac{\beta^2}{2} - \frac{1}{3\beta} \right), \text{ and} \quad (1.18)$$

$$\alpha_3 = \frac{\phi}{6\beta} \left(\frac{1}{\left(\frac{x_u}{l_w} \right)} - 3 \right). \quad (1.19)$$

where $\frac{x_u}{l_w}$ is obtained by solving,

$$\left[0.36 + \phi \left(1 - \frac{\beta}{2} - \frac{1}{2\beta} \right) \right] \left(\frac{x_u}{l_w} \right)^2 + \left(\frac{\phi}{\beta} - \lambda \right) \left(\frac{x_u}{l_w} \right) - \frac{\phi}{5\beta} = 0. \quad (1.20)$$

In the derivation of the above expressions, the vertical steel is represented by an equivalent steel plate along the length of the section, and the design stress-strain curves for concrete and steel (Figure 1.11) are used.

To economize the wall design, the cracked flexural strength of the wall is prescribed to be more than the uncracked flexural strength. Also for walls without boundary elements, extra vertical steel needs to be concentrated at the boundary region to provide additional flexural capacity.

1.7.2.3 Shear Design

Section 9.2 discusses the shear design provisions for RC structural walls. A few relevant clauses therein are:

1. The design shear capacity V_{uw} of the wall section is given by,

$$V_{uw} = \tau_c t_w d_w + 0.87 f_y A_h \left(\frac{d_w}{s_{vw}} \right), \quad (1.21)$$

where the first term on the right hand side is the contribution of concrete and the

second term is the contribution of steel. In Eq.(1.21), A_h is the total area of horizontal shear reinforcement, and s_{vw} is the vertical spacing of horizontal shear reinforcement along the height of the wall. The shear strength of concrete τ_c is calculated using Eq.(1.7). The design shear capacity of the wall section is based on the capacity of web portion only. Thus, for walls with boundary elements, the contribution of boundary elements is not addressed.

2. The nominal shear stress τ_{vw} in the section is calculated as,

$$\tau_{vw} = \frac{V_D}{t_w d_w} \quad (1.22)$$

where d_w is the effective depth of wall section to be taken as $0.8l_w$ for rectangular sections. The nominal shear stress should be less than the maximum possible shear stress $\tau_{c,max}$ as in Eq.(1.3).

3. If the design vertical steel comes out to be less than the design horizontal steel, then the code requires that the vertical steel be increased to at least equal the horizontal steel.

1.7.2.4 Design of Boundary Elements

Section 9.4 gives the provisions for the design and detailing of boundary elements. The salient clauses therein are:

1. Boundary elements are to be provided if the maximum compressive stress in the section, due to factored gravity and factored seismic loading, exceeds $0.2f_{ck}$. Such boundary elements are to be continued along the length of the wall until the section where the compressive stress reduces below $0.15f_{ck}$. The compressive stress is to be calculated using linear elastic model and gross section properties.
2. The boundary element is to be designed as a short column for an axial compression P

equal to the sum of the factored gravity axial load P_g and the additional compressive force P_e induced by the seismic force, given by

$$P_e = \frac{M_u - M_{uv}}{C_w}, \quad (1.23)$$

where M_u is the factored design moment on the entire wall section, M_{uv} is the moment of resistance provided by vertical reinforcement along the length, and C_w is the horizontal center to center distance between the boundary elements. Thus the flexural capacity of the wall section is obtained as a linear superposition of the flexural capacity of rectangular web region and the moment contribution from the axial load capacity of the boundary element.

3. In item 2 above, the load factor is to be taken as 0.8 for gravity axial load P_g , if it adds to the strength of the wall.
4. The percentage of vertical steel in the boundary elements is specified to be in the range 0.8-6%; however, the practical upper limit is suggested as 4% to avoid congestion of reinforcement.
5. To sustain repeated cycles of inelastic strains without large degradation of strength, special confining reinforcement is to be provided along the full height of the boundary element.
6. If boundary elements are not provided, special confining reinforcement is to be provided throughout the entire wall.

1.7.3 American Concrete Code ACI 318-99

The American Concrete Code [ACI 318, 1999], in Section 21.6, gives the design provisions for RC structural walls serving as a part of the earthquake force-resisting system.

1.7.3.1 Flexural Design

The flexural strength of any wall section is to be determined considering the combined action of compression and uniaxial bending, and based on strain compatibility analysis of the wall section with boundary elements including the contribution of concentrated vertical reinforcement in the boundary region.

1.7.3.2 Shear Design

The nominal shear strength V_n of the wall section is obtained as sum of contributions of capacity of the concrete and horizontal steel, as

$$V_n = A_{cv}(\alpha_c \sqrt{f'_c} + \rho_n f_y), \quad (1.24)$$

where A_{cv} is the total concrete area in the direction of the shear force (in in^2), f'_c is the specified compressive strength of concrete (in psi), ρ_n is the ratio of area of distributed steel parallel to the plane of A_{cv} to gross concrete area perpendicular to the reinforcement, f_y is the yield strength of reinforcement (in psi), and α_c is the coefficient specifying the contribution of concrete in wall strength, given by Figure 1.12.

For walls with low aspect ratios, the required horizontal reinforcement for shear resistance may be higher than the required vertical reinforcement for flexure. This will lead to under utilization of vertical steel in resisting the earthquake shear forces. Thus, for walls with $\left(\frac{h_w}{l_w}\right) < 2.0$, the vertical steel ratio ρ_v is to be not less than the horizontal steel ratio ρ_n .

1.7.3.3 Walls with Boundary Elements

Two criteria are provided for boundary elements in structural walls, namely:

1. The first criterion decides to provide the boundary elements. Boundary element needs to be provided when the maximum compressive stress in the section exceeds the

nominal critical value of $0.2f'_c$ under the combined action of gravity and lateral loads.

The boundary element may be discontinued where the compressive stress becomes less than $0.15f'_c$. The maximum compressive stress is to be determined using the linear material properties and the gross sectional properties.

2. The second criterion requires the ends of a wall section to be confined during the design displacement. For walls that are effectively continuous from the base to the top and have a single critical section for the design moment and axial load, the full compression zone of the section is to be reinforced with special boundary elements when,

$$c \geq \frac{l_w}{600 \frac{\delta_u}{h_w}}, \quad (1.25)$$

where c is the depth of neutral axis (in *in*) from the extreme compression fibre and is obtained for the factored axial force and nominal moment strength and δ_u is the design displacement (in *in*); the largest neutral axis depth is obtained for consistency with the design displacement δ_u . The minimum value of the rotation δ_u / h_w is specified as 0.007 . The vertical extent of the boundary element is the estimated height of the plastic hinge zone during the base rotation. The minimum vertical height of the boundary element is given by the larger of l_w or $\frac{M_u}{4V_u}$ where M_u and V_u are the factored moment and the factored shear force in the section. The minimum horizontal extent of the boundary element from the extreme compression fibre is the larger of $(c - 0.1l_w)$ and $0.5c$.

1.7.3.4 Wall without boundary elements

If special boundary elements are not required for walls, the boundary regions of the wall need to be confined with additional reinforcement to impart more strength and

prevent the buckling of the vertical steel during high deformation demands.

1.7.4 New Zealand Concrete Structures Code NZS 3101 Part 1-1995

The New Zealand Code of Practice [NZS 3101, 1995] for the design of concrete structures categorizes structures into two groups from the point of view of seismic design, namely (a) *ductile* structures, and (b) structures with *limited ductility*. The salient clauses pertaining to the design of ductile RC walls are:

1. The structural type factors S used in the calculation of design loads for buildings [NZS 4203, 1976] are specified as follows:

(a) For walls in buildings with a single cantilever shear wall,

$$S = 1.2Z . \quad (1.26)$$

(b) For walls in buildings with two or more cantilever walls,

$$S = 1.0Z \leq 2.0 , \quad (1.27)$$

(c) For walls in buildings with two or more ductile coupled structural walls,

$$S = \begin{cases} 0.8Z \leq 2.0 & \text{for } A \geq 0.67 \\ Z - 0.59Z(A - 0.33) & \text{for } 0.33 \leq A \leq 0.67 , \\ Z \leq 2.0 & \text{for } A \leq 0.33 \end{cases} \quad (1.28)$$

where A is the moment ratio and is given by $\frac{Tl}{M_o}$, T is the axial load induced at

the base of coupled shear walls by design earthquake loading, l is the distance between vertical reference axes of coupled shear walls, and M_o is the total overturning moment at the base of shear wall structure.

In Eqs.(1.26) to (1.28),

$$Z = \begin{cases} 1.0 & \text{for } \frac{h_w}{l_w} \geq 3.0 \\ 2.5 - 0.5 \frac{h_w}{l_w} & \text{for } 1.0 \leq \frac{h_w}{l_w} \leq 3.0 , \\ 2.0 & \text{for } \frac{h_w}{l_w} \leq 1.0 \end{cases} \quad (1.29)$$

2. During strong earthquake shaking, the shear demand in wall may be higher than the

shear demand during flexural overstrength. The code recommends the shear demand to be calculated by the capacity design concept as

$$V_{wall} = \omega_v \phi_o V_{code} < \frac{4V_{code}}{S}, \quad (1.30)$$

where ϕ_o is the Flexural Overstrength Factor $\left(= \frac{M_o}{M_{code}} \right)$, M_o is the Overstrength moment of resistance, M_{code} is the Moment resulting from code loading, ω_v is the Dynamic Shear Magnification Factor given in Table 1.1, and V_{code} is the shear resulting from code specified load combinations.

Table 1.1: Variation of dynamic shear magnification factor

Number of Storeys (N)	ω_v
1-5	$0.1N+0.9$
6-9	1.5
10-14	1.7
≥ 15	1.8

To eliminate the possibility of the formation of plastic hinge above the base of the wall, the code recommends curtailment of vertical bars from the end of the plastic hinge zone to the top of the wall with a linear reduction of moment capacity from the bottom to the top (Figure 1.13).

1.7.4.1 Shear Design

The salient clauses of shear design are:

1. The recommended value of effective depth d , used for obtaining the shear stress ν_i at any horizontal section through the wall, is the distance from the extreme compression fibre to the centre of the tension reinforcement. It may also be considered as $0.8l_w$.
2. Under the action of axial compression P_u , the shear strength ν_c of concrete in the wall section with gross cross sectional area A_g is given by

$$\nu_c = 0.2 \left(\sqrt{f'_c} + \frac{P_u}{A_g} \right). \quad (1.31)$$

3. The cracked shear strength of an inclined wall section is given by

- (a) When a principal tensile stress of $0.33\sqrt{f'_c}$ occurs at the centroid of the wall section, then

$$\nu_c = 0.27\sqrt{f'_c} + \frac{P_u}{4A_g}. \quad (1.32)$$

- (b) When flexural tensile stress becomes $0.5\sqrt{f'_c}$ at a distance $\frac{l_w}{2}$ above the section under consideration, then

$$\nu_c = 0.05\sqrt{f'_c} + \frac{l_w \left(0.1\sqrt{f'_c} + 0.2 \frac{P_u}{A_g} \right)}{\frac{M_u}{V_u} - \frac{l_w}{2}}. \quad (1.33)$$

When $\left(\frac{M_u}{V_u} - \frac{l_w}{2} \right)$ is negative, then Eq.(1.31) is to be used.

4. The upper limit $(\nu_c)_{max}$ of the concrete shear strength in the boundary region is specified as,

$$(\nu_c)_{max} = 0.6 \sqrt{\frac{P_e}{A_g}}, \quad (1.34)$$

where P_e is the design axial load in compression due to gravity and seismic loading acting on the member simultaneously during an earthquake.

5. Considering web-crushing as a likely mode of failure in the plastic hinge zone, the limiting shear stress is given as

$$\nu_i \leq (0.3\phi_o S + 0.16)\sqrt{f'_c}. \quad (1.35)$$

6. To ensure yielding of vertical steel before shear failure, the code specifies a minimum ratio of horizontal steel ρ_h as

$$\rho_h = \frac{4}{3} \left(\frac{d_s V_u}{M_u} \frac{f_{yn}}{f_{yh}} \rho_n - \frac{v_c}{f_{yh}} \right), \quad (1.36)$$

where d_s is the distance from centroid of total vertical reinforcement to extreme compression fibre of wall section, and f_{yh} is the specified yield strength of horizontal non-prestressed shear reinforcement.

1.7.5 Japanese Standard AIJ

Different sections of the guidelines provided by the Architectural Institute of Japan [AIJ, 1994] specify the requirements of a building with earthquake-resistant design.

1.7.5.1 Structural Planning

Section 3 addresses yielding in different structural members during an earthquake. Some salient clauses are:

1. The desired locations of yielding in the structural members need to be identified clearly and detailed for the required strength and ductility.
2. Section 3.2 recommends the yielding of beam reinforcement at the time of hinging. The formation of hinges in beam is favourable as it results in stable hysteresis loops.
3. For a frame-wall building, Section 3.3.3 recommends the flexural yielding at the base of the wall. In multistoreyed buildings, the ends of the beams and for basement walls, the ends of the foundation girders are the desired locations of yielding.

1.7.5.2 Design Methods

1.7.5.2.1 Design Philosophies

Two seismic design philosophies are discussed, namely (a) *yield mechanism* design, and (b) *yield assurance* design.

In *yield mechanism* design, the desired regions of hinge formation are to be

provided with adequate strength and ductility to ensure the flexural yielding. The member design forces are determined by linear analysis considering reduction of member stiffness and redistribution of moments in the members. The stiffness reduction factors for structural walls in linear analysis are given in Table 1.2.

Table 1.2: Stiffness Reduction factors for walls

<i>Structural Wall</i>	<i>Flexural Stiffness</i>	<i>Axial Stiffness</i>	<i>Shear Stiffness</i>
Without Hinge	1.0	1.0	0.5-1.0
Yield Hinge	0.3-0.5	1.0	0.3-0.5

In *yield assurance* design, regions other than the desired locations of hinges are to be provided with adequate strength so that failure does not occur at the time of yielding. The member design forces are obtained using dynamic magnification factors on the member forces from nonlinear analysis and appropriate redistributions. Flexural hinge formations in beams or structural walls are to precede the formation of hinges in columns.

1.7.5.2.2 Lateral Deformation Levels

Three lateral deformation levels are also defined for the design, namely, (a) *yield deformation*, which is the lateral deformation corresponding to the simultaneous formation of all desired hinges during seismic action; (b) *design limit deformation*, which is the limiting lateral deformation by the design earthquake motion: the storey drift angle is specified as 0.01 radian; and (c) *assurance deformation*, which is the maximum possible response deformation during an earthquake, considering all the possible uncertain variations in the factors.

1.7.5.2.3 Flexural Strength

Section 5.0 specifies two levels of flexural strengths for RC members, namely (a) *reliable flexural strength*, which is mobilized for the realistic stress distribution during the total yield mechanism of the structure; and (b) *upper bound flexural strength*, which

is mobilized when the structure is strained upto the assurance deformation level. This strength is estimated considering overstrength material properties.

The moment curvature relation (Figure 1.14a) shows the yield point Y, corresponding to the first tensile yielding of reinforcement, and the point U, corresponding to the ultimate compressive strain. Thus, the reliable strength corresponds to the capacity at point U while the upper bound flexural strength is given by the capacity at point M, which corresponds to an extreme fibre compression strain $\varepsilon_c = 0.003$. The deformation, at which the reliable flexural strength is mobilized, is to be less than the Design Limit Deformation R_d (Figure 1.14b).

1.7.5.2.4 Axial Load Limitation

The flexural strength and deformation capacity of a structural wall depends on the level of axial force in the wall. Section 5.5 recommends an upper bound value of axial load for walls as:

$$N_w \leq k_3 A_{core} \sigma_B - A_{ws} \sigma_{wyu}, \quad (1.37)$$

where N_w is the total axial load acting on the wall in the yield assurance design mechanism (kgf), A_{core} is the core area of boundary column on compression side (cm^2), A_{ws} is the area of vertical reinforcement in wall panel (cm^2), σ_B is the compressive strength of concrete (kgf/cm^2), σ_{wyu} is the material strength of vertical reinforcement in wall panel for upper bound flexural strength (kgf/cm^2), and $k_3 = \frac{2}{3}$ but may be taken as 1.0 if adequate confinement reinforcement is provided.

1.7.5.2.5 Shear Design

The philosophy of shear design requires the reliable shear strength of the members to be greater than the design shear in the yield assurance design, and the shear deformation capacities of the members to exceed the assurance displacement demands. The recommended failure mode of shear walls is either flexural yielding at the base or

lifting-up of foundation as both of them can ensure adequate ductile behaviour.

The recommended method for determining the shear demand is by considering the overstrength material characteristics in the analysis method, and then applying dynamic magnification factors on the obtained shear forces. As structural walls tend to carry most of the shear due to dynamic effects, both horizontal and vertical steel should be designed for the shear demand.

1. The equation for shear strength is based on the assumption that shear force is transferred by arch and truss mechanism. The reliable strength V_u of wall at each storey level is calculated by

$$V_u = t_w l_{wb} p_s \sigma_{sy} \cot \phi + 0.5 \tan \theta (1 - \beta) t_w l_{wa} \nu \sigma_B, \quad (1.38)$$

where

$$\tan \theta = \sqrt{\left(\frac{h_w}{l_{wa}}\right)^2 + 1} - \frac{h_w}{l_{wa}}, \quad (1.39)$$

$$\beta = \left(1 + \cot^2 \phi\right) \frac{p_s \sigma_{sy}}{\nu \sigma_B}, \quad (1.40)$$

t_w is the thickness of wall panel, h_w is the height of the wall which may be taken as the inter-storey height, l_{wb} is the equivalent width of wall panel in truss mechanism, l_{wa} is the equivalent width of wall panel in arch mechanism, σ_{sy} is the strength of shear reinforcement within the panel $\leq 4000 \text{ kgf/cm}^2$, p_s is the shear reinforcement ratio within the wall panel, ν is the effectiveness factor for compressive strength of concrete, and ϕ is the angle of compressive strut in truss mechanism ($= 45^\circ$).

In Eq.(1.40), when $p_s \sigma_{sy} > 0.5 \nu \sigma_B$, then $p_s \sigma_{sy}$ is to be taken as $0.5 \nu \sigma_B$.

2. Experimental observations indicate that boundary elements contribute to the shear strength of walls. To account for this contribution, equivalent width of wall has been recommended for both truss and arch mechanisms. The equivalent wall widths in the

two mechanisms are given as

$$l_{wa} = l'_w + D_c + \Delta l_{wa}, \text{ and} \quad (1.41)$$

$$l_{wb} = l'_w + D_c + \Delta l_{wb}. \quad (1.42)$$

where l'_w is the clear span of wall panel, D_c is the width of boundary column, Δl_{wa} is the increment of wall width, and Δl_{wb} is the increment of wall width.

1.7.5.2.6 Confinement

Confinement of bottom portions of the boundary elements is recommended for providing the required strength and ductility at the time of flexural yielding.

1.7.5.2.7 General Requirements

The minimum thickness of walls is to be the larger of 150mm and $\frac{l}{30}$ th of the clear height of wall panel. The prescribed minimum reinforcement along vertical and horizontal directions in wall panel is 0.25% of the gross sectional area. To ensure the ductile behaviour of boundary elements in the hinge regions, the recommended percentage of shear reinforcement is 0.3% .

1.7.6 European Standard Eurocode 8

The Eurocode 8 [EC8, 1994] differentiates between the different failure modes of structural walls. The failure modes are: (a) diagonal tension, (b) diagonal compression (web crushing), and (c) sliding shear. The concrete contribution in shear capacity at the plastic hinge location, is given as

$$V_{cd} = 0.06\sqrt{f'_c}(1.2 + 40\rho_l)b_wz, \quad (1.43)$$

where ρ_l is the ratio of tension reinforcement, b_w is the thickness of web, and z is the effective internal lever arm ($= 0.8l_w$).

The design shear capacity of web reinforcement in wall sections is given by

$$V_{wd} = \begin{cases} \rho_v f_{yd} b_w z & \text{for } a_s \leq 0.3 \\ [\rho_h (a_s - 0.3) + \rho_v (1.3 - a_s)] f_{yd} b_w z & \text{for } 0.3 < a_s < 1.3, \\ \rho_h f_{yd} b_w z & \text{for } a_s \geq 1.3 \end{cases} \quad (1.44)$$

where ρ_h is the ratio of horizontal web reinforcement, ρ_v is the ratio of vertical web reinforcement, and f_{yd} is the design strength of reinforcement. Thus, the vertical steel resists the entire shear for walls with $a_s \leq 0.3$, and the horizontal steel resists the entire shear for walls with $a_s \geq 1.3$. For the intermediate values of a_s , both horizontal and vertical reinforcement are effective in shear resistance.

Inclined bars are recommended in the wall for shear resistance against failure modes. The shear resistance of walls against sliding shear failure is based on the combination of dowel resistance of vertical bars, shear resistance of cross-inclined bars and frictional resistance. For squat walls $\left(\frac{h_w}{l_w} < 2.0 \right)$, bidiagonal bars are to carry at least half of design shear at base.

1.7.7 Swiss Standard SIA 160

The provisions of Swiss Standard SIA 160 [Bachmann and Linde, 1995] recommend the capacity design philosophy for the structural walls. The capacity design method is based on an equivalent “*elastic*” static force reduced in two stages by a *displacement ductility* factor and an *overstrength reduction* factor. The salient features of the provisions are:

1. For the flexural yielding at the base of the wall, a plastic hinge region is identified. The region stretches over a height of l_w or $\frac{h_w}{6}$, whichever is larger. The region of plastic hinge is detailed to enable the confined concrete to undergo large strains during the flexural yielding of vertical reinforcement.
2. For calculating the lateral force, displacement ductility factor μ_Δ and overstrength reduction factor C_d are considered. For fully ductile walls, the reduction factor is

maximum and $\mu_{\Delta} = 5.0$, whereas for walls with restricted ductility, $\mu_{\Delta} = 3.0$. The overstrength reduction factor C_d is calculated as

$$C_d = \frac{1}{\gamma_R \lambda_o}, \quad (1.45)$$

where γ_R is the resistance factor, usually taken as 1.2, and λ_o is the overstrength factor for reinforcing steel (usually 1.2 or more).

3. The overstrength moment demand M_i is determined from

$$M_i = \gamma_R M_E, \quad (1.46)$$

where M_E is the static bending moment obtained from distribution of forces.

4. Overstrength shear demand is determined from

$$V_w = \omega_v \Phi_{o,w} V_E, \quad (1.47)$$

where $\Phi_{o,w}$ is the flexural overstrength factor for the wall $= \lambda_o \frac{M_R}{M_E}$, ω_v is the dynamic magnification factor depending on the number of storeys of the building, and V_E is the static shear force obtained from distribution of forces.

Thus, the design shear and design moment are always determined for the overstrength condition.

1.7.8 Balkan Codes

1.7.8.1 Turkish National Code 1975

Section 6.7 of the Turkish National Code [UNIDO, 1985] specifies the general design requirements for RC structural walls. The minimum thickness of the wall is prescribed to be the greater of $\frac{1}{20}$ th of the width of wall or storey height and 150mm.

The minimum reinforcement is recommended as 0.25% of the gross sectional area along the horizontal direction and 0.2% of the gross sectional area along the vertical direction. The maximum spacing of vertical bars is specified to be less than the smaller of 1.5 times

the wall thickness and 300mm.

1.7.8.2 Bulletin d'Information No. 160

The CEB Standard [UNIDO, 1985] assigns any of the three ductility levels to different structures, namely (a) *ductility level I* (DL I) for which no specific aseismic provisions are recommended, (b) *ductility level II* (DL II), for which aseismic provisions are recommended for deforming the structures in the inelastic range of response under repeated reversible loading, and (c) *ductility level III* (DL III) for which stringent aseismic design provisions are recommended for the structures to ensure large energy-dissipation capacities.

The code recommends the use of linear analysis in determining the design force resultants on structural walls. Appropriate dynamic magnifications of bending moment and shear force are also considered for design. For shear forces, the amplification factor is given by,

$$\omega = 0.1N + 0.9 \quad (1.48)$$

The design shear force is to be compatible with the actual flexural strength developed at the base of the wall. The actual shear forces are obtained by multiplying the design shear force with the factor γ_n (≤ 4) given as,

$$\gamma_n = \frac{M_{u,d}}{M_d}, \quad (1.49)$$

where M_d is the design moment obtained from analysis, and $M_{u,d}$ is the flexural strength of the section under actual axial load based on provided reinforcement using the characteristic values of concrete and steel strengths.

1.8 MISCELLANEOUS DESIGN METHODS

1.8.1 Miscellaneous Design Methods

Allen *et. al.* [1973] recommended various design provisions for RC structural

walls. Some salient ones are:

1. *Flexural Design*: The wall should be designed for the combined action of the design axial load and the larger of cracking moment M_{cr} and ultimate design moment M_{ud} , where

$$M_{cr} = Z \left(7.5 \sqrt{f'_c} + \frac{P}{A_g} \right). \quad (1.50)$$

2. *Shear Design*: The design shear force is obtained from,

$$V_u = F_s \times V_{ud}, \quad (1.51)$$

where $F_s = \frac{M_f}{M_{ud}}$, in which M_f is the design moment from analysis, M_{ud} is the

unfactored moment capacity of the section. The shear design is to be entirely based on the capacity of the horizontal steel, neglecting the shear capacity offered by concrete.

3. *Foundation*: The foundation of the wall should be suitably designed, and if necessary, anchored, to mobilize the full flexural strength during yielding of the wall.

The recommended guidelines in ATC 11 [ATC 11, 1983] for the design of RC structural walls in line with the provisions specified in ACI 318-83 are:

1. Undesired configurations and arrangements of walls need to be eliminated in buildings for obtaining favourable response during strong earthquake shaking.
2. The ultimate flexural capacity needs to be determined based on the strain compatibility analysis as specified in ACI 318-83 with the allowable maximum compressive strain in concrete taken as 0.003 (Figure 1.15).
3. The design moment capacity ϕM_n of walls with uniformly distributed vertical steel is given by

$$\phi M_n = \phi \left[0.5 A_s f_y l_w \left(1 + \frac{N_u}{A_s f_y} \right) \left(1 - \frac{c}{l_w} \right) \right] \quad \text{for } \phi N_u < P_{bal}. \quad (1.52)$$

The stress distributions in steel and concrete are shown in Figure 1.15. For coupled walls, interaction diagram is to be obtained for individual walls.

4. Vertical reinforcement needs to be curtailed along the height of the wall for cantilever walls under lateral forces.
5. The structural walls are to be provided with adequate shear capacity to take care of shear demand during flexural yielding.
6. Structural walls need to be properly detailed and designed along with the boundary elements for ductile response and prevent the brittle modes of failure. Confinement of concrete in the boundary region and under-reinforced wall design are required for the ductile design of walls.

For shear design of walls, another design philosophy [Wood, 1990] specified the lower bound of nominal shear strength of walls with distributed vertical steel in the web as $0.5\sqrt{f'_c}$ MPa. Correlating with several test results on wall specimens, the design shear strength as per the ACI code was found to overestimate the actual shear strength of the wall above a threshold ratio of web reinforcement. The recommended nominal shear strength was based on shear friction approach instead of truss analogy approach.

A performance-based two-step design procedure is suggested [Hoogenboom *et al.*, 1999] based on the stringer-panel theory for RC structural walls: (a) the wall section is designed and detailed using linear and nonlinear methods of analysis for all selected load combinations, and (b) wall behaviour is simulated till failure for each selected load combination. Based on the simulated performance, the design is improved if necessary. The design procedure may not be economical but realistic behaviour under each load combination is investigated.

Based on nonlinear finite element analysis of low-rise shear walls, a design

method [Lou *et. al.*, 2001] was proposed to include the contribution of vertical shear reinforcement in the flexural strength of the wall section. The decreased amount of flexural reinforcement has two-fold implication, namely (a) less congestion of reinforcement, and (b) reducing the possibility of brittle shear failure during flexural overstrength.

1.8.2 Displacement Based Design

The philosophy of displacement-based design [Wallace and Moehle, 1992, and Wallace, 1994] of structural walls requires (a) the drift capacity to exceed the imposed displacement demand on the wall, and (b) adequate ductility in the wall. The procedure to check item (a) includes the following steps:

1. *Estimation of Natural Period*: The fundamental natural period T is estimated based on the stiffness of cracked section for wall sections [Wallace and Moehle, 1992] as

$$T = 8.8 \frac{h_w}{l_w} n \sqrt{\frac{wh_s}{gE_c p}}, \quad (1.53)$$

where n is the number of floors, w is the unit floor weight including tributary wall height, h_s is the wall height, p is the ratio of wall area to floor plan area for the walls

aligned in the direction the period is calculated as $\left[p = \frac{\Sigma A_w}{A_f} \right]$, A_w is the web area of

the wall ($= l_w t_w$), and A_f is the floor plan area of a typical floor of a building.

2. *Estimation of Displacement Demand*: Using the fundamental natural period of the building, the spectral displacement S_d is obtained from the response spectrum, and the roof displacement δ_u is related to S_d as

$$\frac{\delta_u}{h_w} = \frac{1.5 S_d}{h_w}. \quad (1.54)$$

The roof drift ratio $\frac{\delta_u}{h_w}$ provides an estimate of global deformation demands on the building.

3. *Estimation of Maximum Compressive Strain in Concrete*: Depending on the shape of the wall, the maximum compressive strain in concrete is given by

$$\varepsilon_{c,max} = \left[\frac{(\rho + \rho'') \frac{\alpha f_y}{f'_c} - \rho' \frac{f'_s}{f'_c} - \frac{0.85b}{t_w l_w} (a - t_w) + \frac{P}{l_w t_w f'_c}}{\left(0.85 \beta_1 + 2 \rho'' \frac{\alpha f_y}{f'_c} \right)} \right] \phi_u l_w. \quad (1.55)$$

where ρ is the tension steel ratio $\left(= \frac{A_s}{t_w l_w} \right)$, ρ' is the compression steel ratio

$\left(= \frac{A'_s}{t_w l_w} \right)$, ρ'' is the distribution steel ratio $\left(= \frac{A''_s}{t_w l_w} \right)$, β_1 is a factor defined in ACI

318-99, P is the axial load, f'_s is the stress in compression steel, b is the length of boundary element, and a is the thickness of boundary element. Eq.(1.55) is based on the assumption that the neutral axis lies within the web of the wall and the depth of neutral axis is not more than the half of wall depth.

4. *Estimation of Displacement Capacity*: Considering elastic and inelastic actions over the height of the wall, the displacement capacity δ_c (Figure 1.16) at the top of the wall is to be estimated as

$$\delta_c = \delta_y + \theta_p h_w = \frac{11}{40} \phi_y h_w^2 + \frac{1}{2} (\phi_u - \phi_y) h_w l_w, \quad (1.56)$$

where δ_y is the displacement from elastic deformation, $\theta_p h_w$ is the displacement from inelastic deformation, ϕ_y is the yield curvature (curvature at first yield of wall steel), ϕ_u is the ultimate curvature, and l_p, θ_p being the plastic hinge length and rotation, respectively. Based on this relation, the assumptions for yield curvature

$\left(\frac{0.0025}{l_w}\right)$ and plastic hinge length $(0.5l_w)$, the rotational deformation imposed at

the base of the wall can be expressed as

$$\phi_u l_w = 0.0025 \left[1 - \frac{1}{2} \frac{h_w}{l_w} \right] + 2 \frac{\delta_u}{h_w}. \quad (1.57)$$

In terms of the aspect ratio of the wall, this rotational deformation is expressed as

$$\phi_u l_w = 0.0025 \left[1 - \frac{1}{2} \frac{h_w}{l_w} \right] + 0.0046 \frac{\delta_u}{h_w} \sqrt{\frac{1}{p}}. \quad (1.58)$$

To check item (b), the ductility factor of wall is required. Ductility factor μ_δ was calculated using [Wallace, 1995],

$$\mu_\delta = \frac{\delta_c}{\delta_y} = 0.00023 \frac{h_w^2}{l_w \delta_y} \sqrt{\frac{1}{p}}, \quad (1.59)$$

where δ_y is the yield displacement. For cantilever walls with linearly increasing load over the wall height, if the yield displacement is approximated by $\delta_y = 0.275 \phi_y h_w^2$

with and the yield curvature by $\phi_y = \frac{0.0025}{l_w}$, then Eq.(1.59) can be written as

$$\mu_\delta = 0.33 \sqrt{\frac{1}{p}}. \quad (1.60)$$

The acceptable value of ductility factor depends on the type of building. For the buildings with walls and having low wall area to floor area ratios, μ_δ of 4-5 have been found to be reasonable [Wallace, 1995]. The displacement-based design approach that includes a check on ductility factor, allows the designer to choose building system with any characteristics, so long as the overall ductility is adequate. However to ensure that the above level of ductility can be achieved, the following need to be ensured:

- (i) *Confinement of concrete*: The region of confinement at the ends of the wall depends on the strain distribution over the section, *i.e.*, the maximum compressive strain at the extreme fibre of the section and the depth of compression zone in the section. The actual depth of compression zone is to be determined by strain-compatibility analysis, but can also be determined as $c = \frac{\varepsilon_{c,max}}{\phi_u}$. Wallace [1995] suggested a limiting strain $\varepsilon_{c,max} = 0.004$, exceeding which confinement is to be provided over the exceedance region.
- (ii) *Sufficient Transverse Reinforcement*: The amount of transverse reinforcement for a wall cross section is to be such that the required maximum compressive strain in concrete can be developed by the consequent confining action, and that the buckling of vertical reinforcement in the end region is prevented. For compressive strain in extreme fibre less than 0.004, provision of special transverse reinforcement is not recommended. Then, the required minimum transverse steel should be provided as per ACI 318-99 recommendations in the boundary elements and the web of the wall.

This approach gave consistent results with the experimental study of a full-scale building and the observed performance of shear-wall buildings in 1985 Chile earthquake [Wallace and Moehle, 1992]. In another study, two ten-storeyed buildings having the same plan area and identical material properties, were designed [Wallace and Thomsen, 1995] as per UBC-91 for Zone-4 requirements. All walls in the two buildings were slender. Building 1 had rectangular walls with aspect ratio 5.0 and C-shaped walls with aspect ratio 7.5, while Building 2 had both rectangular and T-shaped walls with aspect ratio 5.0. The code-prescribed forces were distributed equally on the walls although the actual distribution of forces will be based on their stiffness. The results showed that for symmetrically reinforced geometrically symmetric wall cross-sections, the reinforcement

required at the boundaries was substantially less than the steel required as per UBC-1991. For the rectangular and channel-shaped wall sections, the design approach proposed in the study was simpler than the UBC-1991 method.

Kowalsky [2001] recommended a direct Displacement-Based Design method for performance-based engineering of buildings. The sequential steps are given in Figure 1.18. The final design base shear is calculated by the product of effective stiffness and target displacement of the wall. The shear demand is taken care by the vertical steel and target displacement is achieved by providing confinement details.

1.9 CAPACITY DESIGN

In capacity design philosophy, certain desirable inelastic modes of energy dissipation are identified and specific elements of the structure are designed and detailed to achieve the same. Regions of potential plastic hinges are identified within the selected elements, and are designed to achieve the required strength and ductility. The nonductile regions are designed against the demands when overstrength capacities of the plastic hinges are realised. The nonductile regions are designed to remain elastic during strong earthquake shaking while the ductile regions undergo substantial displacements in the inelastic regime [Paulay and Priestley, 1992].

A prescribed minimum vertical steel needs to be provided for flexural design in order to keep the overstrength shear demand minimum [Paulay and Williams, 1980]. An overstrength factor ϕ_o is defined as,

$$\phi_o = \frac{M^o}{M_{code}}, \quad (1.61)$$

where M^o is the overstrength moment capacity. The value of ϕ_o will depend on the grade of reinforcement and the strain level to which it is subjected. To avoid the brittle

shear failure in wall, the shear strength V_{min} in the nonductile regions of the wall, needs to be more than the shear demand at the time of flexural yielding, *i.e.*,

$$V_{min} \geq \phi_o V_{code} . \quad (1.62)$$

The shear demand may be suitably magnified to account for the dynamic effects during strong earthquake shaking.

1.10 SCOPE OF PRESENT STUDY

Based on the above literature review, the behaviour of reinforced concrete structural walls are well understood from experimental and analytical studies, and the failure modes of walls are correlated with the wall characteristics, thus forming the basis of seismic design and detailing. The aim of the present study is to investigate the provisions of the Indian Standards for the design of walls to identify their suitability to capacity design based seismic design. The analytical study examines the capacity design concept for cantilever walls, in multistoreyed building frames. Example walls, designed and detailed as per IS 13920:1993, are analysed in isolation under static lateral loads. These wall sections are checked for compliance with the capacity design philosophy. Finally, the present study aims to propose a capacity-design based seismic design procedure for RC walls in line with the current concrete code IS 456:2000 and the ductile detailing code IS 13920:1993.

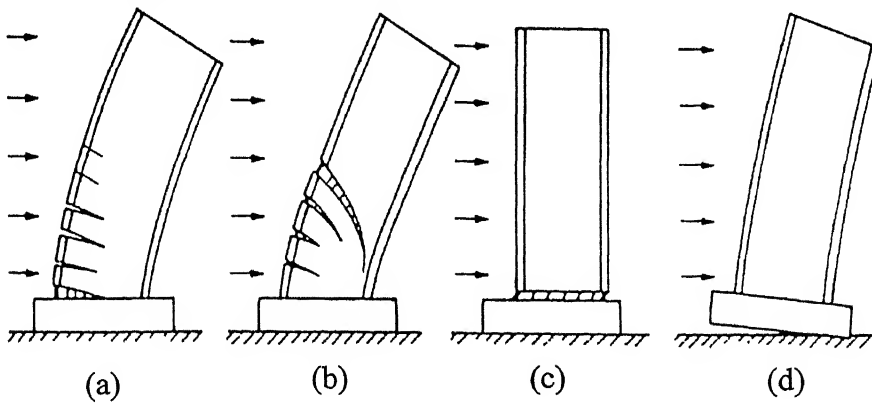


Figure 1.1: Possible modes of failure of slender walls, (a) flexural failure, (b) flexural-shear failure, (c) sliding failure, and (d) overturning failure [Paulay *et. al.*, 1982].

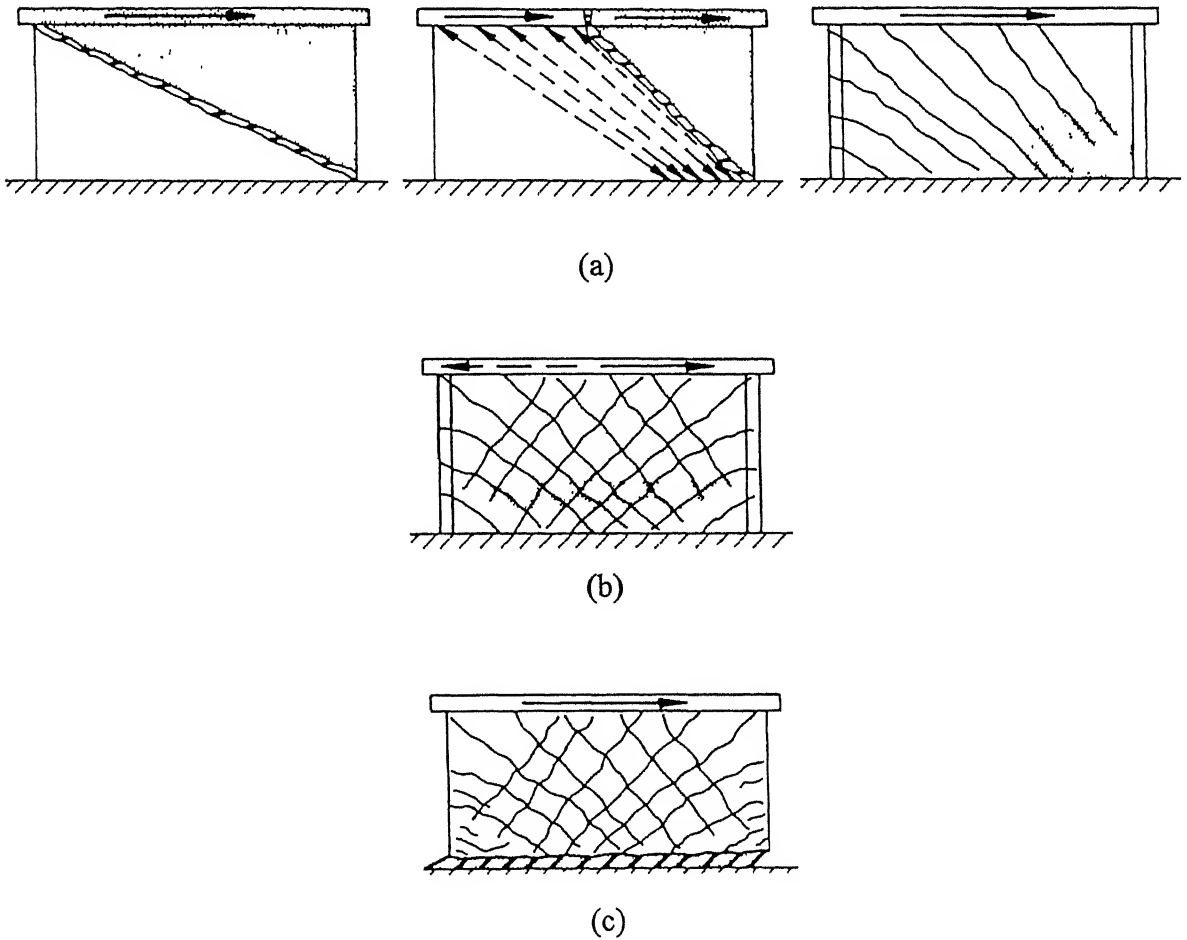
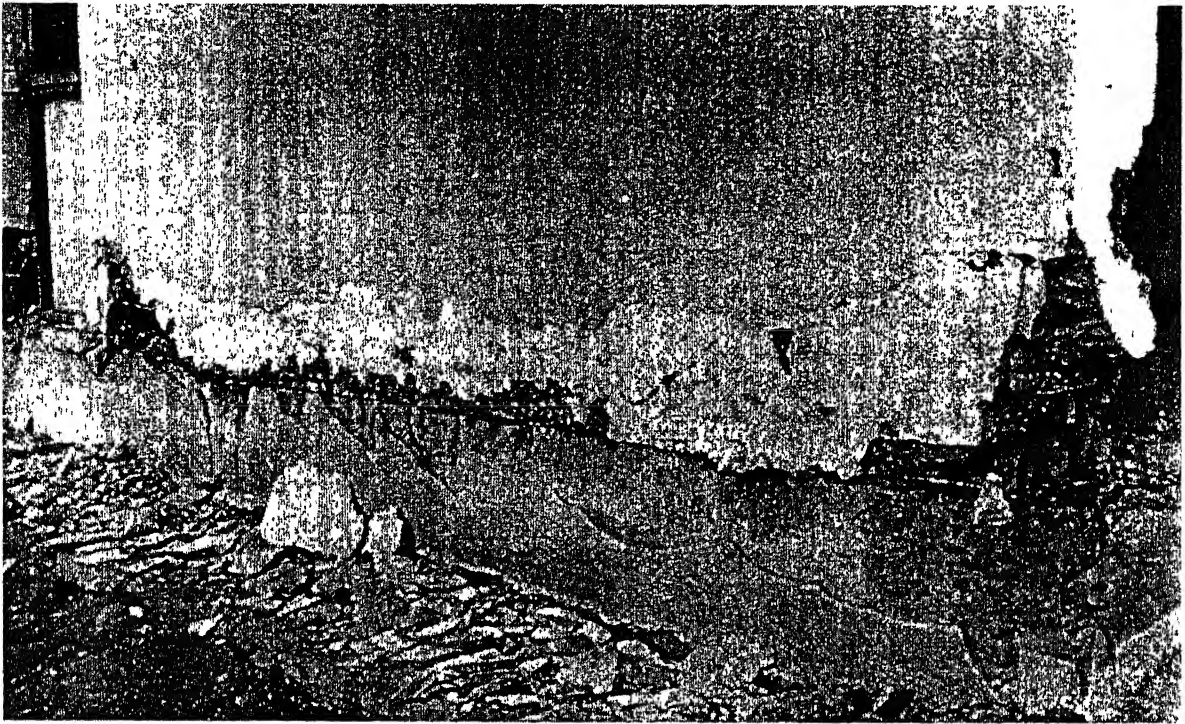


Figure 1.2: Possible modes of failure of squat walls, (a) levels of diagonal tension failure depending on amount of reinforcement, (b) diagonal compression failure, and (c) sliding shear failure [Wakabayashi, 1986].



(a)



(b)



(c)

Figure 1.3: (a) Sliding at construction joint, spalled concrete and buckled edge reinforcement at Canal Beagle [Chile, 1985], Crushing of concrete and buckling of reinforcement in sixteen-storey building [Armenia, 1988], and (c) Diagonal cracking in walls.

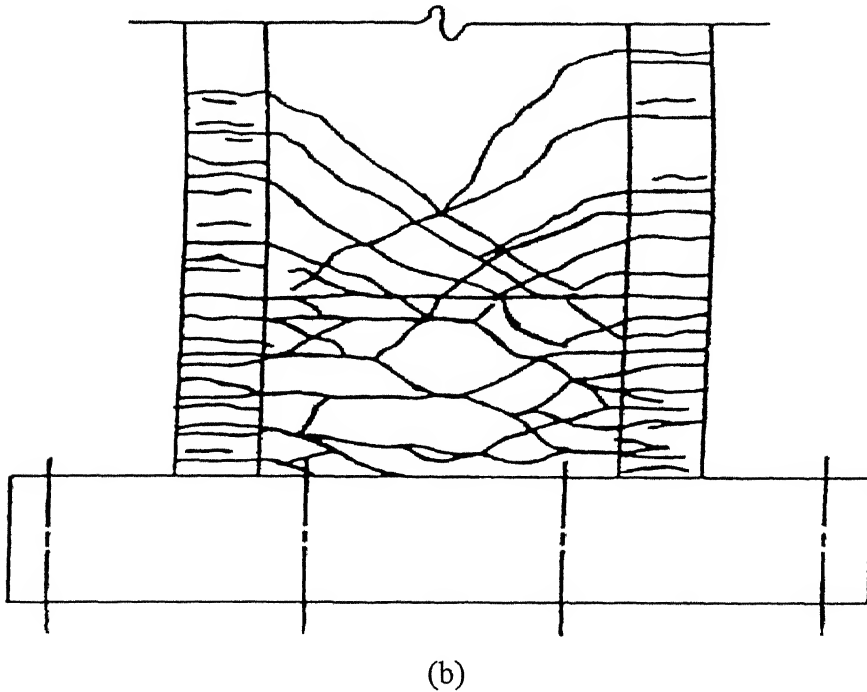
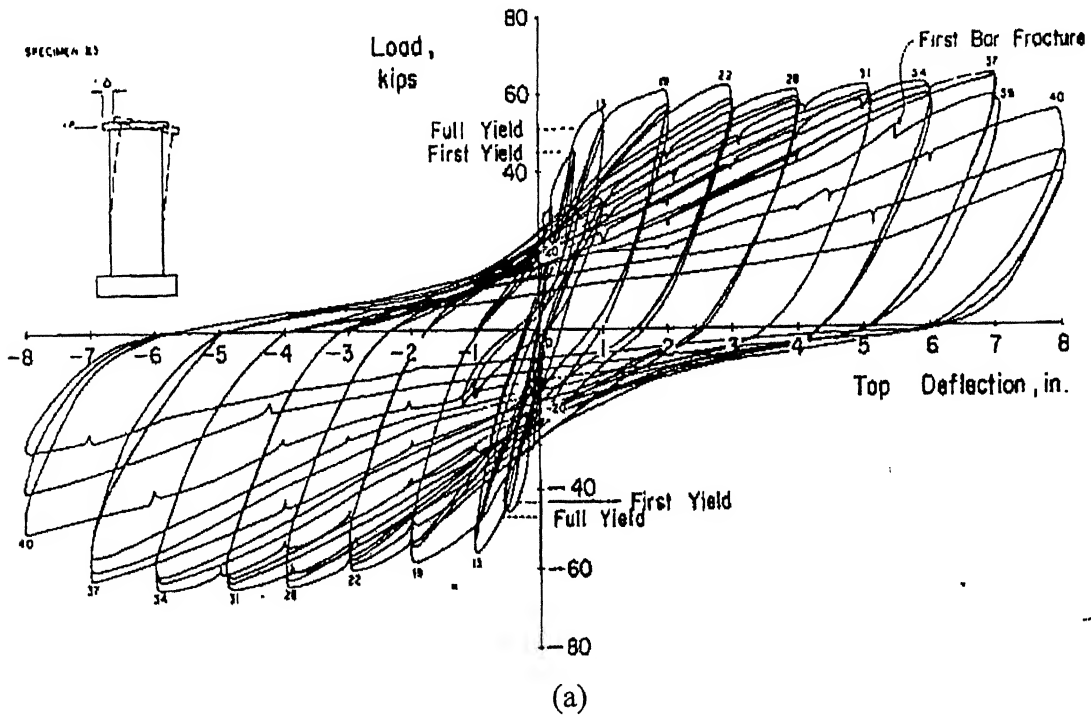


Figure 1.4: Slender RC wall subjected to quasi-static reversed cyclic loading, (a) Load-deformation curve, and (b) Cracking sustained in the lower portion of the wall [ATC 11, 1983].

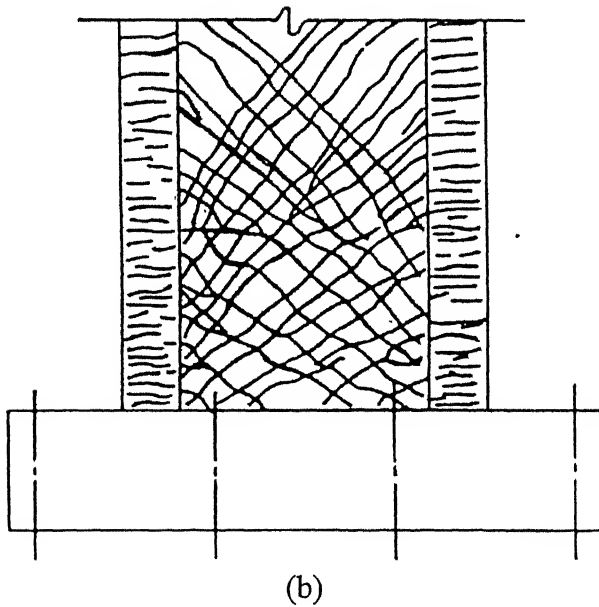
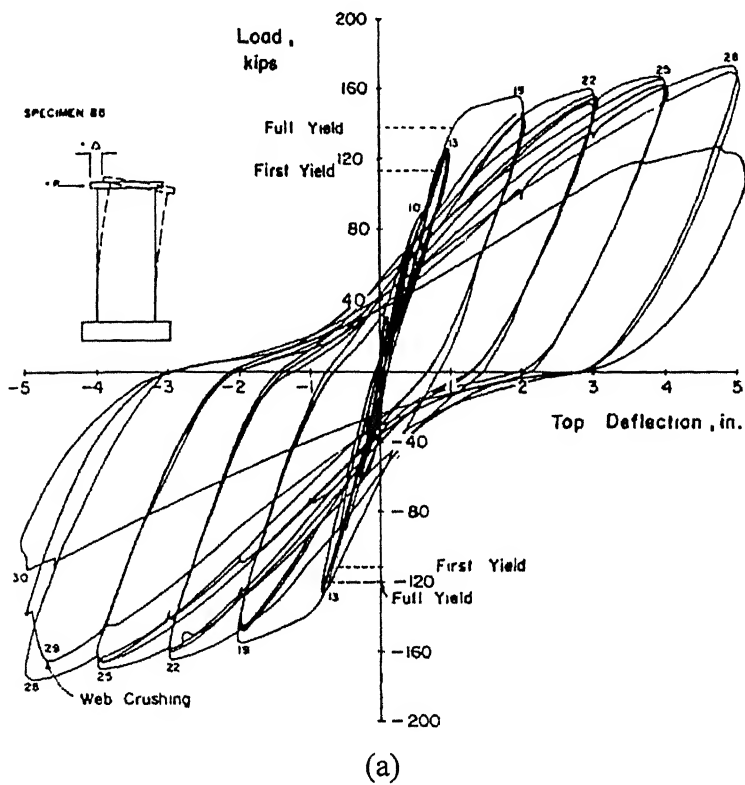


Figure 1.5: Slender RC wall subjected to quasi-static reversed cyclic loading, (a) Load-deformation curve, (b) Cracking sustained in the bottom part of wall [ATC 11, 1983].

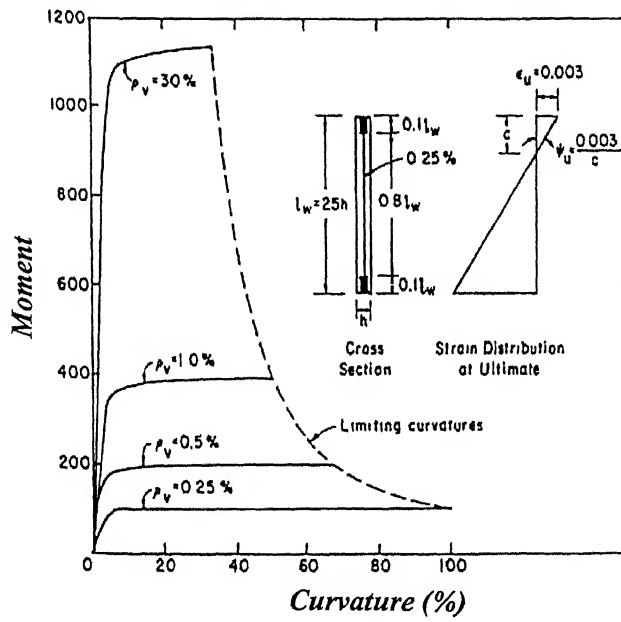
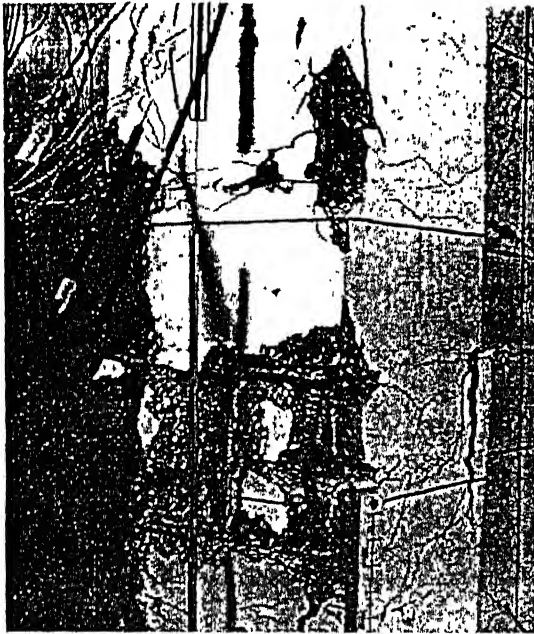
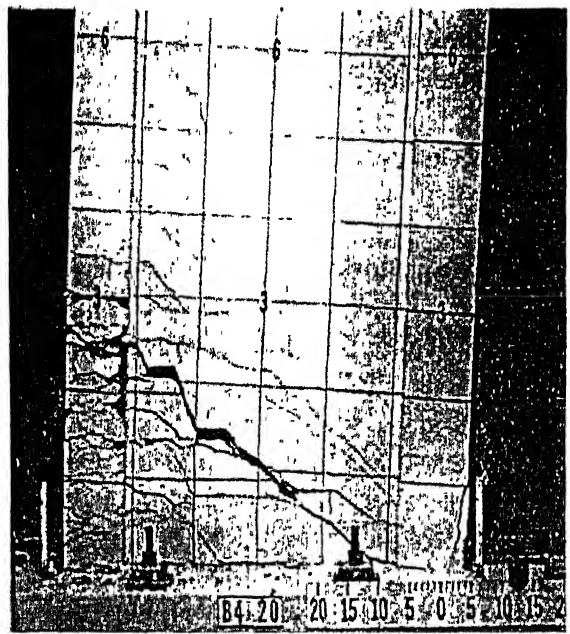


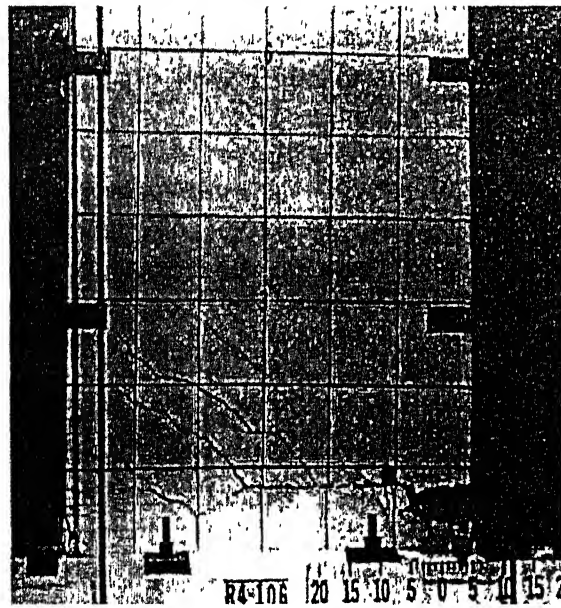
Figure 1.6: Moment curvature diagram of wall with concentrated steel at the ends [Cardenas and Magura, 1973].



(a)



(b)

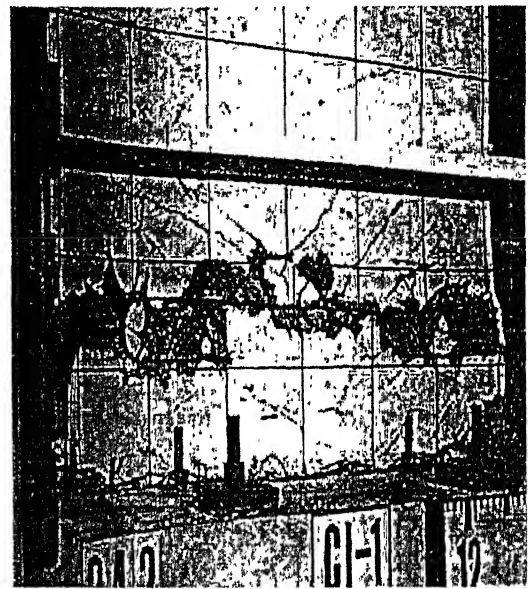


(c)

Figure 1.7: Flexure-dominated failure modes, (a) Buckling of vertical steel, (b) Fracture of vertical steel, and (c) Crushing of concrete [ATC 11, 1983].



(a)



(b)

Figure 1.8: Shear-dominated failure modes, (a) Web Crushing, and (b) Sliding shear [ATC 11, 1983].

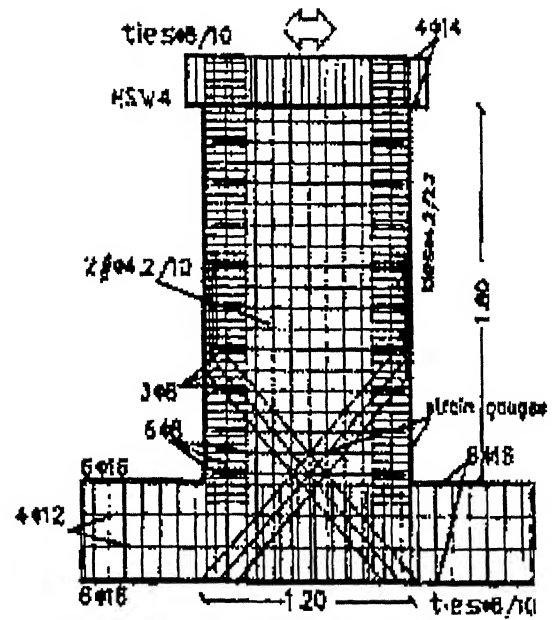
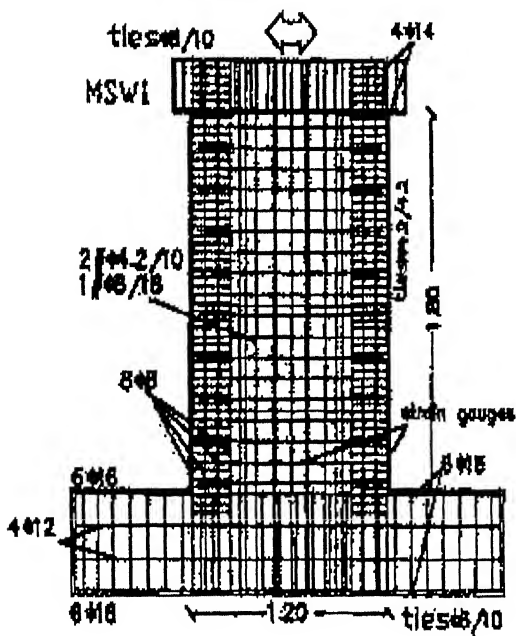


Figure 1.9: Wall specimens with bidirectional reinforcement [Salonikios, 1999].

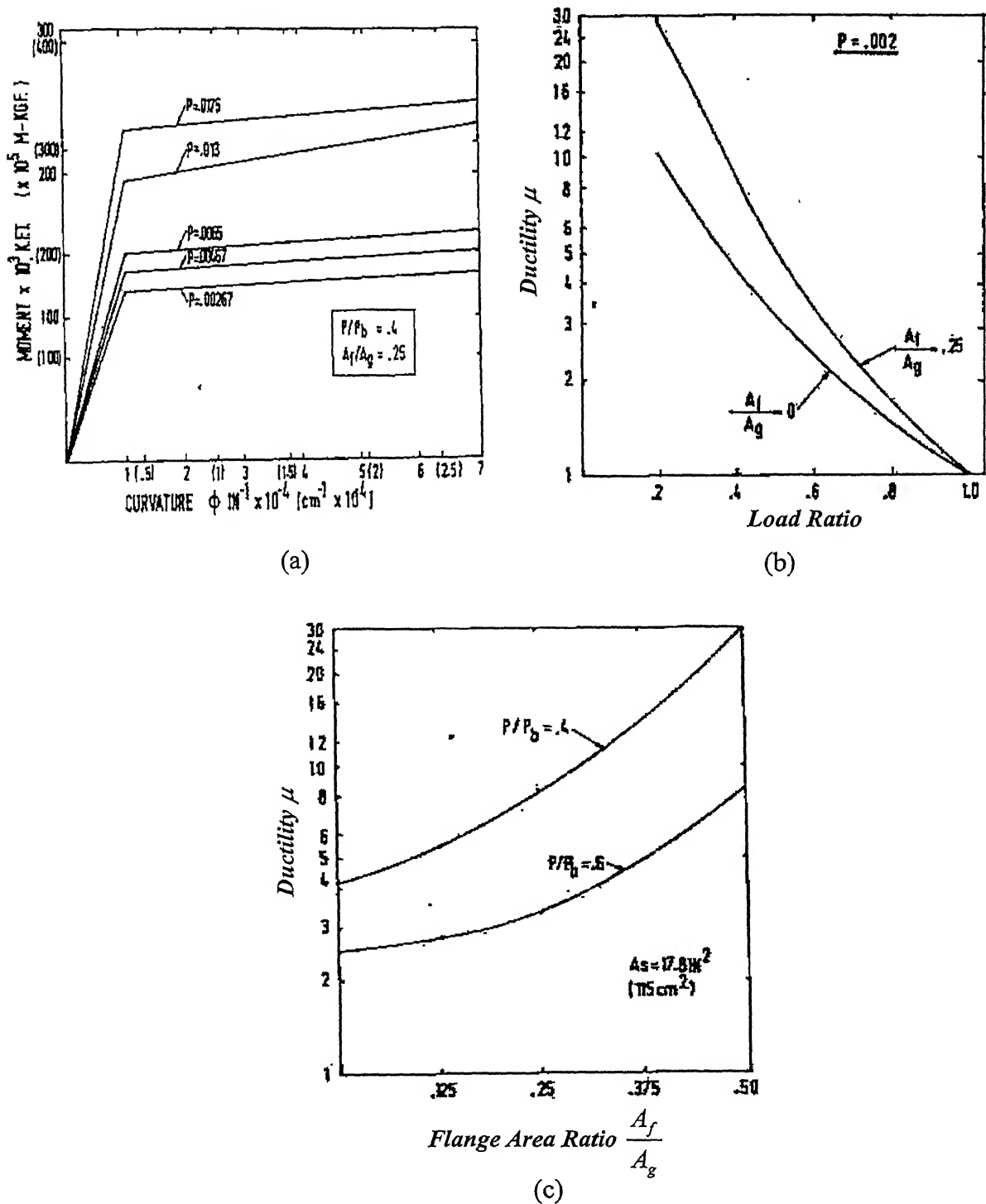


Figure 1.10: (a) Moment curvature diagram for walls, (b) Variation of ductility with load ratio, and (c) Variation of ductility with flange area ratio [Allen *et. al.*, 1973].

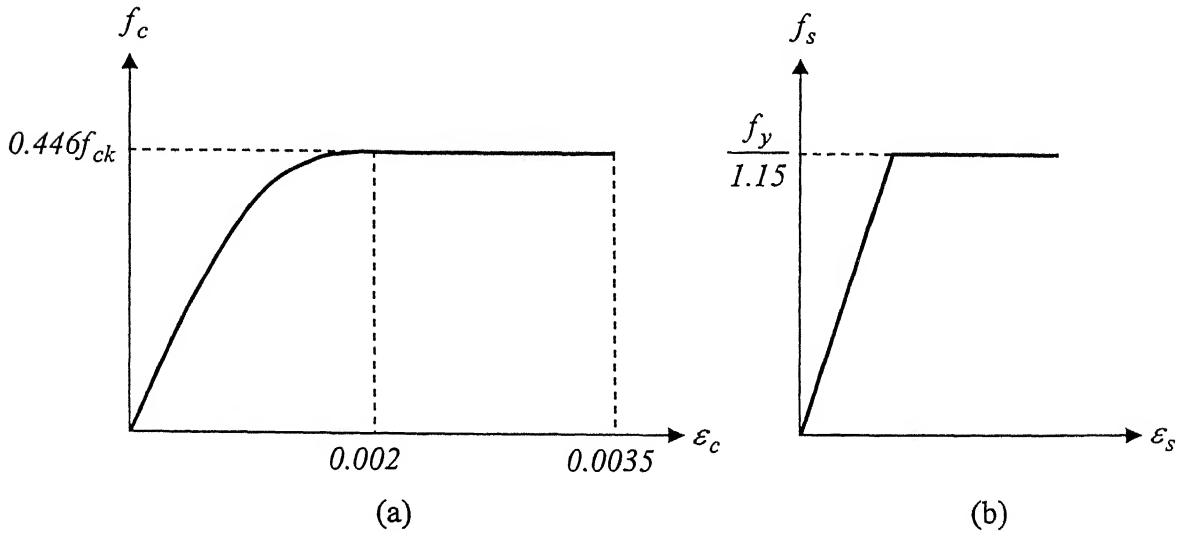


Figure 1.11: Code-specified stress-strain properties for obtaining the design flexural strength of RC wall section, (a) concrete, and (b) steel as per IS 456:2000 [IS 456, 2000].

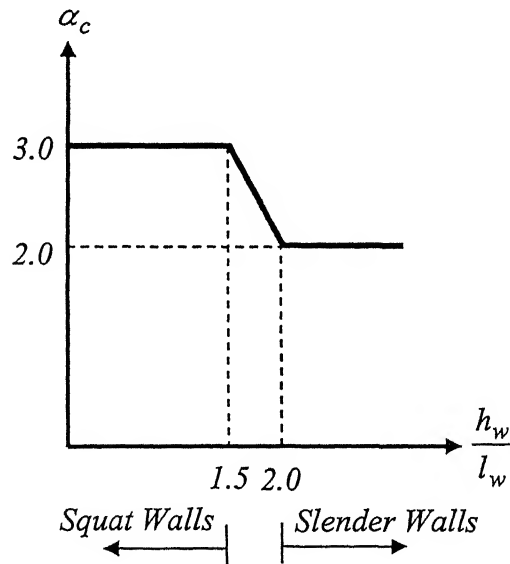


Figure 1.12: Concrete contribution factor for slender and squat walls [ACI 318, 1999].

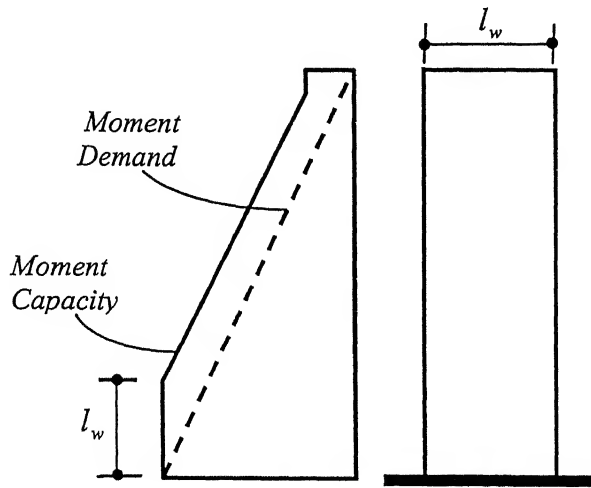


Figure 1.13: Bending moment envelope for design [NZS 3101, 1995].

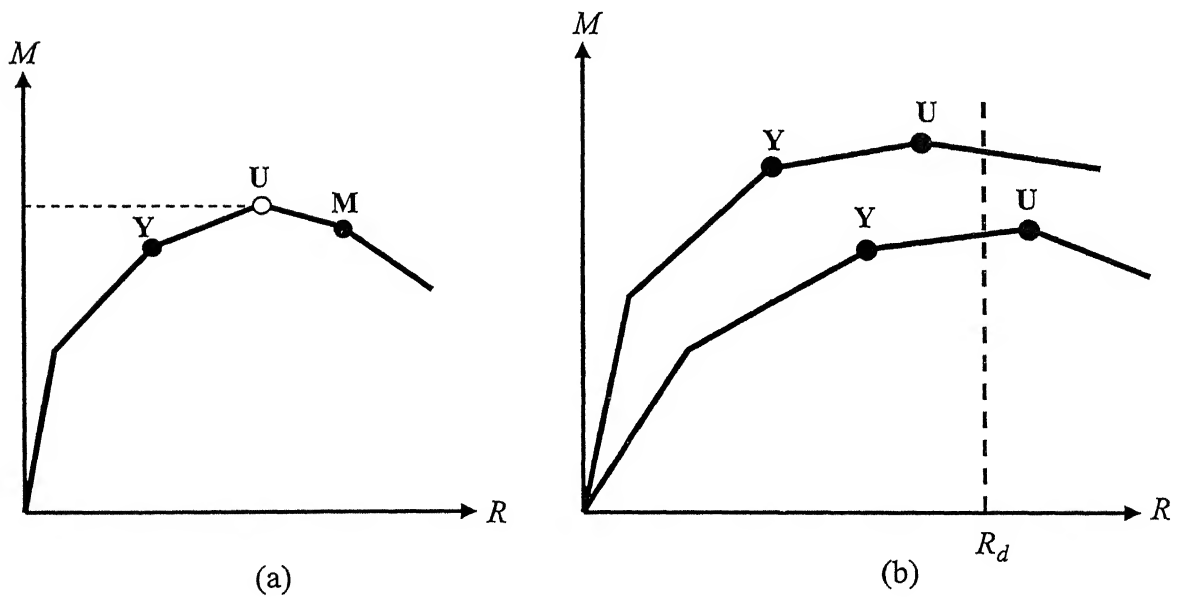


Figure 1.14: (a) Schematic Relation between moment and curvature, and (b) Flexural strengths and Deformations of a wall section with distributed steel [AIJ, 1994].

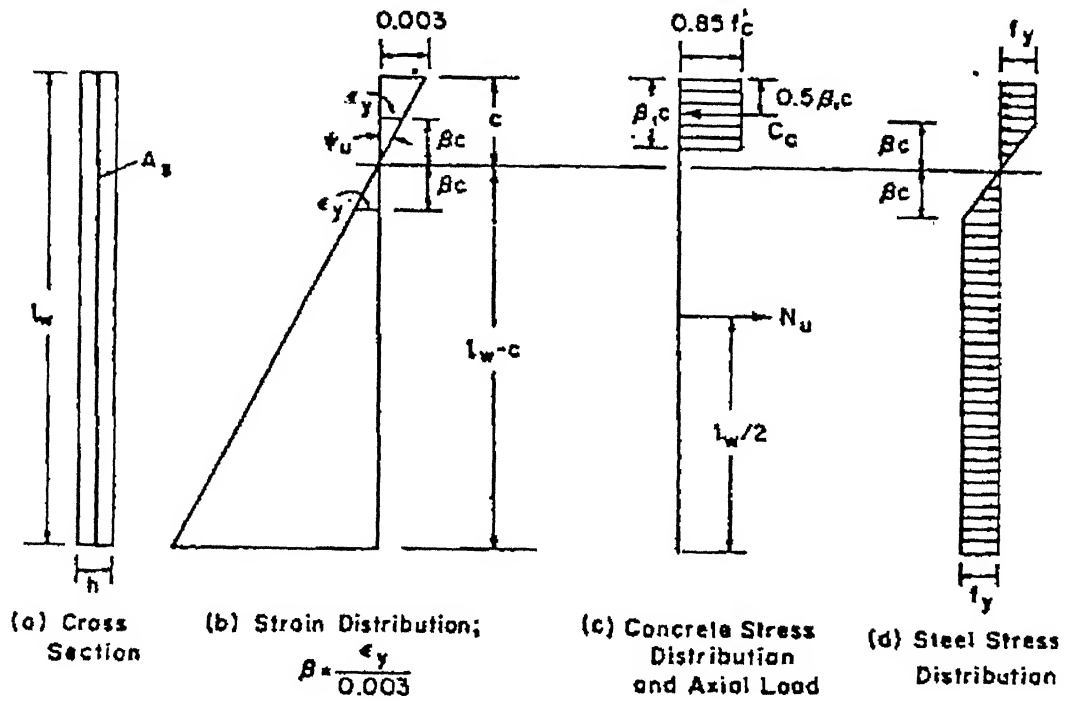


Figure 1.15: Strain and Stress distributions in concrete and steel [ATC 11, 1983].

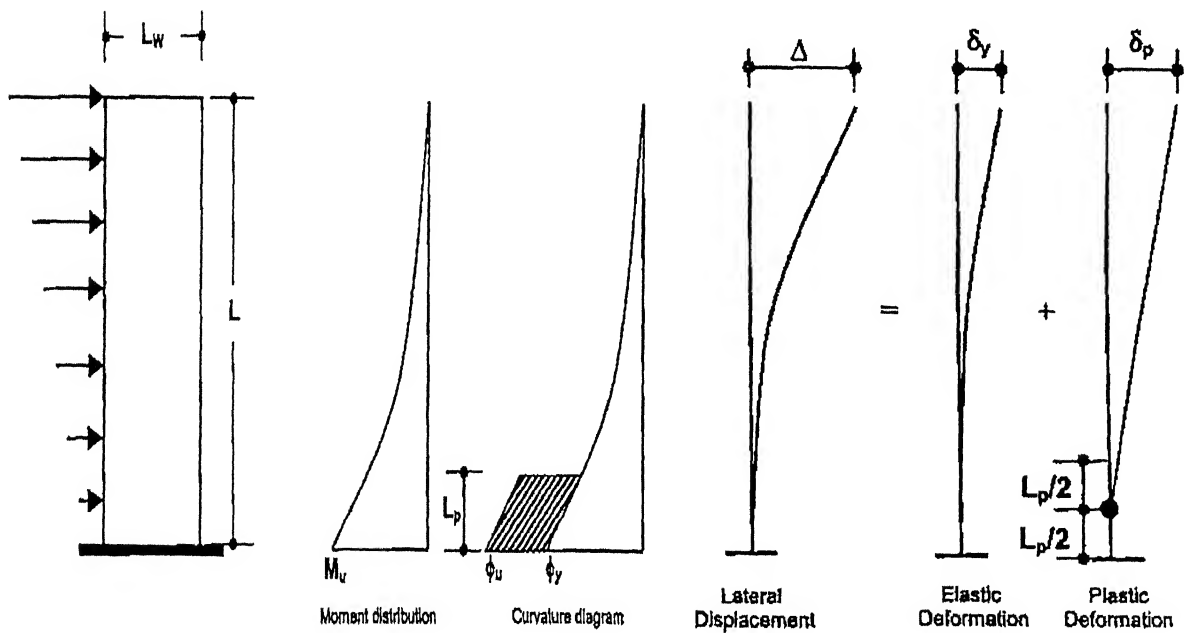


Figure 1.16: Curvature and deformation diagrams for wall [Wallace, 1994].

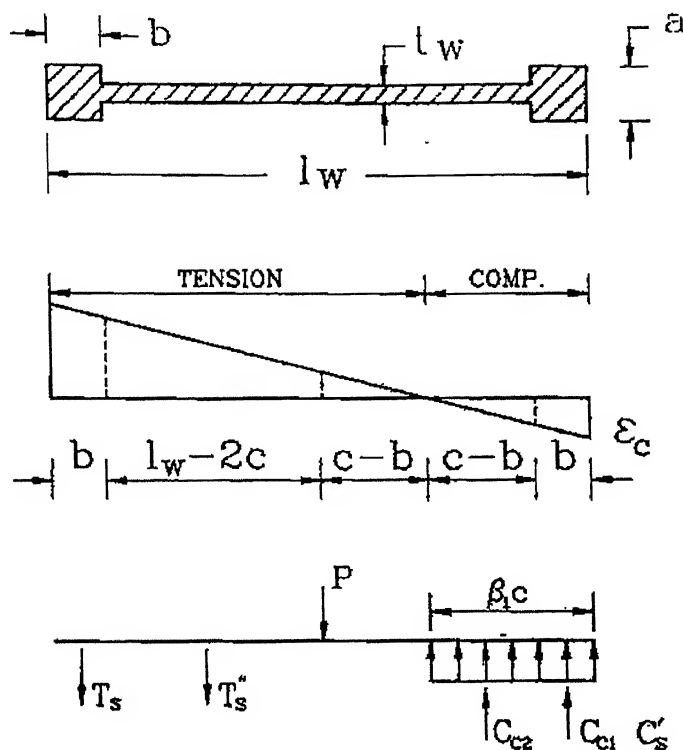


Figure 1.17: Strain and Stress distributions in the proposed design method [Wallace, 1994].

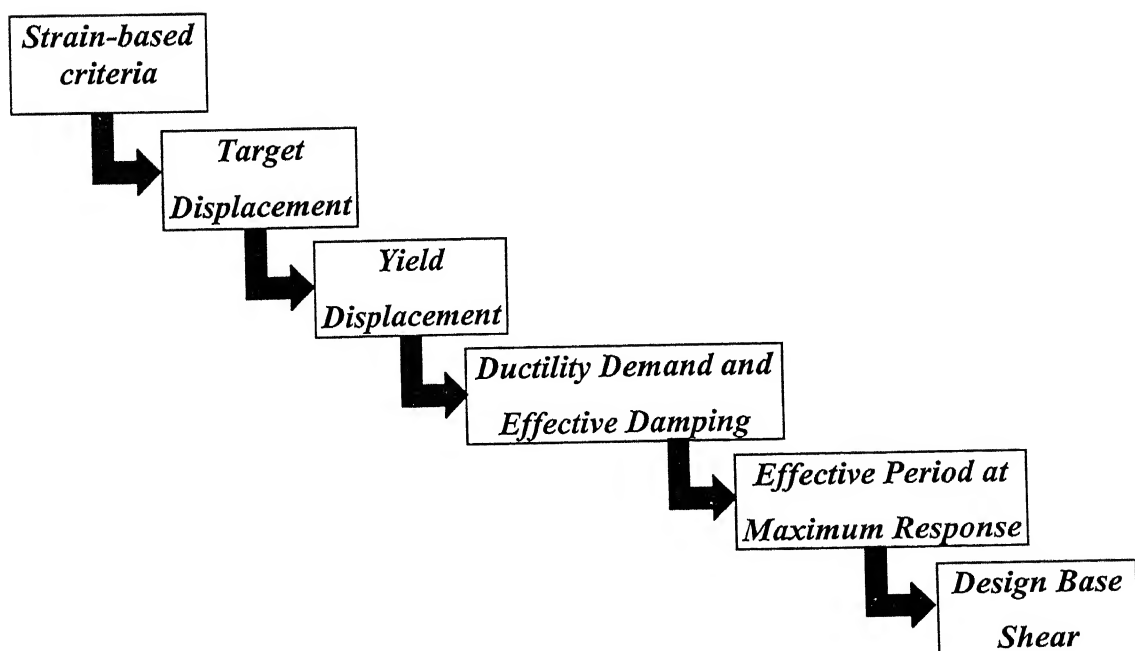


Figure 1.18: Steps in Displacement-Based Design method of walls [Kowalsky, 2001].

Chapter 2

Capacity Design of RC Structural Walls

2.1 INTRODUCTION

In the design of RC structural walls, Indian Codes of Practice [IS 456, 2000; IS 13920, 1993] only feebly link flexure design with shear design. First the design for flexure is performed. Using the percentage of longitudinal steel provided, the design shear stress of concrete is ascertained. This is used in estimating the design shear strength of the section, and ensured to exceed the shear demand obtained from design load combinations. The above procedure does not guarantee that under strong earthquake shaking, the wall section will fail in flexure before the occurrence of brittle shear failure. The development of overstrength plastic moment hinges results in shear demands that often exceed the shear demands estimated from design load combinations based on reduced earthquake forces.

In this chapter, a design procedure that employs the capacity design concept and ensures that premature brittle shear failures are delayed before the occurrence of flexural failure is presented. The provisions for seismic design of RC walls in IS 13920:1993 are investigated. The proposed procedure is a general one and covers RC walls with and without boundary elements.

2.2 OVERSTRENGTH PLASTIC MOMENT CAPACITY

An important input to the Capacity Design Procedure of a RC wall is the estimation of overstrength plastic moment capacity M_{Ω} for the actual axial load (P)

acting on it at overstrength conditions. Since the axial load is a variable, often the full overstrength $P - M_{\Omega}$ interaction curve is derived. In this section the $P - M_{\Omega}$ curves of rectangular RC wall sections are derived. *Appendices A* and *B* provide the expressions of $P - M_{\Omega}$ curves for RC wall sections with boundary elements.

2.2.1 Expressions for P and M_{Ω} for Rectangular Wall Sections

Consider a RC wall section with the following properties: l and t are the length of the wall and the thickness respectively; y_{st} is the location of the steel bar from the edge of compression face of the section and A_{st} is its area; x is the depth of neutral axis from the geometric centroidal axis; and f_{ck} is the grade of concrete. For unconfined concrete, the ultimate strain is taken as $(\varepsilon_c)_{\max} = 0.0035$ (Figure 2.1a). Existing models are used for the stress-strain curves of confined concrete (Figure 2.1a) [Razvi and Saatcioglu, 1999a] and HYSD bars (Figure 2.1b) [Dasgupta, 2000].

The $P - M_{\Omega}$ interaction curve for wall sections with or without boundary elements consists of four segments, namely fully uncracked section region AB with compressive failure, partially cracked region BC with compression failure, partially cracked section region CD with tensile failure and fully cracked section region DE with tensile failure (Figure 2.2). Point C is the balanced failure point with the both concrete and steel simultaneously reaching their main strain values $(\varepsilon_{cc})_{\max}$ and $(\varepsilon_s)_{\max}$ respectively.

In region AB, the depth x of the neutral axis (NA) from the geometric centroidal axis (GCA) of the section, varies from a very large distance outside the section to the edge of the section on the tension face, i.e., $-\infty < x \leq -0.5l$. The failure of the section occurs by the strain in the extreme compression fibre of the core concrete reaching the

maximum confined concrete strain of $(\varepsilon_{cc})_{max}$ with the whole section in compression. In region BC, x varies from the edge of the section on the tension face to a balanced depth x_b , *i.e.*, $-0.5l < x \leq x_b$. Here, x_b corresponds to the balanced point described above. The failure is again by the extreme compression fibre of the core concrete reaching $(\varepsilon_{cc})_{max}$, but a part of the section is in tension. In region CD, x varies from the balanced depth x_b to the edge of the section on the compression face, *i.e.*, $x_b < x \leq 0.5l$. Here, the section fails by the strain in the extreme layer of steel on the tension side reaching the ultimate rupture strain $(\varepsilon_s)_{max}$. In region DE, x varies from the edge of the section on the compression face to a large distance away from the section, *i.e.*, $0.5l < x < \infty$. For this region, the section fails by steel attaining the ultimate rupture strain $(\varepsilon_s)_{max}$.

2.2.1.1 Two Curtains of Vertical Reinforcement

The expressions for P , M_Ω and ϕ_{max} for RC wall sections with two curtains of vertical reinforcement (Figures 2.3 and 2.4) are given below:

For segment AB:

$$(P)_{AB} = 2(P_{cv}^w + P_{cv}^l + P_{cr}) + \sum_{i=1}^{nw} A_{si} \sigma_{si}, \quad (2.1)$$

$$(M_\Omega)_{AB} = 2\left(\left\{\sum P_{cv}^w h_{cv}^w\right\} + \left\{\sum P_{cv}^l h_{cv}^l\right\} + M_{cr}\right) + \sum_{i=1}^{nw} A_{si} \sigma_{si} (0.5l - y_{si}), \text{ and} \quad (2.2)$$

$$(\phi_{max})_{AB} = \frac{|(\varepsilon_{cc})_{max}|}{(-0.5l - x)}, \quad (2.3)$$

where

$$P_{cr} = \begin{cases} 0.5(f_{2c} + f_{3c})l_o(0.5t_o) & \text{for } \varepsilon_2 < \varepsilon_{lc} \\ f_{cr}^t + f_{cr}^p & \text{for } \varepsilon_3 < \varepsilon_{lc} < \varepsilon_2 \end{cases}, \quad (2.4)$$

$$f_{cr}^t = 0.5(f_{3c} + f_{cc})(0.5l_o - x - y_c)(0.5t_o), \quad (2.5)$$

$$f_{cr}^p = f_c(y_c + x + 0.5l_o)(0.5t_o), \quad (2.6)$$

$$M_{cr} = \begin{cases} 0.5(f_{2c} + f_{3c})l_o(0.5t_o) \left[\frac{l_o}{6} \left(\frac{f_{2c} - f_{3c}}{f_{2c} + f_{3c}} \right) \right] & \text{for } \varepsilon_2 < \varepsilon_{lc} \\ f_{cr}^t h_{cr}^t + f_{cr}^p h_{cr}^p & \text{for } \varepsilon_3 < \varepsilon_{lc} < \varepsilon_2 \end{cases}, \quad (2.7)$$

$$h_{cr}^t = (-x - y_c) - \frac{(0.5l_o - x - y_c)}{3} \left[\frac{f_{cc} + 2f_{3c}}{f_{cc} + 2\sigma_{3c}} \right], \quad (2.8)$$

$$h_{cr}^p = -p_l - x, \quad (2.9)$$

$$P_{cv}^w = \begin{cases} 0 & \text{for } \varepsilon_2 < \varepsilon_{lc} \\ 0.5(0.2f_{co} + f_{1a})(0.5l + x + y_d)g & \text{for } \varepsilon_2 < -\varepsilon_{02} < \varepsilon_1 \\ 0.5(0.2f_{co} + f_{1a})(0.5l + x + y_d)g & \text{for } \varepsilon_1 < -\varepsilon_{01} \\ P_{cv}^{tw} + P_{cv}^{pw} & \text{for } \varepsilon_2 < -\varepsilon_{01} < \varepsilon_1 \\ P_{cv}^{tw} + P_{cv}^{pw} & \text{for } \varepsilon_3 < -\varepsilon_{01} < \varepsilon_2 \end{cases}, \quad (2.10)$$

$$P_{cv}^{tw} = -0.408f_{ck}(y_d - y)g, \quad (2.11)$$

$$P_{cv}^{pw} = f_c(0.5l + x + y)g, \quad (2.12)$$

$$P_{cv}^l = \begin{cases} 0 & \text{for } \varepsilon_2 < \varepsilon_{lc} \\ 0.5(0.2f_{co} + f_{1a})(0.5l + x + y_d)(0.5t - g) & \text{for } \varepsilon_2 < -\varepsilon_{02} < \varepsilon_1 \\ 0.5(f_{1a} + f_{2a})(0.5t - g)g & \text{for } \varepsilon_1 < -\varepsilon_{01} \\ P_{cv}^{lt} + P_{cv}^{lp} & \text{for } \varepsilon_2 < -\varepsilon_{01} < \varepsilon_1 \\ f_c g(0.5t - g) & \text{for } \varepsilon_3 < -\varepsilon_{01} < \varepsilon_2 \end{cases}, \quad (2.13)$$

$$P_{cv}^{lt} = 0.5(0.2f_{co} + f_2)(-x - y - 0.5l + g)(0.5t - g), \quad (2.14)$$

$$P_{cv}^{lp} = f_c(0.5l + x + y)(0.5t - g), \quad (2.15)$$

$$h_{cv}^w = \begin{cases} 0 & \text{for } \varepsilon_1 < -\varepsilon_{02} \\ 0.5l - \frac{(0.5l + x + y_d)}{3} \left[\frac{f_{1a} + 0.4f_{co}}{f_{1a} + 0.2f_{co}} \right] & \text{for } \varepsilon_2 < -\varepsilon_{02} < \varepsilon_1, \\ 0.5l - \frac{(0.5l + x + y_d)}{3} \left[\frac{f_{1a} + 0.4f_{co}}{f_{1a} + 0.2f_{co}} \right] & \text{for } \varepsilon_1 < -\varepsilon_{01} \end{cases} \quad (2.16)$$

$$\Sigma(P_{cv}^w h_{cv}^w) = P_{cv}^{tw} h_{cv}^{tw} + P_{cv}^{pw} h_{cv}^{pw}, \quad \text{for } \varepsilon_2 < -\varepsilon_{01} < \varepsilon_1, \varepsilon_3 < -\varepsilon_{01} < \varepsilon_2, \quad (2.17)$$

$$h_{cv}^{tw} = -x - 0.389y_d - 0.611y, \quad (2.18)$$

$$h_{cv}^{pw} = p_l - x - y, \quad (2.19)$$

$$h_{cv}^l = \begin{cases} 0 & \text{for } \varepsilon_2 < \varepsilon_{lc} \\ 0.5l - \frac{(0.5l + x - y_d)}{3} \left[\frac{f_{1a} + 0.4f_{co}}{f_{1a} + 0.2f_{co}} \right] & \text{for } \varepsilon_2 < -\varepsilon_{02} < \varepsilon_1 \\ 0.5l - \frac{g}{3} \left[\frac{f_{1a} + 2f_{2a}}{f_{1a} + f_{2a}} \right] & \text{for } \varepsilon_1 < -\varepsilon_{01} \\ p_l - x - y & \text{for } \varepsilon_3 < -\varepsilon_{01} < \varepsilon_2 \end{cases}, \quad (2.20)$$

$$\Sigma(P_{cv}^l h_{cv}^l) = P_{cv}^{tl} h_{cv}^{tl} + P_{cv}^{pl} h_{cv}^{pl} \quad \text{for } \varepsilon_2 < -\varepsilon_{01} < \varepsilon_1, \quad (2.21)$$

$$h_{cv}^{tl} = (-x - y) - \frac{(-x - y - 0.5l + g)}{3} \left[\frac{f_{co} + 2f_{2a}}{f_{co} + f_{2a}} \right], \quad (2.22)$$

$$h_{cv}^{pl} = p_l - x - y, \quad (2.23)$$

$$y = \varepsilon_{01} \left(\frac{0.5l - x}{|\varepsilon_1|} \right), \quad (2.24)$$

$$y_c = \varepsilon_{lc} \left(\frac{0.5l - x}{\varepsilon_2} \right), \quad (2.25)$$

$$y_d = \varepsilon_{02} \left(\frac{0.5l - x}{\varepsilon_4} \right), \quad (2.26)$$

σ_{si} is the stress in steel corresponding to strain ε_{si} from Figure 2.1b, and

$$\varepsilon_{si} \text{ is the strain in steel} = \varepsilon_1 \left(\frac{0.5l - x - y_{si}}{0.5l - x} \right).$$

For segment BCD:

$$(P)_{BCD} = 2(P_{cv}^w + P_{cv}^l + P_{cv}^2 + P_{cr}) + \sum_{i=1}^{nw} A_{si} \sigma_{si}, \quad (2.27)$$

$$(M_{\Omega})_{BCD} = 2 \left(P_{cv}^w h_{cv}^w + \left\{ \sum P_{cv}^I h_{cv}^I \right\} + \left\{ \sum P_{cv}^2 h_{cv}^2 \right\} + M_{cr} \right) + \sum_{i=1}^{nw} A_{si} \sigma_{si} (0.5l - y_{si}), \quad (2.28)$$

$$(\phi_{max})_{BCD} = \frac{|(\varepsilon_{cc})_{max}|}{(-0.5l - x)}, \quad (2.29)$$

where

$$P_{cr} = \begin{cases} f_{cr}^t + f_{cr}^p & \text{for } \varepsilon_3 < \varepsilon_{lc} < \varepsilon_2, \varepsilon_2 < 0 \\ f_{cr}^t + f_{cr}^{pp} & \text{for } \varepsilon_3 < \varepsilon_{lc} < \varepsilon_2, \varepsilon_2 \geq 0 \end{cases}, \quad (2.30)$$

$$f_{cr}^t = 0.5(f_{3c} + f_{cc})(0.5l_o - x - y_c)(0.5t_o), \quad (2.31)$$

$$f_{cr}^p = f_c(y_c + x + 0.5l_o)(0.5t_o), \quad (2.32)$$

$$f_{cr}^{pp} = f_c y_c (0.5t_o), \quad (2.33)$$

$$M_{cr} = \begin{cases} f_{cr}^t h_{cr}^t + f_{cr}^{pp}(-p_l - x) & \text{for } \varepsilon_3 < \varepsilon_{lc} < \varepsilon_2, \varepsilon_2 < 0 \\ f_{cr}^t h_{cr}^t + f_{cr}^{pp}(-p_l - x) & \text{for } \varepsilon_3 < \varepsilon_{lc} < \varepsilon_2, \varepsilon_2 \geq 0 \end{cases}, \quad (2.34)$$

$$h_{cr}^t = (-x - y_c) - \frac{(0.5l_o - x - y_c)}{3} \left[\frac{f_{cc} + 2f_{3c}}{f_{cc} + f_{3c}} \right], \quad (2.35)$$

$$P_{cv}^w = -0.36 f_{ck} y_d g, \quad (2.36)$$

$$P_{cv}^I = \begin{cases} f_c(-x - 0.5l + g)g & \text{for } \varepsilon_3 < -\varepsilon_{02} < \varepsilon_2, \varepsilon_2 < 0 \\ 0 & \text{for } \varepsilon_3 < -\varepsilon_{02} < \varepsilon_2, \varepsilon_2 > 0 \end{cases}, \quad (2.37)$$

$$h_{cv}^w = -x - 0.42 y_d, \quad (2.38)$$

$$h_{cv}^I = \begin{cases} p_l - x - y & \text{for } \varepsilon_3 < -\varepsilon_{02} < \varepsilon_2, \varepsilon_2 < 0 \\ 0 & \text{for } \varepsilon_3 < -\varepsilon_{02} < \varepsilon_2, \varepsilon_2 > 0 \end{cases}, \quad (2.39)$$

σ_{si} is the stress in steel corresponding to strain ε_{si} from Figure 2.1b, and

$$\varepsilon_{si} \text{ is the strain in steel} = \varepsilon_l \left(\frac{0.5l - x - y_{si}}{0.5l - x} \right). \quad (2.40)$$

For segment DE:

$$(P)_{DE} = \sum_{i=1}^{nw} A_{si} \sigma_{si}, \text{ and} \quad (2.41)$$

$$(M_{\Omega})_{DE} = \sum_{i=1}^{nw} A_{si} \sigma_{si} (0.5l - y_{si}), \quad (2.42)$$

where

σ_{si} is the stress in steel corresponding to strain ε_{si} from Figure 2.1b, and

$$\varepsilon_{si} \text{ is the strain in steel} = \varepsilon_l \left(\frac{0.5l - x - y_{si}}{0.5l - x} \right). \quad (2.43)$$

2.2.1.2 One Curtain of Vertical Reinforcement

The expressions for P , M_{Ω} and ϕ_{max} for RC wall sections with a single curtain of vertical reinforcement (Figure 2.3) are given below:

For segment AB:

$$(P)_{AB} = P_{cv}^w + \sum_{i=1}^{nw} A_{si} \sigma_{si}, \quad (2.44)$$

$$(M_{\Omega})_{AB} = \sum P_{cv}^w h_{cv}^w + \sum_{i=1}^{nw} A_{si} \sigma_{si} (0.5l - y_{si}), \text{ and} \quad (2.45)$$

$$(\phi_{max})_{AB} = \frac{|\varepsilon_{02}|}{(-0.5l - x)}, \quad (2.46)$$

where

$$P_{cv}^w = \begin{cases} 0.5(0.2f_{co} + f_{la})(0.5l + x + y_d) & \text{for } \varepsilon_1 < -\varepsilon_{01} \\ -0.408f_{ck}(y_d - y) + f_c(0.5l + x + y) & \text{for } \varepsilon_2 < -\varepsilon_{01} < \varepsilon_1 \end{cases}, \quad (2.47)$$

$$\sum P_{cv}^w h_{cv}^w = \begin{cases} 0.5(0.2f_{co} + f_{la})(0.5l + x + y_d) h_{cv}^w & \text{for } \varepsilon_1 < -\varepsilon_{01} \\ -0.4f_{ck}(y_d - y)gh_{cv}^{tw} + f_c(0.5l + x + y)gh_{cv}^{pw} & \text{for } \varepsilon_2 < -\varepsilon_{01} < \varepsilon_1 \end{cases}, \quad (2.48)$$

$$h_{cv}^w = 0.5l - \frac{(0.5l + x + y_d)}{3} \left[\frac{f_{la} + 0.4f_{co}}{f_{la} + 0.2f_{co}} \right], \quad (2.49)$$

$$h_{cv}^{tw} = -x - 0.389y_d - 0.611y, \quad (2.50)$$

$$h_{cv}^{pw} = p_l - x - y, \quad (2.51)$$

where

σ_{si} is the stress in steel corresponding to strain ε_{si} from Figure 2.1b, and

$$\varepsilon_{si} \text{ is the strain in steel} = \varepsilon_l \left(\frac{0.5l - x - y_{si}}{0.5l - x} \right). \quad (2.52)$$

For segment BCD:

$$(P)_{BCD} = P_{cv}^w + \sum_{i=1}^{nw} A_{si} \sigma_{si}, \quad (2.53)$$

$$(M_{\Omega})_{BCD} = \sum P_{cv}^w h_{cv}^w + \sum_{i=1}^{nw} A_{si} \sigma_{si} (0.5l - y_{si}), \text{ and} \quad (2.54)$$

$$(\phi_{max})_{BCD} = \frac{|\varepsilon_{02}|}{(-0.5l - x)}, \quad (2.55)$$

where

$$P_{cv}^w = -0.36f_{ck}y_d t, \quad (2.56)$$

$$h_{cv}^w = -x - 0.42y_d, \quad (2.57)$$

σ_{si} is the stress in steel corresponding to strain ε_{si} from Figure 2.1b, and

$$\varepsilon_{si} \text{ is the strain in steel} = \varepsilon_l \left(\frac{0.5l - x - y_{si}}{0.5l - x} \right). \quad (2.58)$$

2.2.2 Step-wise Procedure for Obtaining $P - M_{\Omega}$ Curves

The overstrength $P - M_{\Omega}$ interaction curve of the RC wall section (Figure 2.2) is obtained by the following step-wise procedure:

Step 1: Model the wall section as in Figure 2.5 or as in Figure 2.5, depending on the

number of curtains of vertical steel in the web.

Step 2: Choose the depth of neutral axis x . x is varied from $-\infty$ to $+\infty$. When x is in the range $[-5l, +5l]$, a large number of values of x may be chosen to obtain the smooth $P - M_{\Omega}$ curves.

Step 3: Identify the region in which x lies, i.e., $-\infty < x \leq -0.5l$ for region AB, $-0.5l < x \leq x_b$ for region BC, $x_b < x \leq 0.5l$ for region CD and $0.5l < x < +\infty$ for segment DE.

Step 4: Calculate P and M_{Ω} using the expressions given in Section 2.2.1 for rectangular wall sections and in Appendices A and B for RC wall sections with boundary elements on the $P - M_{\Omega}$ interaction curves.

Step 5: Normalize P with respect to $f_{ck}tl$ and M_{Ω} with $f_{ck}tl^2$. This gives a point on the $P - M_{\Omega}$ interaction curve.

Step 6: Change the value of x and repeat the procedure from *Step 2* until the curve is generated for all the four regions AB, BC, CD and DE.

For the ascending curved portion of confined concrete stress-strain diagram, 16-point Gauss-Legendre quadrature formulae are used for numerical integration. Although a closed form solution of the integral is obtainable using hypergeometric function, the numerical method is preferred due to some constraints on the values of the parameters that make the computation of the functions complicated.

2.3 PROPOSED CAPACITY DESIGN METHOD

The proposed method of shear design of an RC section, based on capacity design philosophy, is summarised in the following steps:

Step 1: Generate the overstrength axial load P -moment M_{Ω} interaction curve by

applying a partial factor of safety γ_m of 1.0 for concrete and $\frac{1}{1.25}$ for steel on their respective characteristic strengths, using the procedure described in Section 2.2.

Step 2: Estimate the overstrength moment capacity (M_Ω) from the $P_\Omega - M_\Omega$ curve corresponding to the actual axial load on the section.

Step 3: Calculate the shear demand (V_Ω), corresponding to M_Ω , as

$$V_\Omega = \frac{M_\Omega}{l^*}, \quad (2.59)$$

where l^* is equivalent cantilever length $= \frac{M_D}{V_D}$, M_D and V_D being the design moment and shear force respectively from the analysis of the whole building under the prescribed design load combination.

Step 4: Calculate the design shear strength V_u of the section as,

$$V_u = V_{uc} + V_{us}, \quad (2.60)$$

where V_{uc} and V_{us} are the concrete and steel contributions to the design shear strengths given by Eqs.1.5 and 1.6 respectively.

Step 5: If $V_\Omega > V_u$, the additional horizontal steel $(A_{sv})_{extra}$ required in the section for the extra shear force is given by,

$$(A_{sv})_{extra} = \frac{(V_\Omega - V_u)}{0.87f_y \left(\frac{d}{s_v} \right)}, \quad (2.61)$$

else if $V_\Omega < V_u$, the section has adequate shear strength.

2.4 NUMERICAL STUDY

RC wall sections of the eight frame-wall buildings with identical plans (Figure 2.6), are studied along with the isolated wall section of a two-storeyed building (Figure 2.7) taken from literature [Medhekar and Jain, 1993]. Apart from the overstrength shear demand V_{Ω} , code shear demand V_{Ω}^c and inelastic shear demand V_{Ω}^p from pushover analysis are also determined as discussed in the following sections.

The geometry and reinforcement details of these walls are shown in Tables 3.1. The compliance, or otherwise, of these walls with the capacity design for shear discussed in Section 2.3, is investigated here. While the shear strength of the section is calculated by the procedure described in Step 4 of Section 2.3, the shear demand is estimated by three methods as follows:

- (a) Overstrength Shear Demand V_{Ω} given by Step 3 of Section 2.3,
- (b) Code approach of estimating the shear demand given by,

$$V_{\Omega}^c = \frac{1.4M_u}{l^*}, \quad (2.62)$$

where M_u is the unfactored moment capacity as per IS 13920:1993, and l^* is described in Step 3 of Section 2.3. Although the Indian Standard [IS 13920, 1993] does not specify overstrength shear demand for walls, the provisions suggested for RC columns are extended for walls. The code overstrength moment capacity is obtained as 1.4 times the unfactored moment capacity M_u .

- (c) Inelastic Shear Demand V_{Ω}^p from nonlinear displacement-controlled pushover analysis of the RC wall using wall properties identical to those described in Step 1 of Section 2.3.

The wall modeled in SAP2000 [CSI, 2000] with vertical frame members between

the floors. The wall is considered fixed at its base. For each frame member, three possible types of hinges are considered namely (a) axial force P -moment M hinge (Figure 2.8a), (b) moment M -rotation θ hinge (Figure 2.8b), and (c) shear force V -displacement Δ hinge (Figure 2.8c). For the shear hinge, the yield shear force is calculated as $V_{max} = (V_c)_{max} + (V_s)_{max}$, where $(V_c)_{max}$ is the overstrength shear capacity of concrete and $(V_s)_{max}$ is the overstrength shear capacity of reinforcement. Pushover analysis is performed under floor displacements in proportion to the lateral load distribution given in Indian Seismic Code IS 1893:2002. The storey shears, observed at different floor levels of the wall during yielding, represent the inelastic shear demand.

Table 3.2 shows the shear demands V_Ω , V_Ω^c and V_Ω^p at each wall section. The design shear capacity V_u of the wall section is contributed by both the web and boundary elements (Table 3.3). For each storey, the shear demands V_Ω , V_Ω^c and V_Ω^p are compared with V_u .

2.4.1 Three Storeyed Building

The overstrength $P - M_\Omega$ interaction curve of the third storey wall section in the three storeyed building is shown in Figure 2.9. The Indian Code proposes the superposition of the web and the boundary element contributions to obtain the design moment capacity of the walls. The same strategy is used in overstrength moment capacity calculation also.

The design $P_u - M_u$ curves and the overstrength $P - M_\Omega$ curves are shown in Figure 2.10 for RC wall sections of the three, five, seven and eleven-storeyed buildings. For each building, the $P_u - M_u$ and the $P - M_\Omega$ curves are shown only for the sections at a few floors.

For the RC wall sections in three storeyed building (Tables 3.2 and 3.3), the following observations are made:

1. For the top storey and the first storey, the overstrength shear demand V_{Ω} exceeds the design shear capacity. Thus, shear failure is likely to occur for the top two storeys.
2. The estimated code shear demand V_{Ω}^c is less than V_{Ω} calculated as per the proposed philosophy, except for the RC wall section in the ground storey.
3. For the wall sections in all the storeys, the inelastic shear demand V_{Ω}^P from pushover analysis is less than V_{Ω} . V_{Ω}^P varies from 30%-50% of V_{Ω} .
4. As per Figure 2.11, the minimum value of the ratio (M_{Ω} / M_u) is more than 2.0 for the ground storey wall section in the normalized axial load ratio (P_u / P_{uz}) range of 0-0.3. For the top storey wall section, the ratio is close to 1.5 in this range.

2.4.2 Eleven Storeyed Building

For the eleven storeyed wall section (Tables 3.2 and 3.3), the following observations are made:

1. For the fifth, seventh, ninth and the tenth storeys, V_{Ω} exceeds V_u . The ninth and the tenth storeys are particularly vulnerable to shear failure.
2. Vertical steel in the seventh storey conforms to the IS 13920:1993 provision (*i.e.*, it is at least equal to the horizontal steel). The effect of the overstrength flexural capacity due to the extra steel is large.
3. Except in the tenth storey, in all other storeys, V_{Ω}^c exceeds V_{Ω} calculated as per the proposed philosophy.
4. In all the storeys, V_{Ω}^P is far less than V_{Ω} .
5. The ratio M_{Ω} / M_u varies in the range 1.4-1.6 for walls in all the storeys

corresponding to P_u / P_{uz} in the range of around 0-0.3.

2.4.3 Other Wall Buildings

The following observations are recorded for the wall sections of all other buildings:

1. In wall of three to seven storeyed buildings, storey for each of them, V_Ω exceeds V_u in all other storeys except the ground.
2. The effect of extra vertical steel in the design, as observed in the wall section at the seventh storey of the eleven-storeyed building, is also observed for the top storey of the nine-storeyed wall. V_Ω exceeds V_u by almost 50%.
3. The demand-capacity ratio V_Ω / V_{cap} shows a decreasing trend for wall sections from the top storey towards the ground storey. The ratio depends on the various sectional properties.
4. Depending on the sectional properties, the V_Ω^c varies from V_Ω compared to the overstrength shear demand. Except in the eleven storeyed building, no regular trend is observed.
5. The V_Ω^p is less than both V_Ω and V_Ω^c for all the sections.

2.5 CONCLUSIONS

The following salient conclusions are drawn from the numerical study reported in this chapter:

1. Capacity design of RC structural walls is not specified in the current code philosophy.
The proposed method aims to overcome this shortcoming.
2. The magnification factor of 1.4, specified in Indian Standard [IS 13920, 1993] for estimating the design shear force in columns, is not applicable for structural walls. The

estimated shear force may be exceeded by the shear demand arising from material overstrengths. The geometry, reinforcement details and specification of vertical steel to be at least that of the horizontal steel play a critical role.

3. Nonlinear static pushover analysis may not provide a conservative estimate of inelastic shear demand compared to the shear force estimated by the proposed method.
4. Slender walls designed with vertical steel, which is increased to be at least equal to the horizontal reinforcement as per code specifications, are vulnerable to shear failure under overstrength conditions. Thus, the provision needs to be applied for squat walls as is done in ACI code.
5. In both high-rise and low-rise building walls, the upper storeys are vulnerable to shear failure. Increased shear capacity of the wall section due to high confinement in boundary elements, may prevent the shear failure of the lower storeys.
6. The proposed procedure for the capacity design of RC structural walls renders the Indian Standard provisions for Design and Detailing of RC walls insufficient to protect the walls from brittle shear failure [IS 13920, 1993].

Table 2.1: Geometric and reinforcement details of building wall sections

Building	Storey	Section Name	Wall Dimensions						Boundary Element					
			Dimensions		Vertical Steel		Horizontal Steel		Width (mm)	Longitudinal Steel		Transverse Steel		
			Width (mm)	Depth (mm)	Bar dia (mm)	Spacing (mm)	Bar dia (mm)	Spacing (mm)		No. of bars	Bar dia (mm)	No. of legs	Dia (mm)	Spacing (mm)
A	G	1WG	150	4730	10	200	10	200	230	4	12	2	10	300
B	1	2W1	150	4730	10	200	10	200	230	4	12	2	10	300
	G	2WG	150	4730	10	200	10	200	230	12	12	4	10	300
C	2	3W2	150	4730	10	200	10	200	230	4	12	2	10	300
	1	3W1	150	4730	10	200	10	200	230	12	12	4	10	300
	G	3WG	200	4730	10	230	10	250	230	12	12	4	10	300
D	3	4W3	150	4730	10	200	10	200	230	4	12	2	10	300
	2	4W2	150	4730	10	200	10	200	230	4	12	2	10	300
	1	4W1	200	4730	10	300	10	300	230	8	16	3	10	300
	G	4WG	200	4800	10	300	10	300	300	12	16	4	10	300
E	4	5W4	150	4730	10	200	10	200	230	4	12	2	10	300
	3	5W3	150	4730	10	200	10	200	230	4	12	2	10	300
	2	5W2	200	4850	10	300	10	300	350	12	12	4	10	300
	1	5W1	200	4850	10	285	10	285	350	16	12	5	10	300
	G	5WG	230	4900	10	265	10	265	400	24	16	7	10	300
F	6	7W6	150	4730	10	200	10	200	230	4	12	2	10	300
	5	7W5	150	4730	10	160	10	160	230	4	12	2	10	300
	4	7W4	200	4800	10	245	10	245	300	12	12	4	10	300
	3	7W3	200	4800	10	190	10	200	300	20	16	6	10	300
	2	7W2	230	4950	10	185	10	185	450	20	20	6	10	300
	1	7W1	230	4950	10	175	10	175	450	24	20	7	10	300
	G	7WG	300	5000	10	100	10	175	500	20	25	6	10	300
G	8	9W8	150	4800	10	200	10	200	300	8	12	3	10	300
	7	9W7	150	4800	10	200	10	200	300	8	12	3	10	300
	6	9W6	200	4800	10	300	10	300	300	8	12	3	10	300
	5	9W5	200	4900	10	240	10	240	400	12	12	4	10	300
	4	9W4	200	4900	12	150	10	150	400	12	16	4	10	300
	3	9W3	250	4900	16	135	10	265	400	20	16	6	10	300
	2	9W2	250	5000	16	125	10	250	500	20	16	6	10	300
	1	9W1	250	5000	20	125	10	250	500	20	20	6	10	300
	G	9WG	250	5000	20	100	10	250	500	20	25	6	10	300
H	10	11W10	150	4800	10	200	10	200	300	8	12	3	10	300
	9	11W9	150	4800	10	200	10	200	300	8	12	3	10	300
	8	11W8	200	4850	10	300	10	300	350	12	12	4	10	300
	7	11W7	200	4850	10	300	10	300	350	12	12	4	10	300
	6	11W6	230	4900	10	250	10	250	400	12	12	4	10	300
	5	11W5	230	4900	10	250	10	250	400	20	16	6	10	300
	4	11W4	300	5000	10	200	10	200	500	24	16	7	10	300
	3	11W3	300	5000	10	175	10	175	500	24	20	7	10	300
	2	11W2	350	5100	10	175	10	175	600	24	20	7	10	300
	1	11W1	350	5100	10	175	10	175	600	28	20	8	10	300
	G	11WG	400	5150	10	150	10	150	650	24	25	7	10	300

Table 2.2: Shear Demands for Building Walls

Section	Results from analysis				Unfactored Moment Capacity M_{uc} (kNm)	Estimated Moment Capacity M_{Ω}^c (kN)	Estimated Shear Demand V_{Ω}^c (kN)	Overstrength conditions		Pushover shear demand V_P (kN)
	Axial Force P_{anal} (kN)	Moment M_{anal} (kNm)	Shear Force V_{anal} (kN)	Ratio $\frac{M_{anal}}{V_{anal}}$ (m)				Moment Capacity M_{Ω} (kNm)	Shear Demand V_{Ω} (kN)	
1WG	122	994	255	3.9	1840	2576	661	2693	691	708
2W1	122	976	375	2.6	1840	2576	990	2693	1036	263
2WG	361	2929	465	6.3	3642	5099	801	5001	794	376
3W2	122	1138	379	3.0	1840	2576	858	2693	898	260
3W1	361	3060	640	4.8	3642	5099	1066	5001	1046	440
3WG	617	6360	751	8.5	6458	9041	1068	8920	1053	503
4W3	122	1237	412	3.0	1840	2576	858	2693	898	179
4W2	362	3629	730	5.0	3642	5099	1026	5001	1006	495
4W1	603	6106	892	6.9	6110	8554	1250	8182	1194	645
4WG	858	10542	954	11.1	10500	14700	1330	14314	1295	647
5W4	122	1210	403	3.0	1840	2576	858	2693	898	238
5W3	362	3456	748	4.6	3642	5099	1104	5001	1082	442
5W2	603	6049	970	6.2	8283	11596	1860	11384	1824	573
5W1	867	9630	1087	8.9	10566	14792	1670	14533	1640	642
5WG	1132	15066	1132	13.3	14904	20866	1568	21575	1606	669
7W6	122	1368	456	3.0	1840	2576	859	2693	898	323
7W5	362	4050	894	4.5	4014	5620	1252	5882	1298	633
7W4	603	7699	1216	6.3	8339	11675	1844	11913	1882	861
7W3	863	12006	1435	8.4	12059	16883	2018	17303	2067	1016
7W2	1123	16744	1579	10.6	17679	24751	2334	24715	2332	1118
7W1	1407	21721	1659	13.1	22553	31574	2412	32018	2446	1174
7WG	1692	30343	1690	18.0	30554	42776	2382	42948	2393	1197
9W8	122	1066	365	2.9	2583	3616	1238	3964	1358	178
9W7	361	3631	721	5.0	3677	5148	1022	5029	998	362
9W6	601	6237	1002	6.2	8169	11437	1837	11254	1809	503
9W5	840	9913	1225	8.1	10460	14644	1810	14597	1804	616
9W4	1096	14076	1387	10.2	16850	23590	2324	23852	2350	697
9W3	1351	18576	1500	12.4	19316	27042	2184	27796	2245	754
9W2	1607	23287	1570	14.8	23647	33106	2232	33960	2290	789
9W1	1878	28116	1609	17.5	28436	39810	2278	40786	2335	809
9WG	2149	34896	1626	21.5	35770	50078	2333	50652	2360	817
11W10	122	801	267	3.0	2583	3616	1205	3964	1321	86
11W9	367	2461	553	4.5	3677	5148	1157	5029	1130	179
11W8	612	4833	790	6.1	5333	7466	1220	7293	1192	255
11W7	876	7780	982	7.9	8483	11876	1499	11407	1440	317
11W6	1141	11178	1132	9.9	11279	15791	1599	14742	1494	366
11W5	1420	14922	1248	12.0	15953	22334	1868	21236	1776	403
11W4	1669	18918	1332	14.2	19984	27978	1970	27028	1903	430
11W3	2011	23089	1390	16.6	24539	34355	2068	33185	1998	449
11W2	2323	27369	1426	19.2	29063	40688	2120	39040	2034	461
11W1	2665	31711	1447	21.9	32048	44867	2047	42501	1940	469
11WG	3007	40013	1456	27.5	42789	59905	2180	58872	2142	471
MJ	256	4830	2030	6.9	---	---	---	10071	1457	---

Table 2.3: Demand capacity ratios for building walls

Section	Design shear capacity (IS 456:2000)					Proposed overstrength		Estimated overstrength		Pushover Analysis	
	Contribution of wall		Contribution of boundary elements		Total V_u (kN)	Shear Demand V_Ω (kN)	Ratio $\frac{V_\Omega}{V_u}$	Shear Demand V_Ω^c (kN)	Ratio $\frac{V_\Omega^c}{V_u}$	Shear Demand V_P (kN)	Ratio $\frac{V_P}{V_u}$
	Concrete (kN)	Steel (kN)	Concrete (kN)	Steel (kN)		V_Ω	$\frac{V_\Omega}{V_u}$	V_Ω^c	$\frac{V_\Omega^c}{V_u}$	V_P	$\frac{V_P}{V_u}$
1WG	213	537	29	57	836	691	0.83	661	0.79	708	0.85
2W1	213	537	29	57	836	1036	1.24	990	1.18	263	0.32
2WG	223	537	67	113	940	794	0.84	801	0.85	376	0.40
3W2	213	537	32	57	839	898	1.07	858	1.02	260	0.31
3W1	223	537	67	113	940	1046	1.11	1026	1.09	440	0.47
3WG	339	858	79	85	1361	1053	0.77	1068	0.79	503	0.37
4W3	213	537	32	57	839	898	1.07	858	1.02	179	0.21
4W2	223	537	67	113	940	1006	1.07	1026	1.09	495	0.53
4W1	302	715	79	85	1181	1194	1.01	1250	1.06	645	0.54
4WG	315	726	139	142	1322	1295	0.98	1330	1.01	647	0.49
5W4	213	537	32	57	839	898	1.07	858	1.02	238	0.28
5W3	223	537	67	113	940	1082	1.15	1104	1.22	442	0.47
5W2	307	733	163	132	1335	1824	1.37	1860	1.39	573	0.43
5W1	324	772	176	165	1437	1640	1.14	1670	1.16	642	0.45
5WG	238	265	380	839	1722	1606	0.93	1568	0.91	669	0.39
7W6	213	537	32	57	839	898	1.07	859	1.02	323	0.38
7W5	223	537	70	85	915	1298	1.42	1252	1.37	633	0.69
7W4	333	889	130	113	1465	1882	1.29	1844	1.26	861	0.59
7W3	382	1089	142	170	1783	2067	1.16	2018	1.13	1016	0.57
7W2	432	1214	295	255	2196	2332	1.06	2334	1.06	1118	0.51
7W1	454	1283	315	298	2350	2446	1.04	2412	1.03	1174	0.50
7WG	768	1296	390	425	2879	2393	0.83	2382	0.83	1197	0.42
9W8	216	544	55	85	900	1358	1.51	1238	1.38	178	0.20
9W7	225	544	97	113	979	998	1.02	1022	1.04	362	0.37
9W6	305	726	130	113	1274	1809	1.42	1837	1.44	503	0.39
9W5	349	926	213	151	1639	1804	1.10	1810	1.10	616	0.38
9W4	502	889	240	189	1820	2350	1.29	2324	1.28	697	0.38
9W3	657	889	240	189	1975	2245	1.14	2184	1.11	754	0.38
9W2	785	907	355	284	2331	2290	0.98	2232	0.96	789	0.34
9W1	907	908	366	284	2465	2335	0.94	2278	0.92	809	0.33
9WG	1014	907	389	284	2594	2360	0.91	2333	0.90	817	0.32
11W10	216	544	55	85	900	1321	1.47	1238	1.38	86	0.10
11W9	225	544	97	113	979	1130	1.15	1157	1.18	179	0.18
11W8	308	733	136	132	1309	1192	0.91	1220	0.93	255	0.19
11W7	318	733	163	132	1346	1440	1.07	1499	1.11	317	0.24
11W6	380	889	215	189	1673	1494	0.89	1599	0.96	366	0.22
11W5	391	889	240	189	1709	1776	1.04	1868	1.09	403	0.24
11W4	501	1134	355	284	2274	1903	0.84	1970	0.87	430	0.87
11W3	543	1296	375	284	2498	1998	0.80	2068	0.83	449	0.83
11W2	599	1322	517	397	2835	2034	0.72	2120	0.75	461	0.75
11W1	610	1322	528	340	2800	1940	0.69	2047	0.73	469	0.73
11WG	707	1558	645	492	3402	2142	0.63	2180	0.64	471	0.64
MJ	285	687	322	736	2030	1457	0.72	---	---	---	---

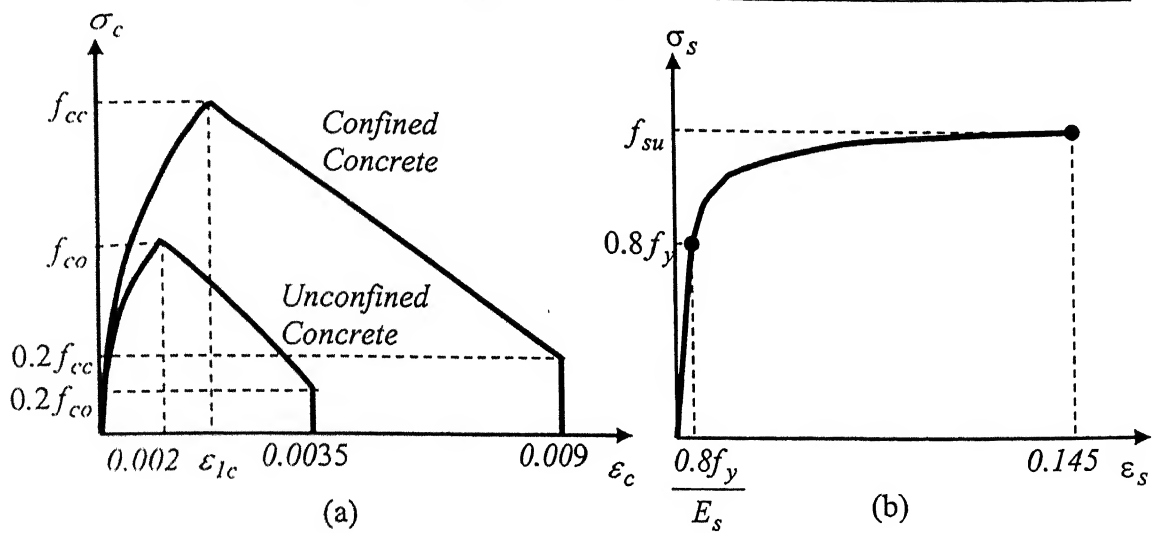


Figure 2.1: Stress-strain curves for $P-M_\Omega$ diagrams: (a) unconfined and confined concrete, and (b) for HYSD bars.

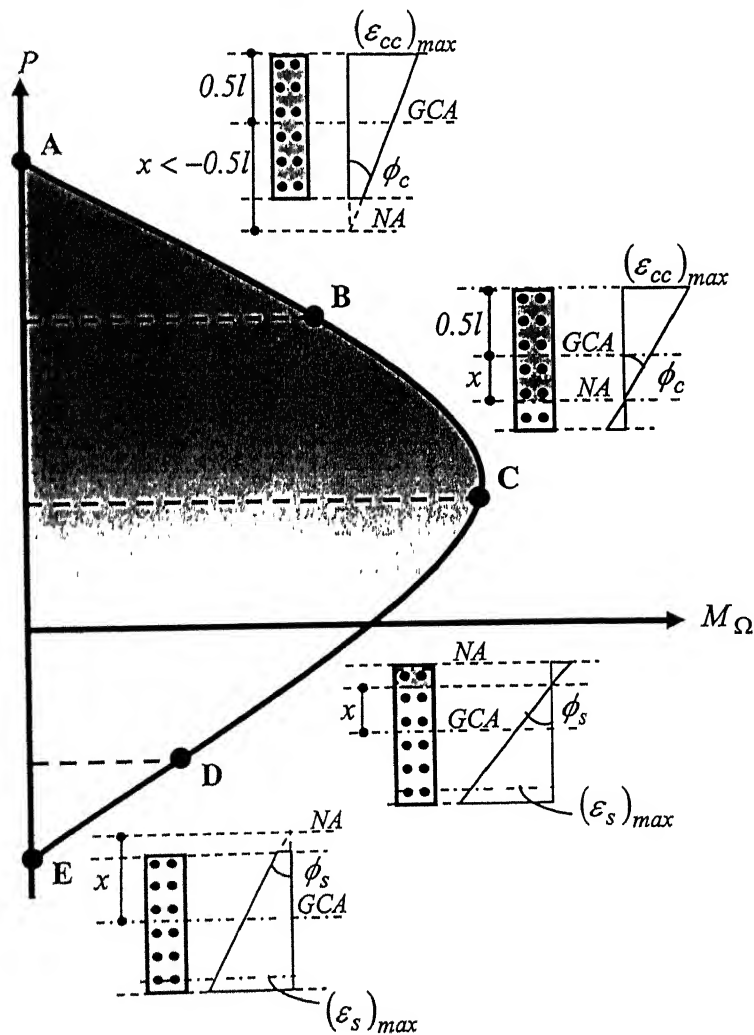


Figure 2.2: General states of a RC cross section and strain distributions under combined axial load and bending moment during overstrength condition.

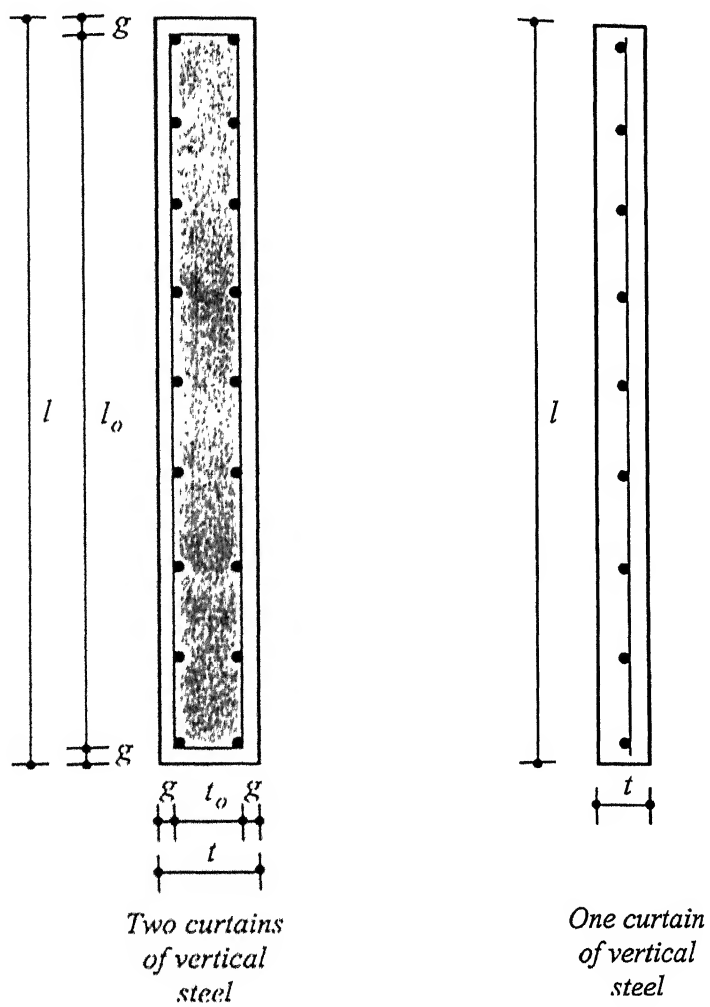


Figure 2.3: General sectional view of wall without boundary elements.

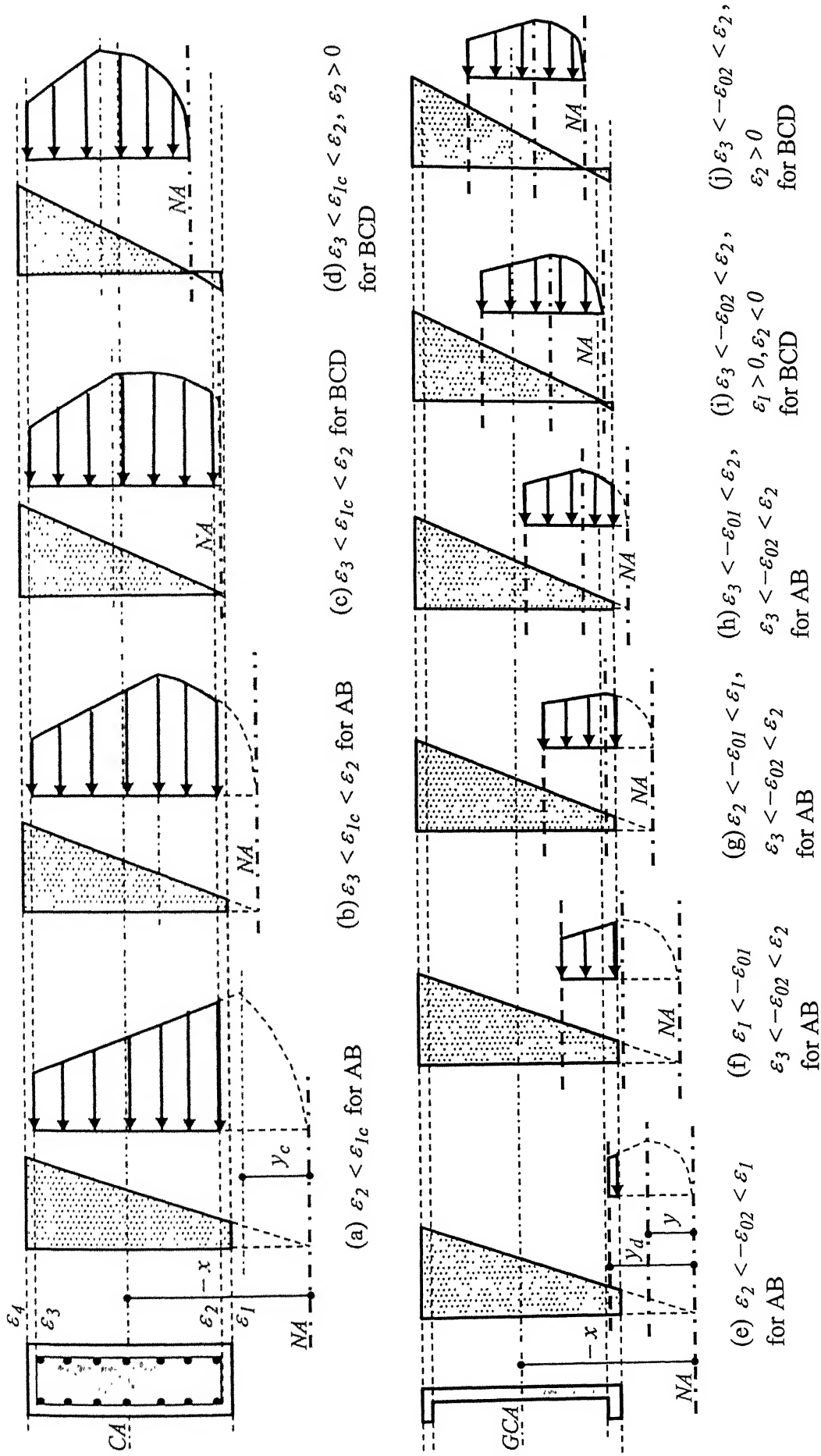


Figure 2.4: Progressive movement of NA into the section and associated strain and stress variations in concrete as per capacity design philosophy: (a) to (d) for confined concrete, and (e) to (j) for unconfined concrete.

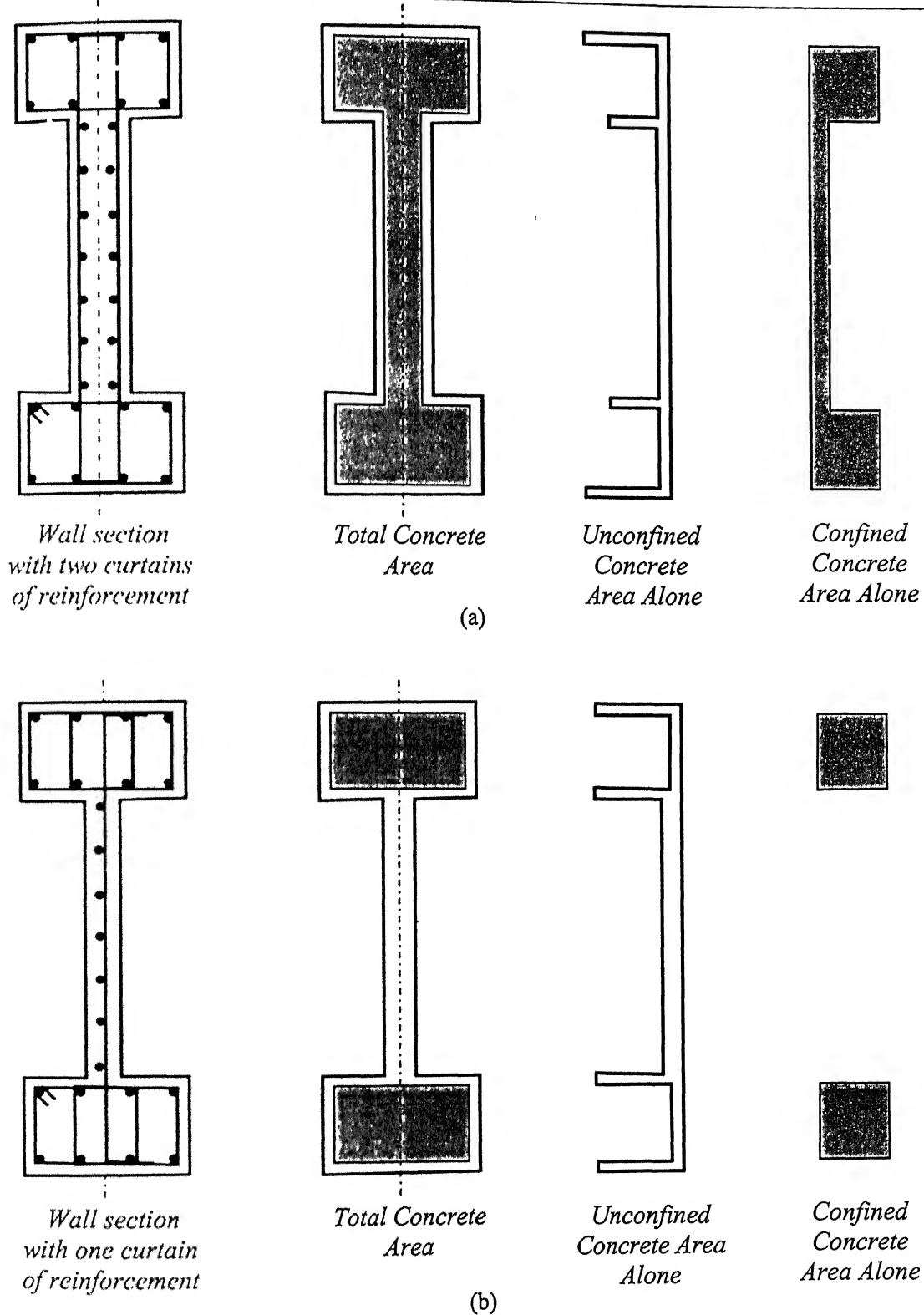
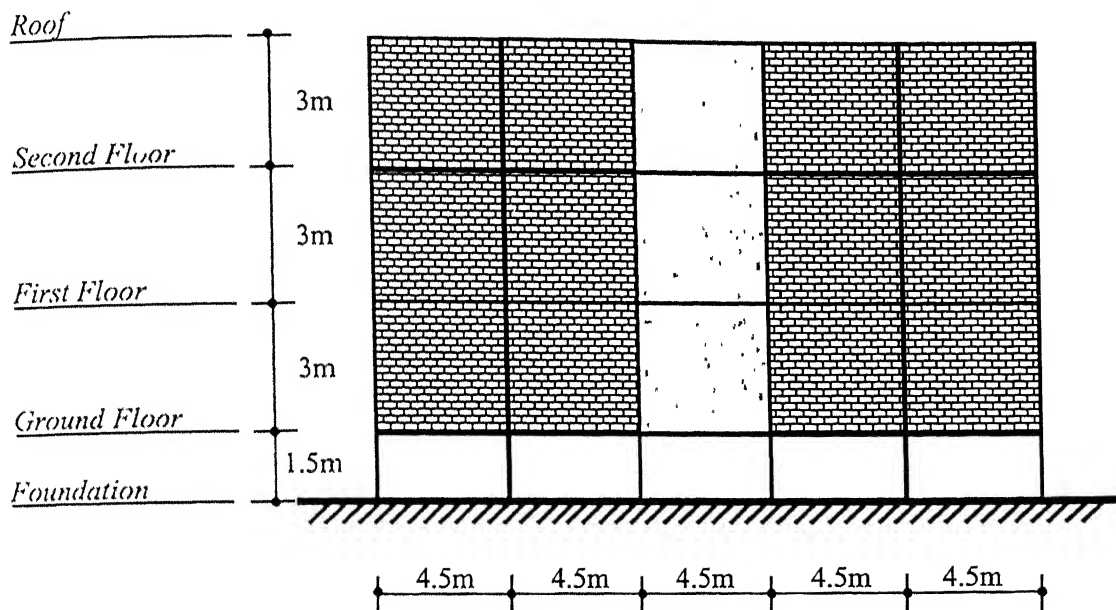
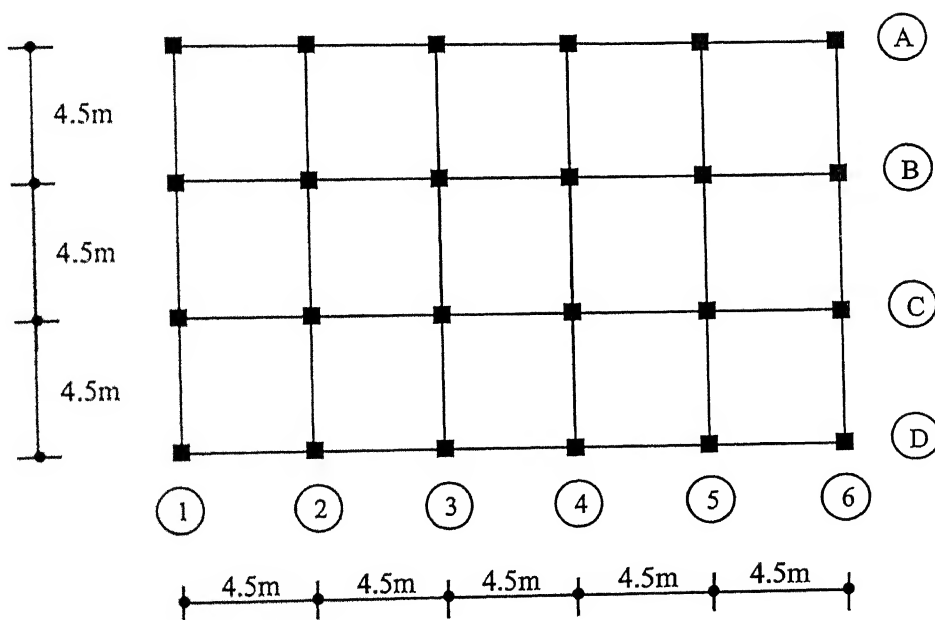


Figure 2.5: Unconfined and confined concrete areas in RC wall sections with (a) two curtains of vertical reinforcement in the web, and (b) one curtain of vertical reinforcement in the web



(a)



(b)

Figure 2.6: Frame-wall building for numerical study: (a) elevation for the three-storeyed building, and (b) typical plan showing frame members.

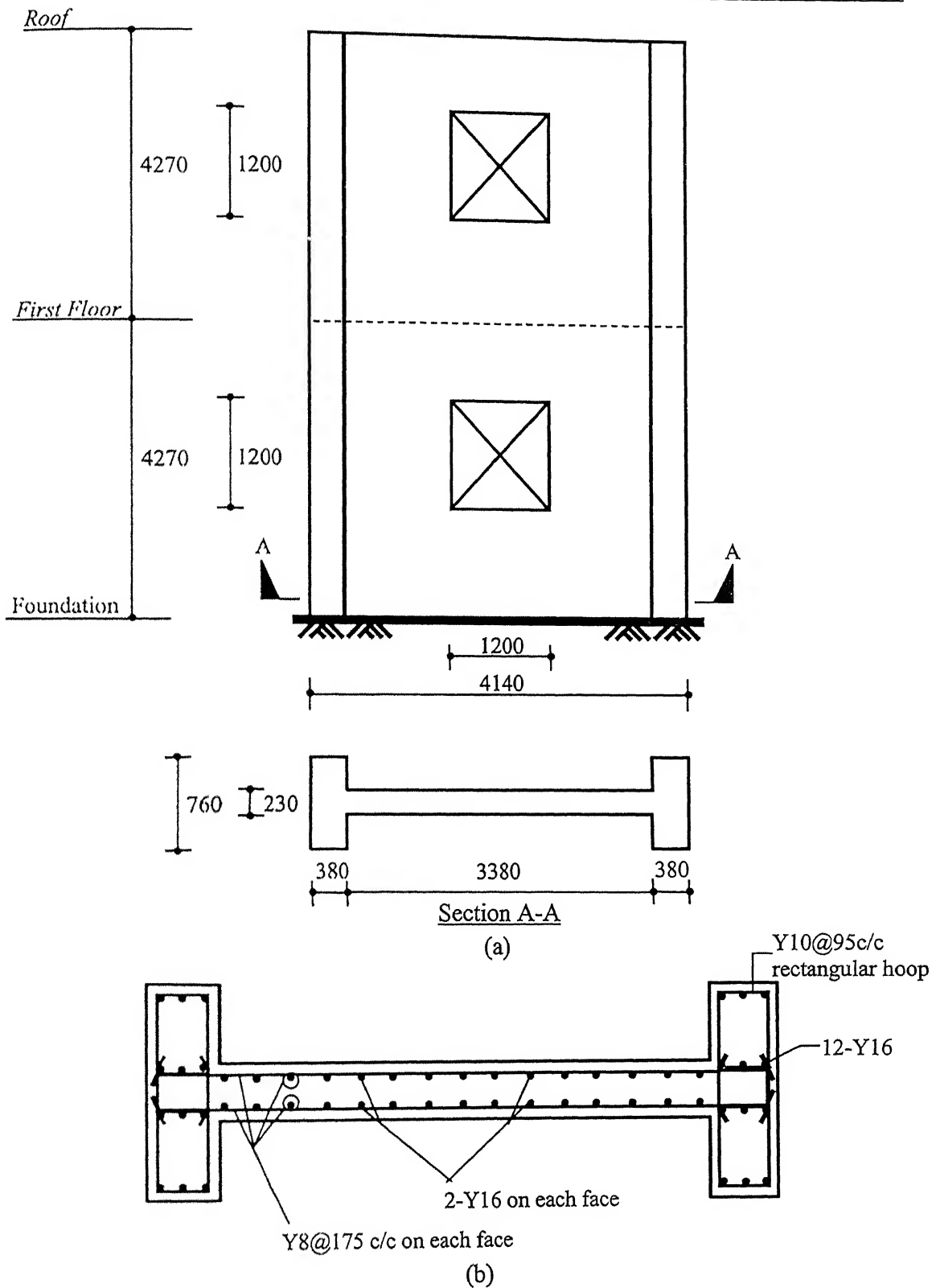


Figure 2.7: Isolated wall section: (a) elevation and sectional plan, and (b) reinforcement details [Medhekar and Jain, 1993].

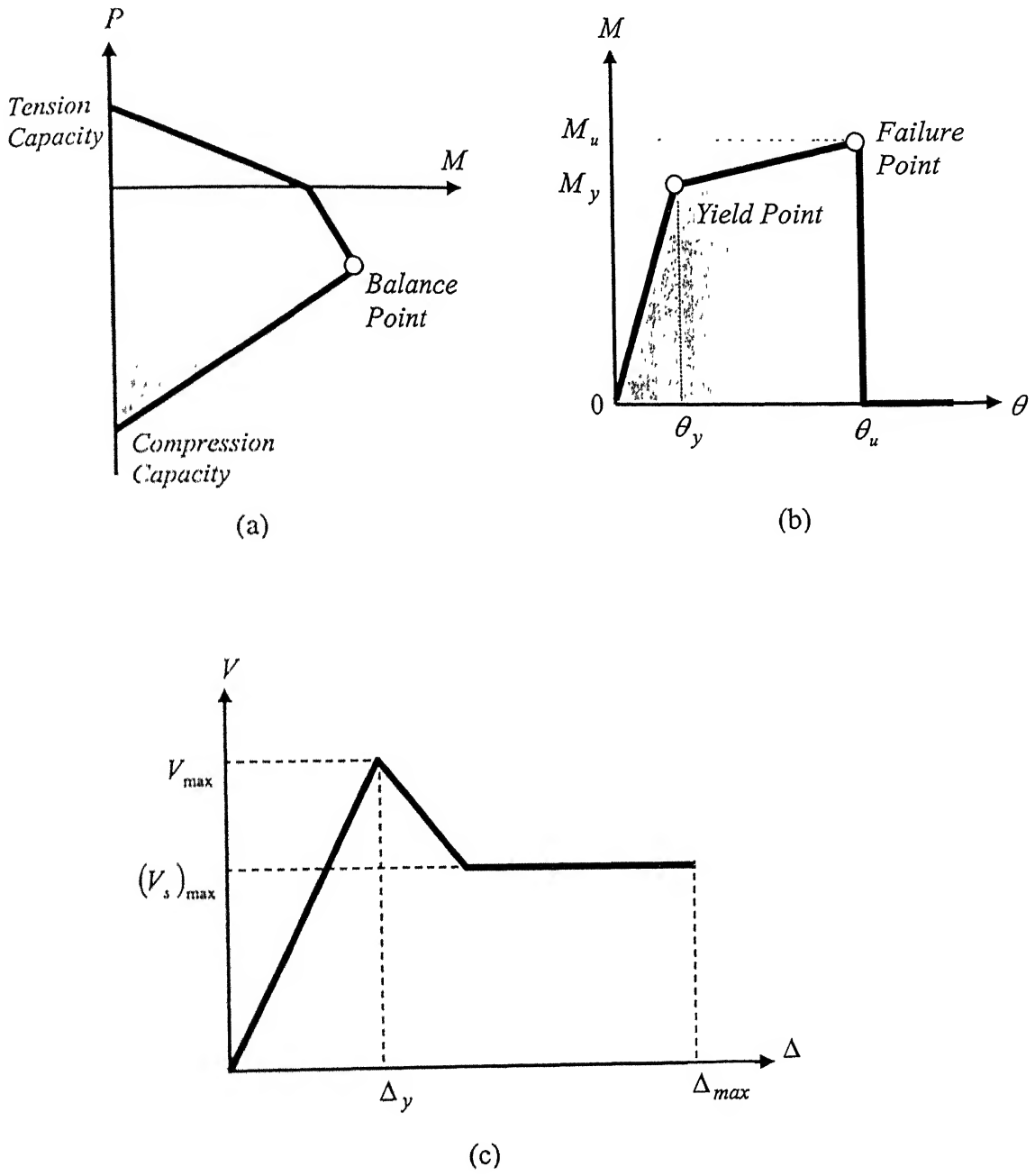


Figure 2.8: Idealized curves and parameters of hinges for pushover analysis, (a) P-M hinge, (b) M- θ hinge, and (c) V- Δ curve.

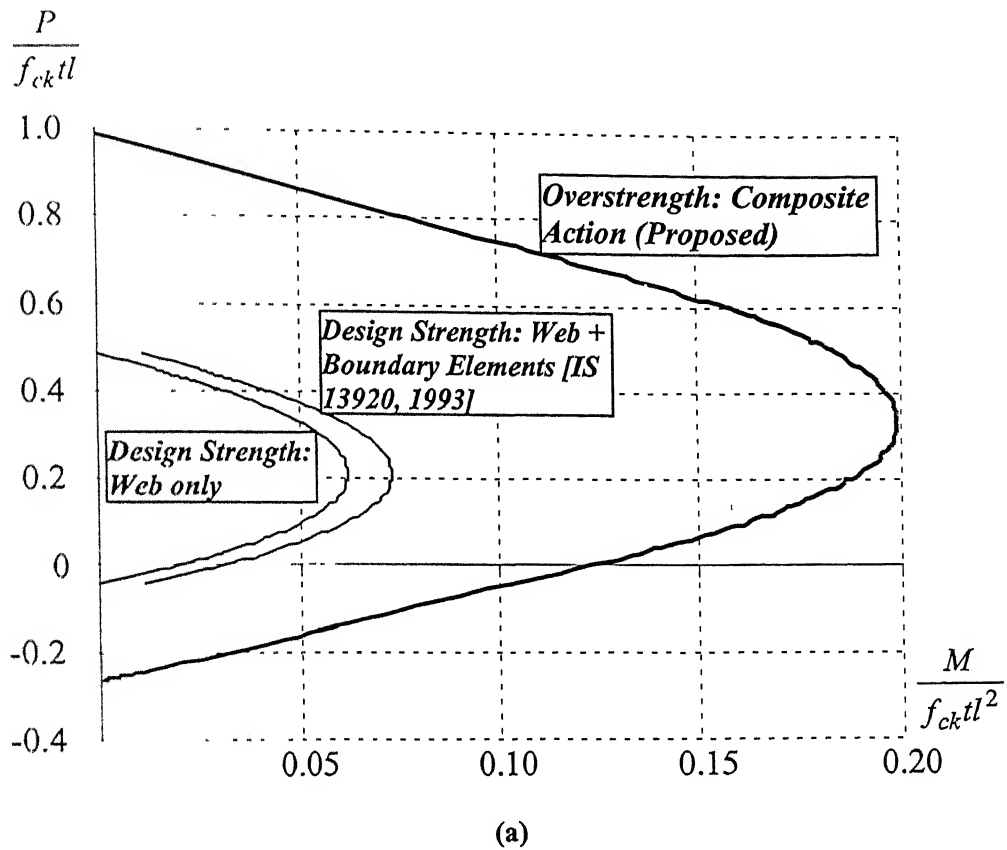


Figure 2.9: Design and Overstrength moment capacities of the third storey in the 3-storey building (Section 3W3 in *Building C*), by the Indian code and the proposed methods respectively.

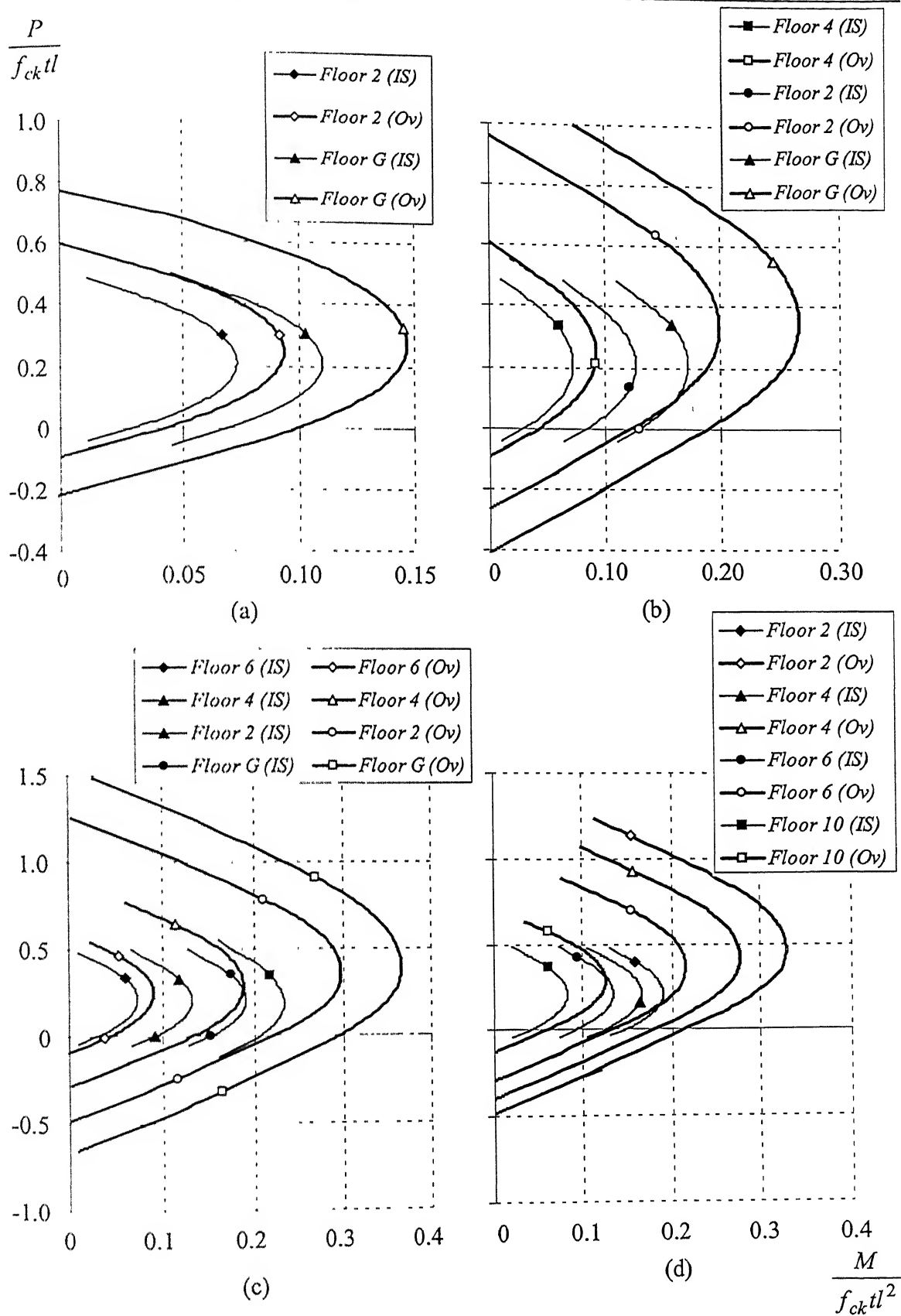


Figure 2.10: $P-M_{\Omega}$ and P_u-M_u [IS 13920, 1993] curves for wall sections in (a) Building C, (b) Building E, (c) Building F, and (d) Building H.

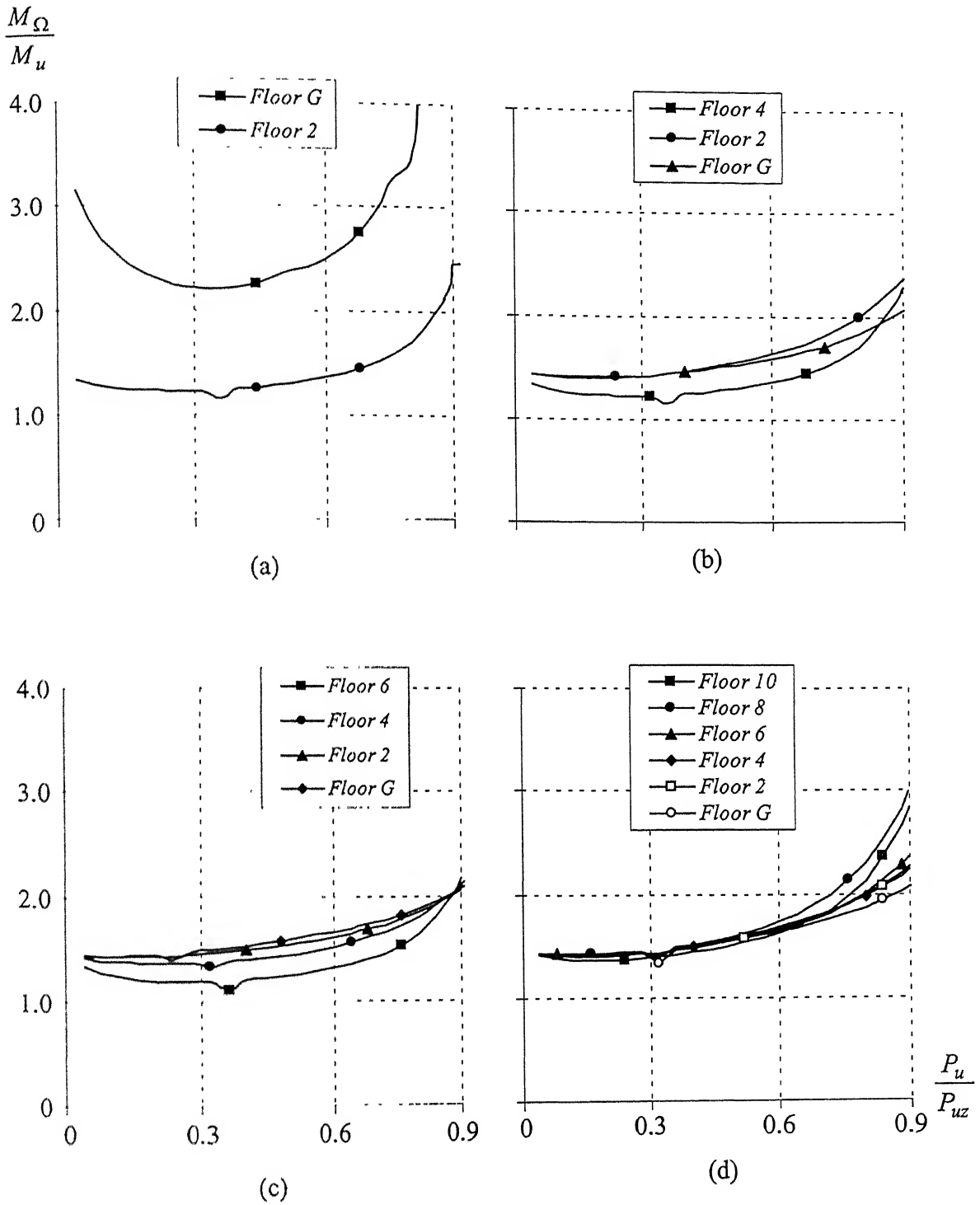


Figure 2.11: Deviation of overstrength moment capacity from the code-specified [IS 456, 2000] flexural capacity for wall sections in (a) *Building C*, (b) *Building E*, (c) *Building F*, and (d) *Building H*.

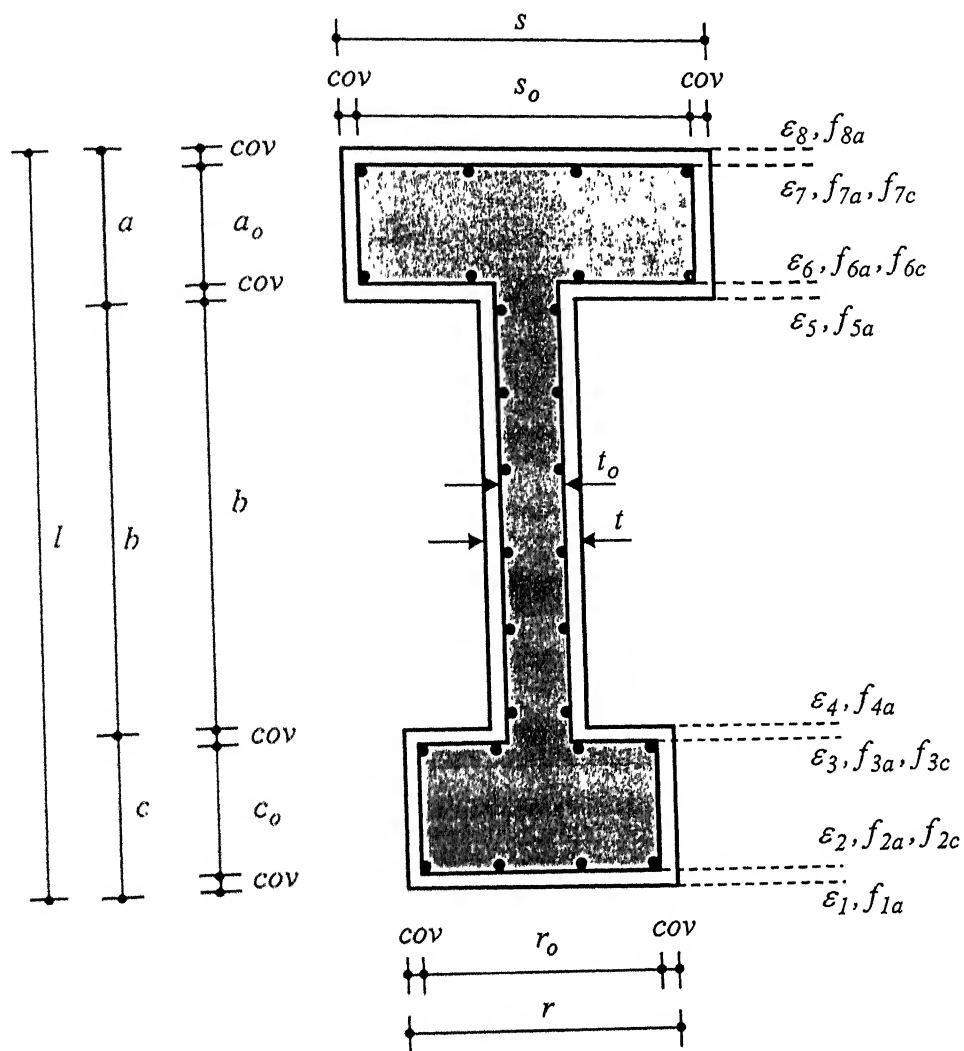


Figure 2.12: Dimensional and stress-strain notations for wall section with boundary elements

Chapter 3

Summary and Conclusions

3.1 INTRODUCTION

RC walls are efficient structural elements for developing desirable ductile seismic behaviour in building systems. They have large lateral stiffness, which reduces the lateral displacement demand on the building system during strong earthquakes. This large stiffness draws significant lateral force on the buildings. Thus, they need to be designed and detailed to possess adequate strength and ductility. The Indian Standard Code of Practice for Ductile Detailing of RC Structures [IS 13920, 1993] prescribes the limit state design of structural walls for flexure and shear, in line with the current Indian Standard Code of Practice for Plain and Reinforced Concrete [IS 456, 2000]. However, the under-reinforced flexural design is not guaranteed through the ductile detailing code provisions. In addition, the capacity design philosophy is not employed in the provisions.

The current study is aimed to review the seismic design provisions for RC structural walls in light of the capacity design philosophy and propose changes in the code revisions.

3.2 SUMMARY

The study covers limit state design of RC structural walls as per the Indian Ductile Detailing Code [IS 13920, 1993]. The following aspects are addressed in this part:

1. The existing philosophy for flexure design of RC structural walls is reviewed and

shortcomings in it are identified.

2. A capacity design method for reinforced concrete structural walls is proposed.
3. Expressions for $P - M_{\Omega}$ interaction curves are analytically derived for building walls using material characteristics under overstrength conditions.
4. The shear demands at various storeys of building walls, obtained from the overstrength moment capacities, are compared with the design shear capacities of the sections. Shear demands based on code procedure for column and inelastic shear demands based on nonlinear static pushover analysis, are also calculated and compared with the design shear capacities. The urgent need for revising the Indian Code provisions for design of RC walls is highlighted.

3.3 CONCLUSIONS

The salient conclusions of this thesis are:

1. For RC walls with boundary elements, the code-specified superposition method incorrectly determines the flexural capacity; the composite action of web and boundary elements needs to be considered.
2. The reinforced concrete structural walls designed by the current code are not protected against premature brittle shear failure.
3. Most of the storeys of multistoreyed buildings are vulnerable to shear failure under material overstrength condition.
4. The current code provision that the provided vertical steel in wall needs to be at least equal to the horizontal steel needs to be specified for squat walls only.
5. The code-specified overstrength factor of 1.4 for estimating the shear force in columns, is not applicable for walls.

3.4 PROPOSED CHANGES IN IS 13920 PROVISIONS

Clauses under Sections 9.2, 9.3 and 9.4 of the Indian Standard Code of Practice for Ductile Detailing of RC structures [IS 13920, 1993], need to be reconsidered. The recommendations are as follows:

1. Superposition of strength contributions from walls and columns, as in Clause 9.4.2 [IS 13920, 1993], is not valid for the estimation of flexural capacity of RC walls with boundary elements.
2. The design flexural capacity of RC walls with boundary elements needs to be calculated considering the composite action of the whole section under the axial force. The code-specified linear superposition may be discontinued.
3. The expressions for the ultimate moment of resistance of rectangular RC wall sections in Annex-A of IS 13920:1993 need to be modified in light of the suggested composite action of web and boundary elements.
4. To ensure ductile under-reinforced response under strong seismic shaking, the design of wall section needs to ensure the balanced axial load to be not more than about 30% of the code-specified ultimate compression capacity.
5. The capacity design method for wall sections needs to be specified explicitly -- the overstrength material characteristics be used, the $P - M_{\Omega}$ interaction be derived, and shear demand be obtained from this overstrength interaction.
6. The shear demand during flexural overstrength needs to be checked against the design shear capacity of the section. Only additional *horizontal* steel be provided in walls where overstrength-based shear demand exceeds the design shear capacity.
7. The requirement of vertical steel to be at least equal to the horizontal steel, as per the Clause 9.2.6, is applicable *only* for squat walls, *i.e.*, in walls with aspect ratio less than 2.0. The current code provision does not have this restriction.

3.5 SCOPE OF FUTURE WORK

The present study is limited to the seismic design of isolated cantilever structural walls. Although the wall sections are designed based on the loads on building frames, the pushover analysis considered walls as single vertical members. To simulate the actual conditions, the frame-wall interaction within the whole building system needs to be considered together in the pushover analysis.

For RC wall sections, interaction of shear capacity with flexural and axial load capacities needs to be considered under overstrength conditions. This may lead to further modifications in shear design provisions.

Displacement-based design of reinforced concrete structural walls is not discussed in the current code provisions [IS 13920, 1993]. Future studies may be aimed towards the drift-based design of reinforced concrete walls.

Soil-foundation interaction mobilised during strong shaking may be considered to better estimate the flexural capacity of RC walls. In turn, this can improve the estimation of shear demand on the RC wall under overstrength conditions.

References

ACI 318-99, (1999), *Building Code Requirement for Reinforced Concrete and Commentary*, American Concrete Institute, Detroit.

Aktan,A.,E., and Bertero,V.,V., (1985), "RC Structural Walls: Seismic Design for Shear," *Journal of Structural Engineering*, ASCE, Vol.111, No.8, pp 1775-1791.

Allen,C.,M., Jaeger,L.,G., and Fenton,V.,C., (1973) "Ductility in Reinforced Concrete Structural Walls", *Response of Multistory Concrete Structures to Lateral Forces*, SP-36, American Concrete Institute, Detroit, pp. 97-118.

Architectural Institute of Japan, (1994), *AIJ Structural Design Guidelines for Reinforced Concrete Buildings*.

Armenia Earthquake Reconnaissance Team, (1989), "Performance of Engineered Structures," *Earthquake Spectra*, Special Supplement, August 1989, pp. 70-92.

ATC 11, (1983), Seismic Resistance of Reinforced Concrete Shear Walls and Frame Joints: Implications of Recent Research for Design Engineers, Applied Technology Council, USA.

Bachmann,H., and Linde,P., (1995) "Dynamic Ductility Demand and Capacity Design of Earthquake-Resistant Reinforced Concrete Walls", *Recent Developments in Lateral Force Transfer in Buildings*, SP-157, American Concrete Institute, Detroit, pp. 117-141.

Cardenas,A.,E., and Magura,D.,D., (1973) "Strength of High-Rise Shear Walls - Rectangular Cross Section", *Response of MultiStorey Concrete Structures to Lateral Forces*, SP-36, American Concrete Institute, Detroit, pp. 119-150.

Cardenas,A.,E., Hanson,J.,M., Corley,W.,G., and Hognestad,E., (1973) "Design Provisions for Shear Walls", *Journal of American Concrete Institute*, Proc. Vol.70, No.3, pp. 221-230.

Cardenas,A.,E., Russell,H.,G., and Corley,W.,G., (1980) "Strength of Low-Rise Structural Walls", *Reinforced Concrete Structures Subjected to Wind and Earthquake Forces*, SP-63-10, American Concrete Institute, Detroit, pp. 221-224.

Cheng,F.,Y., Mertz,G.,E., Sheu,M.,S., and Ger,J.,F., (1993), "Computed versus Observed Inelastic Seismic Low-Rise RC Shear Walls," *Journal of Structural Engineering*, ASCE, Vol.119, No.11, pp. 3255-3275.

Chile Earthquake Reconnaissance Team, (1986), "Performance of Structures," *Earthquake Spectra*, Vol.2, No.2, pp. 293-371.

CSI, (2002), *SAP2000: Integrated Finite Element analysis and Design of Structures*, Computers and Structures Inc., California.

Dasgupta,P., (2000), "Effect of Confinement on Strength and Ductility of Large RC", *Technical Thesis*, Department of Civil Engineering,

Indian Institute of Technology, Kanpur.

EC8, (1994), Eurocode 8 – Design Provisions for Earthquake Resistance of Structures – Part 1-3: General Rules – Specific Rules for Various Materials and Elements, European Committee for Standardisation, Brussels.

Elnashai, A., S., Pilakoutas, K., and Ambraseys, N., N., (1990), “Experimental Behaviour of Reinforced Concrete Walls under Earthquake Loading,” *Earthquake Engineering and Structural Dynamics*, Vol.19, pp.389-407.

Erzincan, Turkey Earthquake Reconnaissance Team, (1993), “Erzincan, Turkey Earthquake Reconnaissance Report: Buildings,” *Earthquake Spectra*, Supplement to Vol.9, pp. 49-85.

Guam Earthquake Reconnaissance Team, (1995), “Guam Earthquake Reconnaissance Report: Buildings,” *Earthquake Spectra*, Supplement B to Vol.11, pp. 63-137.

Hidalgo, P., A., Ledezma, C., A., and Jordan, R., M., (2002), “Seismic Behaviour of Squat Reinforced Concrete Shear Walls,” *Earthquake Spectra*, Vol.18, No.2, pp 287-308.

Hidalgo, P., A., Jordan, R., M., and Martinez, M., P., (2002), “An Analytical Model to Predict the Inelastic Seismic Behaviour of Shear-wall, Reinforced Concrete Structures,” *Engineering Structures*, Vol.24, pp 85-98.

Hoogenboom, P., C., J., Blaauwendraad, J., and Maekawa, K., (1999), “Performance-Based Design of Reinforced Concrete Walls,” *Proceedings of First International Conference on Advances in Structural Engineering and Mechanics, Seoul, Korea*, pp 963-968.

IS 13920-1993, (1993), *Indian Standard Code of Practice for Ductile Detailing of Reinforced Concrete Structures subjected to Seismic Forces*, Bureau of Indian Standards, New Delhi.

IS 1893-2002, (2002), *Indian Standard Criteria of Earthquake Resistant Design of Structures, Part I: General Provisions and Buildings*, Bureau of Indian Standards, New Delhi.

IS 456-2000, (2000), *Code of Practice for Plain and Reinforced Concrete*, Bureau of Indian Standards, New Delhi.

IS 875 (Part I): 1987, (1987), *Code of Practice for Design Loads (other than earthquake) for buildings and structures: Dead Loads – Unit weights of building material and stored materials*, Bureau of Indian Standards, New Delhi.

IS 875 (Part 2): 1987, (1987), *Code of Practice for Design Loads (other than earthquake) for buildings and structures: Imposed Loads*, Bureau of Indian Standards, New Delhi.

Jogala, R., K., R., (1999), “Overstrength and Ductility Capacity of Reinforced Concrete Structural Walls,” *Master of Technology Thesis*, Department of Civil Engineering, Indian Institute of Technology, Kanpur.

Kato,S., Ohya,M., Shimaoka,S., and Takayama,M., (2001), "Finite Element Analysis of Reinforced Concrete Shear Walls with a Crack under Cyclic Loading," *Computational Structural Engineering An International Journal*, Vol.1, No.2, pp 107-116.

Kowalsky,M.,J., (2001), "RC Structural Walls Designed According to UBC and Displacement-Based Methods," *Journal of Structural Engineering*, ASCE, Vol.127, No.5, pp 506-516.

Kwak,H.-G., and Kim,D.-Y., (1999), "Nonlinear Analysis of RC Shear Walls," *Proceedings of First International Conference on Advances in Structural Engineering and Mechanics*, Seoul, Korea, pp 1061-1066.

Lara,A.,M., (1987), "Performance of Eight Engineered Structures," *Earthquake Spectra*, Vol.3, No.3, pp. 543-562.

Lefas,I.,D., Kotsovos,M.,D., and Ambraseys,N.,N., (1990), "Shear Strength of Low-Rise Reinforced Concrete Walls," *ACI Structural Journal*, Vol.87, No.1, pp 23-31.

Lopes,M.,S., (2001), "Experimental Shear-dominated Response of R/C Walls Part I: Objectives, Methodology and Results," *Engineering Structures*, Vol.23, pp 229-239.

Lopes,M.,S., (2001), "Experimental Shear-dominated Response of R/C Walls Part II: Discussion of Results and Design Implications," *Engineering Structures*, Vol.23, pp 564-574.

Lou,K.,Y., Cheng,F.,Y., Sheu,M.,S., and Zhang,X.,Z., (2001), "Load-Displacement Formulations of Low-rise Unbounded RC Walls with or without openings," *Computational Structural Engineering An International Journal*, Vol.1, No.2, pp 117-231.

Mau,S.,T., (1990), "Effect of Tie Spacing on Inelastic Buckling of Reinforcing Bars," *ACI Structural Journal*, Vol.87, No.6, pp 671-677.

Medhekar,M.,S., and Jain,S.,K., (1993) "Seismic Behaviour, Design and Detailing of RC Shear Walls, Part I: Behaviour and Strength", *The Indian Concrete Journal*, July, pp. 311-318.

Medhekar,M.,S., and Jain,S.,K., (1993) "Seismic Behaviour, Design and Detailing of RC Shear Walls, Part II: Design and Detailing", *The Indian Concrete Journal*, September, pp.451-457.

Mochle,J.,P., (1992), "Displacement-Based Design of RC Structures Subjected to Earthquakes", *Earthquake Spectra*, Vol.8, No.3, pp. 403-428.

NZS 4203: 1976, (1976), *Code of Practice for general structural design and design loading for buildings*, Standards Association of New Zealand, Wellington, New Zealand.

NZS 3101 Part-1 & 2: 1995, (1995), *Code of Practice for the Design of Concrete Structures and Commentary*, Standards Association of New Zealand, Wellington, New Zealand.

- Oosterle, R., G., Fiorato, A., E., and Corley, W., G., (1981) "Effect of Reinforcement Details on Seismic Performance of Wall", *Earthquakes and Earthquake Engineering: The Eastern United States*, Ann Arbor Science, Ann Arbor, Michigan, pp. 685-707.
- Oh, Y.-H., Han, S., W., and Lee, L.-H., (2002), "Effect of Boundary Element Details on the Seismic Deformation Capacity of Structural Walls," *Earthquake Engineering and Structural Dynamics*, Vol.31, pp.1583-1602.
- Park, R., and Paulay, T., (1975), *Reinforced Concrete Structures*, John Wiley and Sons, Inc., New York.
- Paulay, T., Priestley, M., J., N., and Syngé, A., J., (1982), "Ductility in Earthquake Resisting Squat Shear Walls," *ACI Structural Journal*, Vol.79, No.4, pp 257-269.
- Paulay, T., (1986), "The Design of Ductile Reinforced Concrete Structural Walls for Earthquake Resistance", *Earthquake Spectra*, Vol.2, No.4, pp. 783 –823.
- Paulay, T., and Priestley, M., J., N., (1992), *Seismic Design of Reinforced Concrete and Masonry Buildings*, John Wiley and Sons, Inc., New York.
- Paulay, T., and Williams, R., L., (1980), "The Analysis and Design of and the Evaluation of Design Actions for Reinforced Concrete Ductile Shear Wall Structures," *Bulletin of New Zealand Society for Earthquake Engineering*, Vol.13, No. 2, pp.73-85.
- Paulay, T., Priestley, M., J., N., and Syngé, A., J., (1982), "Ductility in Earthquake Resisting Squat Shear Walls," *ACI Structural Journal*, Vol.79, No.26, pp 257-269.
- Penelis, G., G., and Kappos, A., J., (1997), *Earthquake Resistant Concrete Structures*, EP & FN SPON, London.
- Priestley, M., J., N., and Kowalsky, M., J., (1998), "Aspects of Drift and Ductility Capacity of Rectangular Concrete Structural Walls," *Bulletin of New Zealand Society for Earthquake Engineering*, Vol.31, No. 2, pp.73-85.
- Razvi, S., R., and Saatcioglu, M., (1999a), "Confinement Model for High-Strength Concrete," *Journal of Structural Engineering*, ASCE, Vol.125, No.3, pp 281-289.
- Salonikios, T., N., (2002), "Shear Strength and Deformation Patterns of R/C Walls with Aspect Ratio 1.0 and 1.5 designed to Eurocode 8 (EC8)," *Engineering Structures*, Vol.24, pp 39-49.
- Salonikios, T., N., Kappos, A., J., Tegos, I., A., and Penelis, G., G., (1999), "Cyclic Load Behaviour of Low-Slenderness Reinforced Concrete Walls: Design Basis and Test Results," *ACI Structural Journal*, Vol.96, No.4, pp 649-660.
- Salonikios, T., N., Kappos, A., J., Tegos, I., A., and Penelis, G., G., (2000), "Cyclic Load Behaviour of Low-Slenderness Reinforced Concrete Walls: Strength and Deformation Analysis, and Design Implications," *ACI Structural Journal*, Vol.97, No.1, pp 132-141.

Sittipunt,C., and Wood,S.,L., (1995), "Influence of Web Reinforcement on the Cyclic Response of Structural Walls," *ACI Structural Journal*, Vol.92, No.6, pp 745-756.

SP: 16-1980, (1980), *Design Aids for Reinforced Concrete*, Bureau of Indian Standards, New Delhi.

Tasnim,A.,A., (2000), "Strength and Deformation of Mid-Rise Shear Walls under Load Reversal," *Engineering Structures*, Vol.22, pp 311-322.

United Nations Industrial Development Organization, (1985), *Seismic Design Codes of the Balkan Region*, Vol.7

Wakabayashi,M., (1986), *Design of Earthquake Resistant Buildings*, McGraw-Hill, New York, 1986, 309p.

Wallace,J.,W., (1993), "Evaluation of UBC-94 Provisions for Seismic Design of RC Structural Walls", *Earthquake Spectra*, Vol.12, No.2, pp. 327 –348.

Wallace,J.,W., (1994), "New Methodology for Seismic Design of RC Shear Walls," *Journal of Structural Engineering*, ASCE, Vol.120, No.3, pp 863-884.

Wallace,J.,W., (1995), "Seismic Design of RC Structural Walls. Part I: New Code Format," *Journal of Structural Engineering*, ASCE, Vol.121, No.1, pp 75-87.

Wallace,J.,W., and Moehle,J.,P., (1993) "An Evaluation of Ductility and Detailing Requirements of Bearing wall Buildings Using Data from the March 3, 1985, Chile Earthquake", *Earthquake Spectra*, Vol.9, No.1, pp. 137 –156.

Wallace,J.,W., and Thomsen IV,J.,H., (1995), "Seismic Design of RC Structural Walls. Part II: Applications," *Journal of Structural Engineering*, ASCE, Vol.121, No.1, pp 88-101.

Wang,Q., (1999), "Numerical Analysis of Reinforced Concrete Shear Wall," *Proceedings of First International Conference on Advances in Structural Engineering and Mechanics*, Seoul, Korea, pp 1091-1096.

Wood,L.,S., (1991), "Performance of Reinforced Concrete Buildings during the 1985 Chile Earthquake: Implications for the Design of Structural Walls", *Earthquake Spectra*, Vol.7, No.4, pp. 607 –637.

Wood,S.,L., (1990), "Shear Strength of Low-Rise Reinforced Concrete Walls," *ACI Structural Journal*, Vol.87, No.1, pp 99-107.

Wyllie, L., et al., (1991), "The Chile Earthquake of March 3 1985", *Earthquake Spectra*, Vol.2, No.2, pp. 249 –512.

Appendix A

Equations for Overstrength P-M Interaction Curve for Confined Web Concrete

The P-M interaction curve has been divided into three segments, namely AB, BC and CD, depending on the strain distribution across the section.

1.0 Segment AB: Neutral axis lies outside the section.

Total axial load and moment of resistance are given by

$$(P_{\Omega})_{AB} = 2(P_{cvt} + P_{crt}) + \sum_{i=1}^n A_{si} \sigma_{si}, \text{ and} \quad (\text{A.1})$$

$$(M_{\Omega})_{AB} = 2(M_{cvt} + M_{crt}) + \sum_{i=1}^n A_{si} \sigma_{si} (0.5l - y_{si}). \quad (\text{A.2})$$

1.1 Subcase 1

The range of strain is, $\varepsilon_2 < \varepsilon_{lc}$. (Figure A.1a)

$$P_{crt} = f_{wc} + f_{f1} + f_{f2}, \text{ and} \quad (\text{A.3})$$

$$M_{crt} = f_{wc} h_{wc} + f_{f1} h_{f1} + f_{f2} h_{f2}, \quad (\text{A.4})$$

where

$$f_{wc} = 0.5[f_{2c} + f_{7c}](0.5t_o)(dl_o), \quad (\text{A.5})$$

$$h_{wc} = \frac{dl_o}{6} \left(\frac{f_{2c} - f_{7c}}{f_{2c} + f_{7c}} \right), \quad (\text{A.6})$$

$$f_{f2} = 0.5(f_{6c} + f_{7c})(0.5a_o)(s_o - t_o), \quad (\text{A.7})$$

$$h_{f2} = (0.5dl_o - a_o) + \frac{a_o}{3} \left(\frac{f_{6c} + 2f_{7c}}{f_{6c} + f_{7c}} \right), \quad (\text{A.8})$$

$$f_{f1} = 0.5(f_{2c} + f_{3c})(0.5c_o)(r_o - t_o), \text{ and} \quad (\text{A.9})$$

$$h_{f1} = 0.5dl_o - \frac{c_o}{3} \left(\frac{f_{2c} + 2f_{3c}}{f_{2c} + f_{3c}} \right). \quad (\text{A.10})$$

1.1.1 Subcase 1.1

The range of strain is, $\varepsilon_1 < -\varepsilon_{02}$.

$$P_{crt} = 0, \text{ and} \quad (\text{A.11})$$

$$M_{cvt} = 0. \quad (\text{A.12})$$

1.2 Subcase 2 (Figure A.1b)

The range of strain is, $\varepsilon_3 < \varepsilon_{lc} < \varepsilon_2$.

$$P_{crt} = f_{wc} + f_{fl} + f_{fp1} + f_{f2}, \text{ and} \quad (\text{A.13})$$

$$M_{crt} = f_{mwc} - f_{fl}h_{fl} - f_{fp1}h_{fp1} + f_{f2}h_{f2}, \quad (\text{A.14})$$

where

$$f_{wc} = f_{wtc} + f_{wpc}, \quad (\text{A.15})$$

$$f_{mwc} = f_{wtc}h_{wtc} + f_{wpc}h_{wpc}, \quad (\text{A.16})$$

$$f_{wtc} = 0.5(f_{7c} + f_{cc})(0.5dl_o - x - y_c)(0.5t_o), \quad (\text{A.17})$$

$$h_{wtc} = (-x - y_c) - \frac{(0.5dl_o - x - y_c)}{3} \left(\frac{f_{cc} + 2f_{7c}}{f_{cc} + f_{7c}} \right), \quad (\text{A.18})$$

$$f_{wpc} = f_c(y_c + x + 0.5dl_o)(0.5t_o), \quad (\text{A.19})$$

$$h_{wpc} = -p_l - x, \text{ and} \quad (\text{A.20})$$

$$y_c = \varepsilon_l \frac{(0.5l - x)}{\varepsilon_8}. \quad (\text{A.21})$$

$$f_{fl} = 0.5(f_{3c} + f_{cc})(-x - y_c - 0.5dl_o + c_o)0.5(r_o - t_o), \quad (\text{A.22})$$

$$h_{fl} = (-x - y_c) - \frac{(x + y_c - 0.5dl_o + c_o)}{3} \left(\frac{f_{cc} + 2f_{3c}}{f_{cc} + f_{3c}} \right). \quad (\text{A.23})$$

$$f_{fp1} = f_c(y_c + x + 0.5dl_o)0.5(r_o - t_o), \quad (\text{A.24})$$

$$h_{fp1} = -p_l - x. \quad (\text{A.25})$$

The force and lever arm for zone 2con are the same as in Eqs.(A.7) and (A.8).

1.2.1 Subcase 2.1

The range of strain is, $\varepsilon_2 < (-\varepsilon_{02}) < \varepsilon_1$.

1.2.1.1 Subcase 2.1.1 (Figure A.2a)

The range of strain is, $\varepsilon_1 < (-\varepsilon_{01})$.

$$P_{cvt} = f_w + f_l, \text{ and} \quad (\text{A.26})$$

$$M_{cvt} = -f_{mw} - f_l h_l. \quad (\text{A.27})$$

where,

$$f_w = 0.5(-0.136f_{ck} + f_{la})(0.5l + x + y_d)cov, \quad (\text{A.28})$$

$$h_w = 0.5l - \frac{(0.5l + x + y_d)}{3} \left(\frac{f_{la} - 0.272f_{ck}}{f_{la} - 0.136f_{ck}} \right), \quad (\text{A.29})$$

$$f_l = 0.5(-0.136f_{ck} + f_{la})(0.5l + y_d + x)(0.5r - cov), \quad (\text{A.30})$$

$$h_l = 0.5l - \frac{(0.5l + y_d + x)}{3} \left(\frac{-0.272f_{ck} + f_{la}}{-0.136f_{ck} + f_{la}} \right), \quad (\text{A.31})$$

$$y = -\epsilon_{01} \frac{(0.5l - x)}{\epsilon_8}, \text{ and} \quad (\text{A.32})$$

$$y_d = -\epsilon_{02} \frac{(0.5l - x)}{\epsilon_8}. \quad (\text{A.33})$$

1.2.2 Subcase 2.2

The range of strain is, $\epsilon_l < (-\epsilon_{02})$.

$$P_{cvt} = 0, \text{ and} \quad (\text{A.34})$$

$$M_{cvt} = 0. \quad (\text{A.35})$$

1.3 Subcase 3 (Figure A.1c)

The range of strain is, $\epsilon_6 < \epsilon_{lc} < \epsilon_3$

$$P_{crt} = f_{wc} + f_{f1} + f_{f2}, \text{ and} \quad (\text{A.36})$$

$$M_{crt} = f_{mwc} - f_{f1}h_{f1} + f_{f2}h_{f2}. \quad (\text{A.37})$$

where

$$f_{f1} = f_c c_o \{0.5(r_o - t_o)\}, \text{ and} \quad (\text{A.38})$$

$$h_{f1} = -p_l - x. \quad (\text{A.39})$$

The force and lever arm for *wall* are the same as in Eqs.(A.15) to (A.20).

The force and lever arm for *zone 1con* are the same as in Eqs.(A.7) to (A.8).

1.3.1 Subcase 3.1

The range of strain is, $\epsilon_l < -\epsilon_{02}$.

$$P_{cvt} = 0, \text{ and} \quad (\text{A.40})$$

$$M_{cvt} = 0. \quad (\text{A.41})$$

1.3.2 Subcase 3.2

The range of strain is, $\epsilon_2 < -\epsilon_{02} < \epsilon_l$.

1.3.2.1 Subcase 3.2.1 (Figure A.2a)

The range of strain is, $\varepsilon_I < (-\varepsilon_{0I})$.

$$P_{cvt} = f_w + f_I, \text{ and} \quad (\text{A.42})$$

$$M_{cvt} = -f_{mw} - f_I h_I. \quad (\text{A.43})$$

The force and lever arm for *wall* and *zone I* are the same as in Eqs.(A.28) to (A.31).

1.3.3 Subcase 3.3

The range of strain is, $\varepsilon_3 < -\varepsilon_{02} < \varepsilon_2$.

1.3.3.1 Subcase 3.3.1 (Figure A.2b)

The range of strain is, $\varepsilon_3 < -\varepsilon_{0I} < \varepsilon_2$.

$$P_{cvt} = f_w + f_I, \text{ and} \quad (\text{A.44})$$

$$M_{cvt} = -f_{mw} - f_I h_I. \quad (\text{A.45})$$

where

$$f_w = f_{wt} + f_{wp}, \quad (\text{A.46})$$

$$f_{mw} = f_{wt} h_{wt} + f_{wp} h_{wp}, \quad (\text{A.47})$$

$$f_{wt} = -0.408 f_{ck} (y_d - y) cov, \quad (\text{A.48})$$

$$h_{wt} = -x - 0.389 y_d - 0.611 y; \quad (\text{A.49})$$

$$f_{wp} = f_c (0.5l + y + x) cov, \quad (\text{A.50})$$

$$h_{wp} = x_p - x - y, \quad (\text{A.51})$$

$$f_I = f_c cov (0.5r - cov), \text{ and} \quad (\text{A.52})$$

$$h_I = x_p - x - y. \quad (\text{A.53})$$

1.3.3.2 Subcase 3.3.2 (Figure A.2c)

The range of strain is, $\varepsilon_2 < -\varepsilon_{0I} < \varepsilon_I$.

$$P_{cvt} = f_w + f_{It} + f_{Ip}, \text{ and} \quad (\text{A.54})$$

$$M_{cvt} = -f_{mw} - f_{It} h_{It} - f_{Ip} h_{Ip}. \quad (\text{A.55})$$

where

$$f_{It} = 0.5(-0.68 f_{ck} + f_{2a})(0.5r - cov)(-x - y - 0.5l + cov), \quad (\text{A.56})$$

$$h_{It} = (-x - y) - \frac{(-x - y - 0.5l + cov)}{3} \left(\frac{-0.68 f_{ck} + 2f_{2a}}{-0.68 f_{ck} + f_{2a}} \right). \quad (\text{A.57})$$

$$f_{lp} = f_c(y + 0.5l + x)(0.5r - cov), \text{ and} \quad (\text{A.58})$$

$$h_{lp} = x_p - x - y. \quad (\text{A.59})$$

The force and lever arm for *wall* are the same as in Eqs.(A.46) to (A.51).

1.3.3.3 Subcase 3.3.3 (Figure A.2d)

The range of strain is, $\varepsilon_I < -\varepsilon_{0I}$.

$$P_{cvt} = f_w + f_I, \text{ and} \quad (\text{A.60})$$

$$M_{cvt} = -f_{mw} - f_I h_I. \quad (\text{A.61})$$

where

$$f_I = 0.5(f_{1a} + f_{2a})(0.5r - cov)cov, \text{ and} \quad (\text{A.62})$$

$$h_I = 0.5l - \frac{cov}{3} \left(\frac{f_{1a} + 2f_{2a}}{f_{1a} + f_{2a}} \right). \quad (\text{A.63})$$

The force and lever arm for *wall* are the same as in Eqs.(A.28) and (A.29).

1.3.4 Subcase 3.4

The range of strain is, $\varepsilon_4 < -\varepsilon_{02} < \varepsilon_3$.

1.3.4.1 Subcase 3.4.1 (Figure A.2e)

The range of strain is, $\varepsilon_3 < -\varepsilon_{0I} < \varepsilon_2$.

$$P_{cvt} = f_w + f_I + f_2, \text{ and} \quad (\text{A.64})$$

$$M_{cvt} = -f_{mw} - f_I h_I - f_2 h_2. \quad (\text{A.65})$$

where

$$f_2 = 0.5(-0.136f_{ck} + f_{3a})(0.5l - cov - c_o + x + y_d)(0.5r - cov), \text{ and} \quad (\text{A.66})$$

$$h_2 = 0.5l - \frac{(0.5l - cov - c_o + x + y_d)}{3} \left(\frac{f_{3a} - 0.272f_{ck}}{f_{3a} - 0.136f_{ck}} \right). \quad (\text{A.67})$$

The force and lever arm for *wall* and *zone 1* are the same as in Eqs.(A.46) to (A.53).

1.3.4.2 Subcase 3.4.2 (Figure A.2f)

The range of strain is, $\varepsilon_2 < -\varepsilon_{0I} < \varepsilon_I$.

$$P_{cvt} = f_w + f_2 + f_{I1} + f_{lp}, \text{ and} \quad (\text{A.68})$$

$$M_{cvt} = -f_{mw} - f_2 h_2 - f_{I1} h_{I1} - f_{lp} h_{lp}. \quad (\text{A.69})$$

The force and lever arm for *wall* are the same as in Eqs.(A.46) to (A.51).

The force and lever arm for *zone 1* are the same as in Eqs.(A.56) to (A.59).

The force and lever arm for *zone 2* are the same as in Eqs.(A.66) and (A.67).

1.3.4.3 Subcase 3.4.3 (Figure A.2g)

The range of strain is, $\varepsilon_I < -\varepsilon_{0I}$.

$$P_{cvt} = f_w + f_I + f_2, \text{ and} \quad (\text{A.70})$$

$$M_{cvt} = -f_{mw} - f_I h_I - f_2 h_2. \quad (\text{A.71})$$

The force and lever arm for *wall* are the same as in Eqs.(A.28) and (A.29).

The force and lever arm for *zone 1* are the same as in Eqs.(A.62) and (A.63).

The force and lever arm for *zone 2* are the same as in Eqs.(A.66) and (A.67).

1.3.5 Subcase 3.5

The range of strain is, $\varepsilon_5 < -\varepsilon_{02} < \varepsilon_4$.

1.3.5.1 Subcase 3.5.1 (Figure A.2h)

The range of strain is, $\varepsilon_5 < -\varepsilon_{0I} < \varepsilon_4$.

$$P_{cvt} = f_w + f_I + f_2, \text{ and} \quad (\text{A.72})$$

$$M_{cvt} = -f_{mw} - f_I h_I - f_2 h_2. \quad (\text{A.73})$$

where

$$f_2 = f_c \text{cov}(0.5r - \text{cov}), \text{ and} \quad (\text{A.74})$$

$$h_2 = x_p - x - y. \quad (\text{A.75})$$

The force and lever arm for *wall* and *zone 1* are the same as in Eqs.(A.46) to (A.53).

1.3.5.2 Subcase 3.5.2 (Figure A.2i)

The range of strain is, $\varepsilon_4 < -\varepsilon_{02} < \varepsilon_3$.

$$P_{cvt} = f_w + f_{2t} + f_{2p} + f_I, \text{ and} \quad (\text{A.76})$$

$$M_{cvt} = -f_{mw} - f_{2t} h_{2t} - f_{2p} h_{2p} - f_I h_I. \quad (\text{A.77})$$

where

$$f_{2t} = 0.5(-0.68f_{ck} + f_{4a})(-0.5l - x - y + c)(0.5r - \text{cov}), \quad (\text{A.78})$$

$$h_{2t} = (-x - y) - \frac{(-0.5l - x - y + c)}{3} \left(\frac{-0.68f_{ck} + 2f_{4a}}{-0.68f_{ck} + f_{4a}} \right), \quad (\text{A.79})$$

$$f_{2p} = f_c(y + 0.5l + x - c_o - \text{cov})(0.5r - \text{cov}), \quad (\text{C.80})$$

$$h_{2p} = x_p - x - y. \quad (A.81)$$

The force and lever arm for *wall* and *zone 1* are the same as given in Eqs.(A.46) to (A.53).

1.3.5.3 Subcase 3.5.3 (Figure A.2j)

The range of strain is, $\varepsilon_3 < -\varepsilon_{01} < \varepsilon_2$.

$$P_{cvt} = f_w + f_1 + f_2, \text{ and} \quad (A.82)$$

$$M_{cvt} = -f_{mw} - f_1 h_1 - f_2 h_2. \quad (A.83)$$

where

$$f_2 = 0.5(f_4 + f_3) \text{cov}(0.5r - \text{cov}), \text{ and} \quad (A.84)$$

$$h_2 = (0.5l - \text{cov} - c_o) - \frac{\text{cov}}{3} \left(\frac{f_3 + 2f_4}{f_3 + f_4} \right). \quad (A.85)$$

The force and lever arm for *wall* and *zone 1* are the same as given in Eqs.(A.46) to (A.53).

1.3.5.4 Subcase 3.5.4 (Figure A.2k)

The range of strain is, $\varepsilon_2 < -\varepsilon_{02} < \varepsilon_1$.

$$P_{cvt} = f_w + f_{1t} + f_{1p} + f_2, \text{ and} \quad (A.86)$$

$$M_{cvt} = -f_{mw} - f_{1t} h_{1t} - f_{1p} h_{1p} - f_2 h_2. \quad (A.87)$$

The force and lever arm for *wall* are the same as in Eqs.(A.46) to (A.51).

The force and lever arm for *zone 1* are the same as in Eqs.(A.56) to (A.59).

The force and lever arm for *zone 2* are the same as in Eqs.(A.84) and (A.85).

1.3.5.5 Subcase 3.5.5 (Figure A.2l)

The range of strain is, $\varepsilon_1 < -\varepsilon_{01}$.

$$P_{cvt} = f_w + f_1 + f_2, \text{ and} \quad (A.88)$$

$$M_{cvt} = -f_{mw} - f_1 h_1 - f_2 h_2. \quad (A.89)$$

The force and lever arm for *wall* are the same as in Eqs.(A.28) and (A.29).

The force and lever arm for *zone 1* are the same as in Eqs.(A.62) and (A.63).

The force and lever arm for *zone 2* are the same as in Eqs.(A.84) and (A.85).

2.0 Segments BC and CD

The following equations have been derived based on the strain distribution over

$$h_{2p} = x_p - x - y. \quad (\text{A.81})$$

The force and lever arm for wall and zone 1 are the same as given in Eqs.(A.46) to (A.53).

1.3.5.3 Subcase 3.5.3 (Figure A.2j)

The range of strain is, $\varepsilon_3 < -\varepsilon_{01} < \varepsilon_2$.

$$P_{cvl} = f_w + f_l + f_2, \text{ and} \quad (\text{A.82})$$

$$M_{cvl} = -f_{mw} - f_l h_l - f_2 h_2. \quad (\text{A.83})$$

where

$$f_2 = 0.5(f_4 + f_3) \text{cov}(0.5r - \text{cov}), \text{ and} \quad (\text{A.84})$$

$$h_2 = (0.5l - \text{cov} - c_o) - \frac{\text{cov}}{3} \left(\frac{f_3 + 2f_4}{f_3 + f_4} \right). \quad (\text{A.85})$$

The force and lever arm for wall and zone 1 are the same as given in Eqs.(A.46) to (A.53).

1.3.5.4 Subcase 3.5.4 (Figure A.2k)

The range of strain is, $\varepsilon_2 < -\varepsilon_{02} < \varepsilon_1$.

$$P_{cvl} = f_w + f_{lt} + f_{lp} + f_2, \text{ and} \quad (\text{A.86})$$

$$M_{cvl} = -f_{mw} - f_{lt} h_{lt} - f_{lp} h_{lp} - f_2 h_2. \quad (\text{A.87})$$

The force and lever arm for wall are the same as in Eqs.(A.46) to (A.51).

The force and lever arm for zone 1 are the same as in Eqs.(A.56) to (A.59).

The force and lever arm for zone 2 are the same as in Eqs.(A.84) and (A.85).

1.3.5.5 Subcase 3.5.5 (Figure A.2l)

The range of strain is, $\varepsilon_1 < -\varepsilon_{01}$.

$$P_{cvl} = f_w + f_l + f_2, \text{ and} \quad (\text{A.88})$$

$$M_{cvl} = -f_{mw} - f_l h_l - f_2 h_2. \quad (\text{A.89})$$

The force and lever arm for wall are the same as in Eqs.(A.28) and (A.29).

The force and lever arm for zone 1 are the same as in Eqs.(A.62) and (A.63).

The force and lever arm for zone 2 are the same as in Eqs.(A.84) and (A.85).

2.0 Segments BC and CD

The following equations have been derived based on the strain distribution over

the section. The strain distribution is determined by the minimum of the two curvature values, based on the allowable maximum compressive strain in concrete and the maximum rupture strain in steel respectively.

Curvature is defined as either

$$|\varphi_s| = \frac{0.145}{y_{ns} - 0.5l + x}, \text{ or} \quad (\text{A.90})$$

$$|\varphi_c| = \frac{\varepsilon_{c,max}}{0.5l - x - cov}. \quad (\text{A.91})$$

where $\varepsilon_{c,max}$ is the maximum compressive strain in confined concrete, and the rupture strain in steel is 0.145.

Total axial load and moment of resistance are given by

$$(P_{\Omega})_{BC} = 2(P_{cvt} + P_{crt}) + \sum_{i=1}^n A_{si} \sigma_{si}, \text{ and} \quad (\text{A.92})$$

$$(M_{\Omega})_{BC} = 2(M_{cvt} + M_{crt}) + \sum_{i=1}^n A_{si} \sigma_{si} (0.5l - y_{si}). \quad (\text{A.93})$$

2.1 Subcase 1

Neutral axis lies in zone I.

2.1.1 Subcase 1.1 (Figure A.1d)

The range of strain values is, $\varepsilon_6 < \varepsilon_{lc} < \varepsilon_3$.

$$P_{crt} = f_{wc} + f_{f1} + f_{f2}, \text{ and} \quad (\text{A.94})$$

$$M_{crt} = -f_{mwc} - f_{f1}h_{f1} + f_{f2}h_{f2}. \quad (\text{A.95})$$

where

$$f_{wc} = f_{wte} + f_{wpc}, \quad (\text{A.96})$$

$$f_{mwc} = f_{wte}h_{wte} + f_{wpc}h_{wpc}, \quad (\text{A.97})$$

$$f_{wte} = 0.5(f_{cc} + f_{7c})(0.5dl_o - y_c - x)0.5t_o, \quad (\text{A.98})$$

$$h_{wte} = (-x - y_c) - \frac{(0.5dl_o - y_c - x)}{3} \left(\frac{f_{cc} + 2f_{7c}}{f_{cc} + f_{7c}} \right), \quad (\text{A.99})$$

$$f_{wpc} = f_c(y_c + 0.5dl_o + x)0.5t_o, \quad (\text{A.100})$$

$$h_{wpc} = -x_p - x, \quad (\text{A.101})$$

$$f_{f2} = 0.5(f_{7c} + f_{6c}) \frac{a_o}{2} (s_o - t_o), \quad (\text{A.102})$$

$$h_{f2} = 0.5dl_o - a_o + \frac{a_o}{3} \left(\frac{f_{6c} + 2f_{7c}}{f_{6c} + f_{7c}} \right), \quad (\text{A.103})$$

$$f_{f1} = 0.5(f_{2c} + f_{3c}) \frac{c_o}{2} (r_o - t_o), \text{ and} \quad (\text{A.104})$$

$$h_{f1} = 0.5dl_o + \frac{a_o}{3} \left(\frac{f_{2c} + 2f_{3c}}{f_{2c} + f_{3c}} \right). \quad (\text{A.105})$$

2.1.1.1 Subcase 1.1.1

The range of strain is, $\varepsilon_5 < -\varepsilon_{02} < \varepsilon_4$.

2.1.1.1.1 Subcase 1.1.1.1 (Figure A.3a)

The range of strain is, $\varepsilon_3 < -\varepsilon_{01} < \varepsilon_2$.

$$P_{cvt} = f_w + f_1 + f_2, \text{ and} \quad (\text{A.106})$$

$$M_{cvt} = -f_{mw} - f_1 h_1 - f_2 h_2. \quad (\text{A.107})$$

where

$$f_{mw} = f_w h_w, \quad (\text{A.108})$$

$$f_w = -0.36f_{ck} y_d \text{cov}, \quad (\text{A.109})$$

$$h_w = -x - 0.58 y_d, \quad (\text{A.110})$$

$$f_2 = 0.5(f_3 + f_4) \text{cov} (0.5r - \text{cov}), \quad (\text{A.111})$$

$$h_2 = (0.5l - c) + \frac{\text{cov}}{3} \left(\frac{f_{3a} + 2f_{4a}}{f_{3a} + f_{4a}} \right), \quad (\text{A.112})$$

$$f_1 = f_c [y - (\text{cov} - 0.5l - x)] (0.5r - \text{cov}), \text{ and} \quad (\text{A.113})$$

$$h_1 = -x - y + x_p. \quad (\text{A.114})$$

2.1.1.1.2 Subcase 1.1.1.2 (Refer Figure A.3b)

The range of strain is, $\varepsilon_4 < -\varepsilon_{01} < \varepsilon_3$.

$$P_{cvt} = f_w + f_1 + f_{2t} + f_{2p}, \text{ and} \quad (\text{A.115})$$

$$M_{cvt} = -f_{mw} - f_1 h_1 - f_{2t} h_{2t} - f_{2p} h_{2p}. \quad (\text{A.116})$$

where

$$f_{2t} = \frac{(-0.68f_{ck} + f_{4a})}{2} (0.5r - \text{cov}) [-x - y - (0.5l - c)], \quad (\text{A.117})$$

$$h_{2t} = (-x - y) + \frac{\text{cov}}{3} \left(\frac{-0.68f_{ck} + 2f_{4a}}{-0.68f_{ck} + f_{4a}} \right), \quad (\text{A.118})$$

$$f_{2p} = f_c [(0.5l - \text{cov} - c_o) + x + y](0.5r - \text{cov}), \text{ and} \quad (\text{A.119})$$

$$h_{2p} = x_p - x - y. \quad (\text{A.120})$$

The *force* and *lever arm* for wall are the same as in Eqs.(A.109) and (A.110).

The *force* and *lever arm* for zone 1 are the same as in Eqs.(A.113) and (A.114).

2.1.1.1.3 Subcase 1.1.1.3 (Figure A.3c)

The range of strain is, $\varepsilon_5 < -\varepsilon_{01} < \varepsilon_4$.

$$P_{cvt} = f_w + f_1 + f_2, \text{ and} \quad (\text{A.121})$$

$$M_{cvt} = -f_{mw} - f_1 h_1 - f_2 h_2. \quad (\text{A.122})$$

where

$$f_2 = f_c (0.5r - \text{cov}) \text{cov}, \text{ and} \quad (\text{A.123})$$

$$h_2 = x_p - y - x. \quad (\text{A.124})$$

The *force* and *lever arm* for wall are the same as in Eqs.(A.109) and (A.110).

The *force* and *lever arm* for zone 1 are the same as in Eqs.(A.113) and (A.114).

2.2 Subcase 2

In this case, the neutral axis lies between zone 1 and zone 2

2.2.1 Subcase 2.1 (Figure A.1e)

The range of strain values is, $\varepsilon_6 < \varepsilon_{1c} < \varepsilon_3$.

$$P_{crt} = f_{wc} + f_{f1} + f_{f2}, \text{ and} \quad (\text{A.125})$$

$$M_{crt} = -f_{mwc} - f_{f1} h_{f1} + f_{f2} h_{f2}. \quad (\text{A.126})$$

where

$$f_{f1} = f_c (-x - 0.5dl_o + c_o) 0.5(r_o - t_o), \text{ and} \quad (\text{A.127})$$

$$h_{f1} = -x_p - x. \quad (\text{A.128})$$

The *force* and *lever arm* for wall are the same as in Eqs.(A.96) and (A.101).

The *force* and *lever arm* for zone 2 are the same as in Eqs.(A.102) and (A.103).

2.2.1.1 Subcase 2.1.1

The range of strain values is, $\varepsilon_5 < -\varepsilon_{02} < \varepsilon_4$.

2.2.1.1.1 Subcase 2.1.1.1 (Figure A.3d)

The range of strain values is, $\varepsilon_3 < -\varepsilon_{0I} < \varepsilon_2$.

$$P_{cvt} = f_w + f_2, \text{ and} \quad (\text{A.129})$$

$$M_{cvt} = -f_{mw} - f_2 h_2. \quad (\text{A.130})$$

The *force* and *lever arm* for wall and zone 2 are the same as in Eqs.(A.108) to (A.112).

2.2.1.1.2 Subcase 2.1.1.2 (Figure A.3e)

The range of strain values is, $\varepsilon_4 < -\varepsilon_{0I} < \varepsilon_3$.

$$P_{cvt} = f_w + f_{2t} + f_{2p}, \text{ and} \quad (\text{A.131})$$

$$M_{cvt} = -f_{mw} - f_{2t} h_{2t} - f_{2p} h_{2p}. \quad (\text{A.132})$$

The *force* and *lever arm* for wall are the same as in Eqs.(A.109) and (A.110).

The *force* and *lever arm* for zone 2 are the same as in Eqs.(A.117) to (A.120).

2.2.1.1.3 Subcase 2.1.1.3 (Figure A.3f)

The range of strain values is, $\varepsilon_5 < -\varepsilon_{0I} < \varepsilon_4$.

$$P_{cvt} = f_w + f_2, \text{ and} \quad (\text{A.133})$$

$$M_{cvt} = -f_{mw} - f_2 h_2. \quad (\text{A.134})$$

The *force* and *lever arm* for wall are the same as in Eqs.(A.109) and (A.110).

The *force* and *lever arm* for zone 2 are the same as in Eqs.(A.111) and (A.112).

2.3 Subcase 3

In this case, the neutral axis lies in zone 2.

2.3.1 Subcase 3.1 (Figure A.1f)

The range of strain values is, $\varepsilon_6 < \varepsilon_{Ic} < \varepsilon_3$.

$$P_{crt} = f_{wc} + f_{f2}, \text{ and} \quad (\text{A.135})$$

$$M_{crt} = -f_{mwc} + f_{f2} h_{f2}. \quad (\text{A.136})$$

The *force* and *lever arm* for wall and zone 2con are the same as in Eqs.(A.96) to (A.103).

2.3.1.1 Subcase 3.1.1

The range of strain values is, $\varepsilon_5 < -\varepsilon_{02} < \varepsilon_4$.

2.3.1.1.1 Subcase 3.1.1.1 (Figure A.3g)

The range of strain values is, $\varepsilon_5 < -\varepsilon_{01} < \varepsilon_4$.

$$P_{cvt} = f_w + f_2, \text{ and} \quad (\text{A.137})$$

$$M_{cvt} = -f_{mw} - f_2 h_2. \quad (\text{A.138})$$

where

$$f_2 = f_c(-x - 0.5l + c)(0.5r - cov), \text{ and} \quad (\text{A.139})$$

$$h_2 = x_p - y - x. \quad (\text{A.140})$$

The *force* and *lever arm* for *wall* are the same as in Eqs.(A.109) and (A.110).

2.4 Subcase 4

In this case, the neutral axis lies between *zone 2* and *zone 3*.

2.4.1 Subcase 4.1 (A.1f)

The range of strain values is, $\varepsilon_6 < \varepsilon_{1c} < \varepsilon_3$.

$$P_{crt} = f_{wc} + f_{f2}, \text{ and} \quad (\text{A.141})$$

$$M_{crt} = -f_{mwc} + f_{f2} h_{f2}. \quad (\text{A.142})$$

The *force* and *lever arm* for *wall* and *zone 2con* are the same as in Eqs.(A.96) to (A.103).

2.4.1.1 Subcase 4.1.1

The range of strain values is, $\varepsilon_5 < -\varepsilon_{02} < \varepsilon_4$.

2.4.1.1.1 Subcase 4.1.1.1

The range of strain values is, $\varepsilon_5 < -\varepsilon_{01} < \varepsilon_4$ (Figure A.3h).

$$P_{cvt} = f_w, \text{ and} \quad (\text{A.143})$$

$$M_{cvt} = -f_{mw}. \quad (\text{A.144})$$

The *force* and *lever arm* for *wall* are the same as in Eqs.(A.109) and (A.110).

2.4.2 Subcase 4.2 (Figure A.1g)

The range of strain values is, $\varepsilon_7 < \varepsilon_{1c} < \varepsilon_6$.

$$P_{crt} = f_{wc} + f_{f2} + f_{fp2}, \text{ and} \quad (\text{A.145})$$

$$M_{crt} = -f_{mwc} + f_{f2} h_{f2} + f_{fp2} h_{fp2}. \quad (\text{A.146})$$

where

$$f_{f2} = f_c(y_c + x + c_o - 0.5dl_o)0.5(s_o - t_o), \quad (\text{A.147})$$

$$h_{f12} = (y_c + x) - \frac{(0.5dl_o - y_c - x)}{3} \left(\frac{f_{cc} + 2f_{7c}}{f_{cc} + f_{7c}} \right), \quad (\text{A.148})$$

$$f_{fp2} = f_c (y_c + x + c_o - 0.5dl_o) 0.5(s_o - t_o), \text{ and} \quad (\text{A.149})$$

$$h_{fp2} = -x_p - x. \quad (\text{A.150})$$

The *force* and *lever arm* for *wall* are the same as in Eqs.(A.96) to (A.101).

2.4.2.1 Subcase 4.2.1

The range of strain values is, $\varepsilon_5 < -\varepsilon_{02} < \varepsilon_4$.

2.4.2.1.1 Subcase 4.2.1.1 (Figure A.3h)

The range of strain values is, $\varepsilon_5 < -\varepsilon_{01} < \varepsilon_4$

$$P_{cvt} = f_w, \text{ and} \quad (\text{A.151})$$

$$M_{cvt} = -f_{mw}. \quad (\text{A.152})$$

The *force* and *lever arm* for *wall* are the same as in Eqs.(A.109) and (A.110).

2.4.2.2 Subcase 4.2.2

The range of strain values is, $\varepsilon_6 < -\varepsilon_{02} < \varepsilon_5$.

2.4.2.2.1 Subcase 4.2.2.1

The range of strain values is, $\varepsilon_5 < -\varepsilon_{01} < \varepsilon_4$ (Figure A.3i).

$$P_{cvt} = f_w + f_3, \text{ and} \quad (\text{A.153})$$

$$M_{cvt} = -f_{mw} + f_3 h_3. \quad (\text{A.154})$$

where

$$f_3 = 0.5(-0.136f_{ck} + f_{5a})(0.5s - cov)(y_d + x - 0.5l + a), \text{ and} \quad (\text{A.155})$$

$$h_3 = (y_d + x) + \frac{(y_d + x - 0.5l + a)}{3} \left(\frac{f_{5a} - 0.272f_{ck}}{f_{5a} - 0.136f_{ck}} \right). \quad (\text{A.156})$$

The *force* and *lever arm* for *wall* are the same as in Eqs.(A.109) and (A.110).

2.4.2.3 Subcase 4.2.3

The range of strain values is, $\varepsilon_7 < -\varepsilon_{02} < \varepsilon_6$.

2.4.2.3.1 Subcase 4.2.3.1

The range of strain values is, $\varepsilon_5 < -\varepsilon_{01} < \varepsilon_4$ (Figure A.3j).

$$P_{cvt} = f_w + f_3, \text{ and} \quad (\text{A.157})$$

$$M_{cvt} = -f_{mw} + f_3 h_3. \quad (\text{A.158})$$

where

$$f_3 = 0.5(f_{5a} + f_{6a})\text{cov}(0.5s - \text{cov}), \text{ and} \quad (\text{A.159})$$

$$h_3 = (0.5l - a) + \frac{\text{cov}}{3} \left(\frac{f_{5a} + 2f_{6a}}{f_{5a} + f_{6a}} \right). \quad (\text{A.160})$$

The *force* and *lever arm* for wall are the same as in Eqs.(A.109) and (A.110).

2.4.2.3.2 Subcase 4.2.3.2

The range of strain values is, $\varepsilon_6 < -\varepsilon_{0I} < \varepsilon_5$ (Figure A.3k).

$$P_{cvt} = f_w + f_{3p} + f_{3t}, \text{ and} \quad (\text{A.161})$$

$$M_{cvt} = f_{mw} + f_{3p}h_{3p} + f_{3t}h_{3t}. \quad (\text{A.162})$$

where

$$f_{3t} = 0.5(-0.68f_{ck} + f_{6a})(0.5s - \text{cov})(0.5l - \text{cov} - c_o - x - y), \text{ and} \quad (\text{A.163})$$

$$h_{3t} = (x + y) + \frac{(0.5l - \text{cov} - c_o - x - y)}{3} \left(\frac{-0.68f_{ck} + 2f_{6a}}{-0.68f_{ck} + f_{6a}} \right). \quad (\text{A.164})$$

$$f_{3p} = f_c(x + y - 0.5l + a)(0.5s - \text{cov}), \text{ and} \quad (\text{A.165})$$

$$h_{3p} = x + y + x_p. \quad (\text{A.166})$$

The *force* and *lever arm* for wall are the same as in Eqs.(A.109) and (A.110).

2.4.2.3.3 Subcase 4.2.3.3

The range of strain values is, $\varepsilon_7 < -\varepsilon_{0I} < \varepsilon_6$ (Figure A.3l).

$$P_{cvt} = f_w + f_3, \text{ and} \quad (\text{A.167})$$

$$M_{cvt} = f_{mw} + f_3h_3. \quad (\text{A.168})$$

where

$$f_3 = f_c\text{cov}(0.5s - \text{cov}), \text{ and} \quad (\text{A.169})$$

$$h_3 = x + y + x_p. \quad (\text{A.170})$$

The *force* and *lever arm* for wall are the same as in Eqs.(A.109) and (A.110).

2.4.3 Subcase 4.3

The range of strain values is, $\varepsilon_7 > \varepsilon_{Ic}$ (Figure A.1h).

$$P_{crt} = f_{wc} + f_{j2}, \text{ and} \quad (\text{A.171})$$

$$M_{crt} = f_{mwc} + f_{j2}h_{j2}. \quad (\text{A.172})$$

where

$$f_{wc} = f_c(0.5l - x)0.5t_o, \quad (\text{A.173})$$

$$h_{wc} = x + x_p, \quad (\text{A.174})$$

$$f_{f2} = f_c s_o 0.5(s_o - t_o), \text{ and} \quad (\text{A.175})$$

$$h_{f2} = x + x_p. \quad (\text{A.176})$$

2.4.3.1 Subcase 4.3.1

The range of strain values is, $\varepsilon_5 < -\varepsilon_{02} < \varepsilon_4$.

2.4.3.1.1 Subcase 4.3.1.1

The range of strain values is, $\varepsilon_5 < -\varepsilon_{01} < \varepsilon_4$ (Figure A.3h).

$$P_{cvt} = f_w, \text{ and} \quad (\text{A.177})$$

$$M_{cvt} = f_{mw}. \quad (\text{A.178})$$

The *force* and *lever arm* for *wall* are the same as in Eqs.(A.109) and (A.110).

2.4.3.2 Subcase 4.3.2

The range of strain values is, $\varepsilon_6 < -\varepsilon_{02} < \varepsilon_5$.

2.4.3.2.1 Subcase 4.3.2.1

The range of strain values is, $\varepsilon_5 < -\varepsilon_{01} < \varepsilon_4$ (Figure A.3i).

$$P_{cvt} = f_w + f_3, \text{ and} \quad (\text{A.179})$$

$$M_{cvt} = f_{mw} + f_3 h_3. \quad (\text{A.180})$$

The *force* and *lever arm* for *wall* are the same as in Eqs.(A.109) and (A.110).

The *force* and *lever arm* for *zone 3* are the same as in Eqs.(A.155) and (A.156).

2.4.3.3 Subcase 4.3.3

The range of strain values is, $\varepsilon_7 < -\varepsilon_{02} < \varepsilon_6$.

2.4.3.3.1 Subcase 4.3.3.1

The range of strain values is, $\varepsilon_5 < -\varepsilon_{01} < \varepsilon_4$ (Figure A.3j).

$$P_{cvt} = f_w + f_3, \text{ and} \quad (\text{A.181})$$

$$M_{cvt} = f_{mw} + f_3 h_3. \quad (\text{A.182})$$

where

$$f_3 = 0.5(f_{5a} + f_{6a}) \text{ cov}(0.5s - \text{cov}), \text{ and} \quad (\text{A.183})$$

$$h_3 = (y_d + x) \frac{\text{cov} \left(\frac{f_{5a} + 2f_{6a}}{f_{5a} + f_{6a}} \right)}{3}. \quad (\text{A.184})$$

The *force* and *lever arm* for *wall* are the same as in Eqs.(A.109) and (A.110).

2.4.3.3.2 Subcase 4.3.3.2

The range of strain values is, $\varepsilon_6 < -\varepsilon_{0I} < \varepsilon_5$ (Figure A.3k).

$$P_{\text{cvt}} = f_w + f_{3p} + f_{3t}, \text{ and} \quad (\text{A.185})$$

$$M_{\text{cvt}} = f_{mw} + f_{3p}h_{3p} + f_{3t}h_{3t}. \quad (\text{A.186})$$

The *force* and *lever arm* for *wall* are the same as in Eqs.(A.109) and (A.110).

The *force* and *lever arm* for *zone 3* are the same as in Eqs.(A.163) to (A.166).

2.4.3.3.3 Subcase 4.3.3.3

The range of strain values is, $\varepsilon_7 < -\varepsilon_{0I} < \varepsilon_6$ (Figure A.3l).

$$P_{\text{cvt}} = f_w + f_3, \text{ and} \quad (\text{A.187})$$

$$M_{\text{cvt}} = f_{mw} + f_3h_3. \quad (\text{A.188})$$

The *force* and *lever arm* for *wall* are the same as in Eqs.(A.109) and (A.110).

The *force* and *lever arm* for *zone 3* are the same as in Eqs.(A.169) and (A.170).

2.4.3.4 Subcase 4.3.4

The range of strain values is, $\varepsilon_8 < -\varepsilon_{02} < \varepsilon_7$.

2.4.3.4.1 Subcase 4.3.4.1

The range of strain values is, $\varepsilon_6 < -\varepsilon_{0I} < \varepsilon_5$ (Figure A.3m).

$$P_{\text{cvt}} = f_w + f_{3t} + f_{3p} + f_4, \text{ and} \quad (\text{A.189})$$

$$M_{\text{cvt}} = f_{mw} + f_{3t}h_{3t} + f_{3p}h_{3p} + f_4h_4. \quad (\text{A.190})$$

where

$$f_4 = 0.5(0.136f_{ck} + f_{7a})(0.5s - \text{cov})(y_d + x - 0.5l + \text{cov}), \text{ and} \quad (\text{A.191})$$

$$h_4 = (y_d + x) \frac{(y_d + x - 0.5l + \text{cov})}{3} \left(\frac{f_{7a} - 0.272f_{ck}}{f_{7a} - 0.136f_{ck}} \right). \quad (\text{A.192})$$

The *force* and *lever arm* for *wall* are the same as in Eqs.(A.109) and (A.110).

The *force* and *lever arm* for *zone 3* are the same as in Eqs.(A.163) to (A.166).

2.4.3.4.2 Subcase 4.3.4.2

The range of strain values is, $\varepsilon_7 < -\varepsilon_{0I} < \varepsilon_6$ (Figure A.3n).

$$P_{\text{cvt}} = f_w + f_{3t} + f_{3p} + f_4, \text{ and} \quad (\text{A.193})$$

$$M_{cvt} = -f_{mw} + f_3 h_3 + f_4 h_4. \quad (A.194)$$

The *force* and *lever arm* for *wall* are the same as in Eqs.(A.109) and (A.110).

The *force* and *lever arm* for *zone 3* are the same as in Eqs.(A.169) and (A.170).

The *force* and *lever arm* for *zone 4* are the same as in Eqs.(A.191) and (A.192).

2.4.3.5 Subcase 4.3.5

The range of strain values is, $\varepsilon_8 > -\varepsilon_{02}$.

2.4.3.5.1 Subcase 4.3.5.1

The range of strain values is, $\varepsilon_6 < -\varepsilon_{01} < \varepsilon_5$ (Figure A.3o).

$$P_{cvt} = f_w + f_{3t} + f_{3p} + f_4, \text{ and} \quad (A.195)$$

$$M_{cvt} = -f_{mw} + f_{3t} h_{3t} + f_{3p} h_{3p} + f_4 h_4. \quad (A.196)$$

where

$$f_w = f_{wt} + f_{wp}, \quad (A.197)$$

$$f_{mw} = f_{wt} h_{wt} + f_{wp} h_{wp}, \quad (A.198)$$

$$f_{wt} = 0.5(-0.68f_{ck} + f_{8a})(0.5l - y - x)cov, \quad (A.199)$$

$$h_{wt} = (x + y) - \frac{(0.5l - y - x)}{3} \left(\frac{-0.68f_{ck} + 2f_{8a}}{-0.68f_{ck} + f_{8a}} \right), \quad (A.200)$$

$$f_{wp} = f_c y.cov, \quad (A.201)$$

$$h_{wp} = -x_p + x + y, \quad (A.202)$$

$$f_4 = 0.5(f_{8a} + f_{7a})(0.5s - cov)cov, \text{ and} \quad (A.203)$$

$$h_4 = (0.5l - cov) + \frac{cov}{3} \left(\frac{f_{7a} + 2f_{8a}}{f_{7a} + f_{8a}} \right). \quad (A.204)$$

The *force* and *lever arm* for *zone 3* are the same as in Eqs.(A.163) to (A.166).

2.4.3.5.2 Subcase 4.3.5.2

The range of strain values is, $\varepsilon_7 < -\varepsilon_{01} < \varepsilon_6$ (Figure A.3p).

$$P_{cvt} = f_w + f_3 + f_4, \text{ and} \quad (A.205)$$

$$M_{cvt} = -f_{mw} + f_3 h_3 + f_4 h_4. \quad (A.206)$$

The *force* and *lever arm* for *wall* are the same as in Eqs.(A.197) to (A.202).

The *force* and *lever arm* for *zone 3* are the same as in Eqs.(A.169) and (A.170).

The *force* and *lever arm* for *zone 4* are the same as in Eqs.(A.203) and (A.204).

2.4.3.5.3 Subcase 4.3.5.3

The range of strain values is, $\varepsilon_8 < -\varepsilon_{0l} < \varepsilon_7$ (Figure A.4a).

$$P_{cvt} = f_w + f_3 + f_{4t} + f_{4p}, \text{ and} \quad (\text{A.207})$$

$$M_{cvt} = -f_{mw} + f_3 h_3 + f_{4p} h_{4p} + f_{4t} h_{4t}. \quad (\text{A.208})$$

where

$$f_{4t} = 0.5(-0.68f_{ck} + f_{7a})(0.5s - cov)(0.5l - x - y), \quad (\text{A.209})$$

$$h_{4t} = (x + y) - \frac{(0.5l - y - x)}{3} \left(\frac{-0.68f_{ck} + 2f_{7a}}{-0.68f_{ck} + f_{7a}} \right), \quad (\text{A.210})$$

$$f_{4p} = f_c(x + y + cov - 0.5l)(0.5s - cov), \text{ and} \quad (\text{A.211})$$

$$h_{4p} = -x_p + x + y. \quad (\text{A.212})$$

The *force* and *lever arm* for *wall* are the same as in Eqs.(A.197) to (A.202).

The *force* and *lever arm* for *zone 3* are the same as in Eqs.(A.169) and (A.170).

2.4.3.5.4 Subcase 4.3.5.4

The range of strain values is, $\varepsilon_8 > -\varepsilon_{0l}$ (Figure A.4b).

$$P_{cvt} = f_w + f_3 + f_4, \text{ and} \quad (\text{A.213})$$

$$M_{cvt} = -f_{mw} + f_3 h_3 + f_4 h_4. \quad (\text{A.214})$$

where

$$f_w = f_c(0.5l - x).cov, \quad (\text{A.215})$$

$$h_w = -x_p + x + y, \quad (\text{A.216})$$

$$f_4 = f_c.cov(0.5s - cov), \text{ and} \quad (\text{A.217})$$

$$h_4 = -x_p + x + y. \quad (\text{A.218})$$

The *force* and *lever arm* for *zone 3* are the same as in Eqs.(A.169) and (A.170).

2.5 Subcase 5

In this case, the neutral axis lies in *zone 3*.

2.5.1 Subcase 5.1

The range of strain values is, $\varepsilon_7 < \varepsilon_{lc} < \varepsilon_6$ (Figure A.1g).

$$P_{crt} = f_{wc} + f_{fi2} + f_{fp2}, \text{ and} \quad (\text{A.219})$$

$$M_{crt} = -f_{mwc} + f_{fi2} h_{fi2} + f_{fp2} h_{fp2}. \quad (\text{A.220})$$

The *force* and *lever arm* for *wall* are the same as in Eqs.(A.96) to (A.101).

The *force* and *lever arm* for *zone 2con* are the same as in Eqs.(A.147) and (A.150).

2.5.1.1 Subcase 5.1.1

The range of strain values is, $\varepsilon_7 < -\varepsilon_{02} < \varepsilon_6$.

2.5.1.1.1 Subcase 5.1.1.1

The range of strain values is, $\varepsilon_7 < -\varepsilon_{0I} < \varepsilon_6$ (Figure A.4A).

$$P_{cvt} = f_w + f_3, \text{ and} \quad (\text{A.221})$$

$$M_{cvt} = -f_{mw} + f_3 h_3. \quad (\text{A.222})$$

where

$$f_3 = f_c (0.5l - x - a_o - cov)(0.5s - cov), \text{ and} \quad (\text{A.223})$$

$$h_3 = x + y - x_p. \quad (\text{A.224})$$

The *force* and *lever arm* for *wall* are the same as in Eqs.(A.109) and (A.110).

2.5.2 Subcase 5.2

The range of strain values is, $\varepsilon_7 > \varepsilon_{Ic}$ (Figure A.1h).

$$P_{crt} = f_{wc} + f_{f2}, \text{ and} \quad (\text{A.225})$$

$$M_{crt} = -f_{mwc} + f_{f2} h_{f2}. \quad (\text{A.226})$$

where

$$f_{wc} = f_c (0.5l - x) 0.5t_o, \quad (\text{A.227})$$

$$h_{wc} = x + y_c - x_p, \quad (\text{A.228})$$

$$f_{f2} = f_c s_o 0.5(s_o - t_o), \text{ and} \quad (\text{A.229})$$

$$h_{f2} = x + x_p. \quad (\text{A.230})$$

2.5.2.1 Subcase 5.2.1

The range of strain values is, $\varepsilon_7 < -\varepsilon_{02} < \varepsilon_6$.

2.5.2.1.1 Subcase 5.2.1.1

The range of strain values is, $\varepsilon_7 < -\varepsilon_{0I} < \varepsilon_6$ (Figure A.4c).

$$P_{cvt} = f_w + f_3, \text{ and} \quad (\text{A.231})$$

$$M_{cvt} = -f_{mw} + f_3 h_3. \quad (\text{A.232})$$

The *force* and *lever arm* for *wall* are the same as in Eqs.(A.109) and (A.110).

The *force* and *lever arm* for zone 3 are the same as in Eqs.(A.223) and (A.224).

2.5.2.2 Subcase 5.2.2

The range of strain values is, $\varepsilon_8 < -\varepsilon_{02} < \varepsilon_7$.

2.5.2.2.1 Subcase 5.2.2.1

The range of strain values is, $\varepsilon_7 < -\varepsilon_{01} < \varepsilon_6$ (Figure A.4d).

$$P_{cvt} = f_w + f_3 + f_4, \text{ and} \quad (\text{A.233})$$

$$M_{cvt} = -f_{mw} + f_3 h_3 + f_4 h_4. \quad (\text{A.234})$$

where

$$f_3 = f_c \cdot (x + y - 0.5l + a_o + cov)(0.5s - cov), \text{ and} \quad (\text{A.235})$$

$$h_3 = -x_p + x + y. \quad (\text{A.236})$$

The *force* and *lever arm* for wall are the same as in Eqs.(A.109) and (A.110).

The *force* and *lever arm* for zone 4 are the same as in Eqs.(A.191) and (A.192).

2.5.2.3 Subcase 5.2.3

The range of strain values is, $\varepsilon_8 > -\varepsilon_{02}$.

2.5.2.3.1 Subcase 5.2.3.1

The range of strain values is, $\varepsilon_7 < -\varepsilon_{01} < \varepsilon_6$ (Figure A.4e).

$$P_{cvt} = f_w + f_3 + f_4, \text{ and} \quad (\text{A.237})$$

$$M_{cvt} = -f_{mw} + f_3 h_3 + f_4 h_4. \quad (\text{A.238})$$

The *force* and *lever arm* for wall are the same as in Eqs.(A.197) to (A.202).

The *force* and *lever arm* for zone 3 are the same as in Eqs.(A.235) and (A.236).

The *force* and *lever arm* for zone 4 are the same as in Eqs.(A.203) and (A.204).

2.5.2.3.2 Subcase 5.2.3.2

The range of strain values is, $\varepsilon_8 < -\varepsilon_{01} < \varepsilon_7$ (Figure A.4f).

$$P_{cvt} = f_w + f_3 + f_{4t} + f_{4p}, \text{ and} \quad (\text{A.239})$$

$$M_{cvt} = -f_{mw} + f_3 h_3 + f_{4p} h_{4p} + f_{4t} h_{4t}. \quad (\text{A.240})$$

The *force* and *lever arm* for wall are the same as in Eqs.(A.197) to (A.202).

The *force* and *lever arm* for zone 3 are the same as in Eqs.(A.235) and (A.236).

The *force* and *lever arm* for zone 4 are the same as in Eqs.(A.209) to (A.212).

2.5.2.3.3 Subcase 5.2.3.3

The range of strain values is, $\varepsilon_8 > -\varepsilon_{01}$ (Figure A.4g).

$$P_{cvt} = f_w + f_3 + f_4, \text{ and} \quad (\text{A.241})$$

$$M_{cvt} = -f_{mw} + f_3 h_3 + f_4 h_4. \quad (\text{A.242})$$

The *force* and *lever arm* for *wall* are the same as in Eqs.(A.215) and (A.216).

The *force* and *lever arm* for *zone 3* are the same as in Eqs.(A.235) and (A.236).

The *force* and *lever arm* for *zone 4* are the same as in Eqs.(A.217) and (A.218).

2.6 Subcase 6

In this case, the neutral axis lies between *zones 3* and *4*.

2.6.1 Subcase 6.1

The range of strain values is, $\varepsilon_7 > \varepsilon_{1c}$ (Figure A.1i).

$$P_{crt} = f_{wc} + f_{f2}, \text{ and} \quad (\text{A.243})$$

$$M_{crt} = -f_{mwc} + f_{f2} h_{f2}. \quad (\text{A.244})$$

where

$$f_{f2} = f_c (0.5l - x) 0.5(s_o - t_o), \text{ and} \quad (\text{A.245})$$

$$h_{f2} = x + x_p. \quad (\text{A.246})$$

The *force* and *lever arm* for *wall* are the same as in Eqs.(A.227) and (A.228).

2.6.1.1 Subcase 6.1.1

The range of strain values is, $\varepsilon_8 < -\varepsilon_{02} < \varepsilon_7$.

2.6.1.1.1 Subcase 6.1.1.1

The range of strain values is, $\varepsilon_7 < -\varepsilon_{01} < \varepsilon_6$ (Figure A.4h).

$$P_{cvt} = f_w + f_4, \text{ and} \quad (\text{A.247})$$

$$M_{cvt} = -f_{mw} + f_4 h_4. \quad (\text{A.248})$$

The *force* and *lever arm* for *wall* are the same as in Eqs.(A.109) and (A.110).

The *force* and *lever arm* for *zone 4* are the same as in Eqs.(A.191) and (A.192).

2.6.1.2 Subcase 6.1.2

The range of strain values is, $\varepsilon_8 > -\varepsilon_{02}$.

2.6.1.2.1 Subcase 6.1.2.1

The range of strain values is, $\varepsilon_7 < -\varepsilon_{01} < \varepsilon_6$ (Figure A.4i).

$$P_{cvt} = f_w + f_4, \text{ and} \quad (\text{A.249})$$

$$M_{cvt} = -f_{mw} + f_4 h_4. \quad (\text{A.250})$$

The *force* and *lever arm* for *wall* and *zone 4* are the same as in Eqs.(A.197) to (A.204).

2.6.1.2.2 Subcase 6.1.2.2

The range of strain values is, $\varepsilon_8 < -\varepsilon_{0I} < \varepsilon_7$ (Figure A.4j).

$$P_{cvt} = f_w + f_4, \text{ and} \quad (\text{A.251})$$

$$M_{cvt} = -f_{mw} + f_4 h_4. \quad (\text{A.252})$$

The *force* and *lever arm* for *wall* are the same as in Eqs.(A.197) to (A.202).

The *force* and *lever arm* for *zone 4* are the same as in Eqs.(A.209) to (A.212).

2.6.1.2.3 Subcase 6.1.2.3

The range of strain values is, $\varepsilon_8 > -\varepsilon_{0I}$ (Figure A.4k).

$$P_{cvt} = f_w + f_4, \text{ and} \quad (\text{A.253})$$

$$M_{cvt} = -f_{mw} + f_4 h_4. \quad (\text{A.254})$$

The *force* and *lever arm* for *wall* are the same as in Eqs.(A.235) and (A.236).

The *force* and *lever arm* for *zone 4* are the same as in Eqs.(A.217) and (A.218).

2.7 Subcase 7

In this case, the neutral axis lies between *zones 3* and *4*.

2.7.1 Subcase 7.1

The range of strain values is, $\varepsilon_7 > \varepsilon_{1c}$ (Figure A.1i).

$$P_{crt} = f_{wc} + f_{f2}, \text{ and} \quad (\text{A.255})$$

$$M_{crt} = -f_{mwc} + f_{f2} h_{f2}. \quad (\text{A.256})$$

where

The *force* and *lever arm* for *wall* are the same as in Eqs.(A.227) and (A.228).

The *force* and *lever arm* for *zone 2con* are the same as in Eqs.(A.245) and (A.246).

2.7.1.1 Subcase 7.1.1

The range of strain values is, $\varepsilon_8 > -\varepsilon_{02}$.

2.6.1.1.1 Subcase 7.1.1.1

The range of strain values is, $\varepsilon_8 > -\varepsilon_{0I}$ (Figure A.4l).

$$P_{cvt} = f_w + f_4, \text{ and} \quad (\text{A.257})$$

$$M_{cvt} = -f_{mw} + f_4 h_4. \quad (\text{A.258})$$

where

$$f_w = f_c \cdot (0.5l - x) cov, \text{ and} \quad (\text{A.259})$$

$$h_w = -x_p + x + y. \quad (\text{A.260})$$

$$f_4 = f_c \cdot (0.5l - x)(0.5s - cov), \text{ and} \quad (\text{A.261})$$

$$h_4 = -x_p + x + y. \quad (\text{A.262})$$

Table A1: Index Table of Figures for Appendices A and B

Subcase		Figure	
Confined concrete	Unconfined Concrete	Confined concrete	Unconfined Concrete
1.1	1.1.1	A.1a	-
1.2	1.2.1	A.1b	A.2a
	1.2.2	A.1b	-
1.3	1.3.1	A.1c	-
	1.3.2.1	A.1c	A.2a
	1.3.3.1	A.1c	A.2b
	1.3.3.2	A.1c	A.2c
	1.3.3.2	A.1c	A.2d
	1.3.4.1	A.1c	A.2e
	1.3.4.2	A.1c	A.2f
	1.3.4.3	A.1c	A.2g
	1.3.4.1	A.1c	A.2h
	1.3.4.2	A.1c	A.2i
	1.3.4.3	A.1c	A.2j
	1.3.4.1	A.1c	A.2k
	1.3.4.2	A.1c	A.2l
2.1.1	2.1.1.1.1	A.1d	A.3a
	2.1.1.1.2	A.1d	A.3b
	2.1.1.1.3	A.1d	A.3c
2.2.1	2.2.1.1.1	A.1e	A.3d
	2.2.1.1.2	A.1e	A.3e
	2.2.1.1.3	A.1e	A.3f
2.3.1	2.3.1.1.1	A.1f	A.3g
2.4.1	2.4.1.1.1	A.1f	A.3h
2.4.2	2.4.2.1.1	A.1g	A.3h
	2.4.2.2.1	A.1g	A.3i
	2.4.2.3.1	A.1g	A.3j
	2.4.2.3.2	A.1g	A.3k
	2.4.2.3.3	A.1g	A.3l
2.4.3	2.4.3.1.1	A.1h	A.3h
	2.4.3.2.1	A.1h	A.3i
	2.4.3.3.1	A.1h	A.3j
	2.4.3.3.2	A.1h	A.3k
	2.4.3.3.3	A.1h	A.3l
	2.4.3.4.1	A.1h	A.3m
	2.4.3.4.2	A.1h	A.3n
	2.4.3.5.1	A.1h	A.3o
	2.4.3.5.2	A.1h	A.3p
	2.4.3.5.3	A.1h	A.4a
	2.4.3.5.4	A.1h	A.4b
2.5.1	2.5.1.1.1	A.1g	A.4c
2.5.2	2.5.2.1.1	A.1h	A.4c
	2.5.2.2.1	A.1h	A.4d
	2.5.2.3.1	A.1h	A.4e
	2.5.2.3.2	A.1h	A.4f
	2.5.2.3.3	A.1h	A.4g
2.6.1	2.6.1.1.1	A.1i	A.4h
	2.6.1.2.1	A.1i	A.4i
	2.6.1.2.2	A.1i	A.4j
	2.6.1.2.3	A.1i	A.4k
2.7.1	2.7.1.1.1	A.1i	A.4l

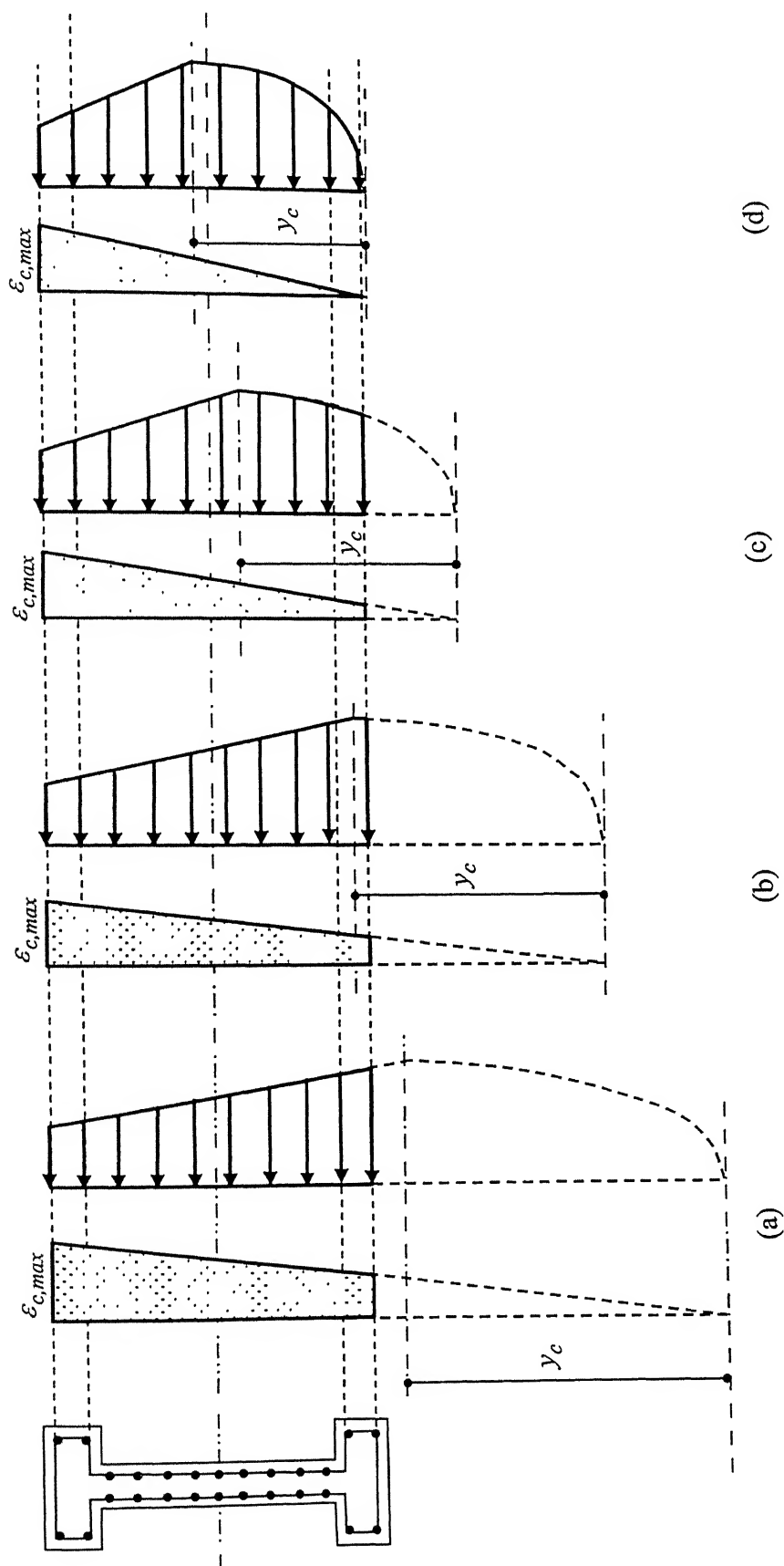


Figure A.1: Progressive movement of NA in the section with associated strain and stress variations in confined concrete.

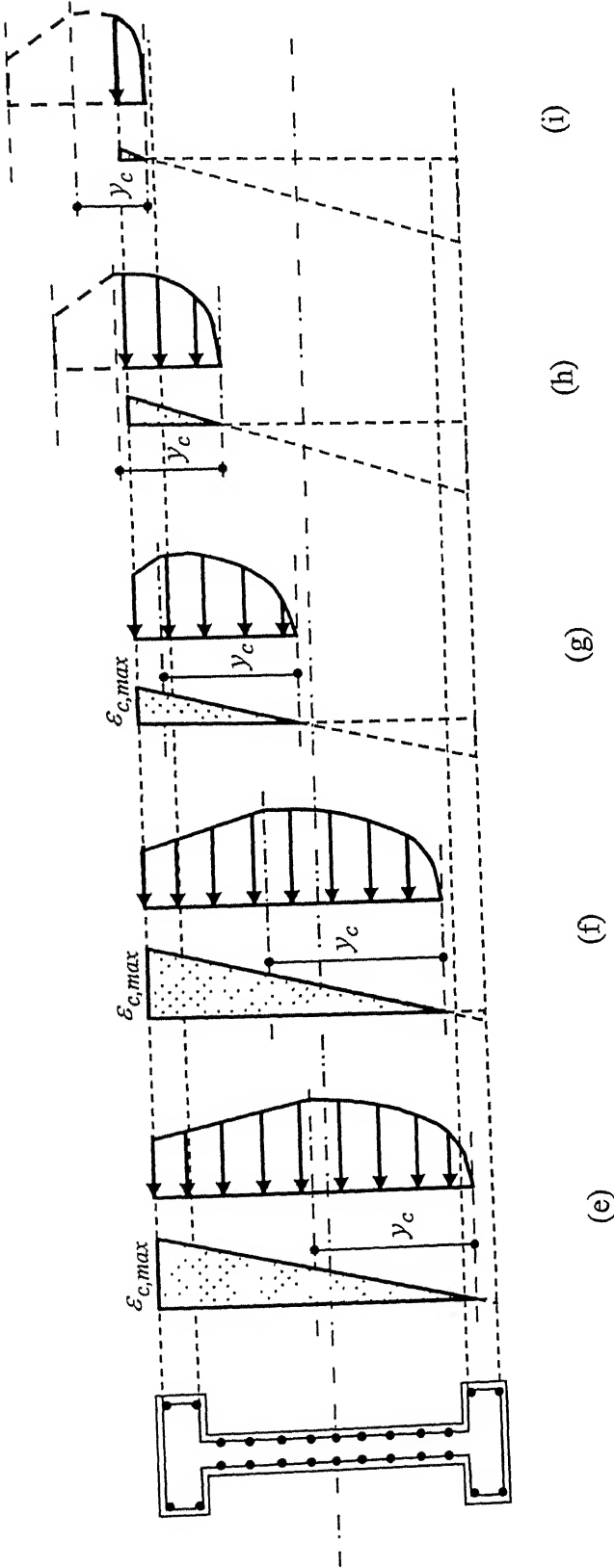


Figure A.1 contd...

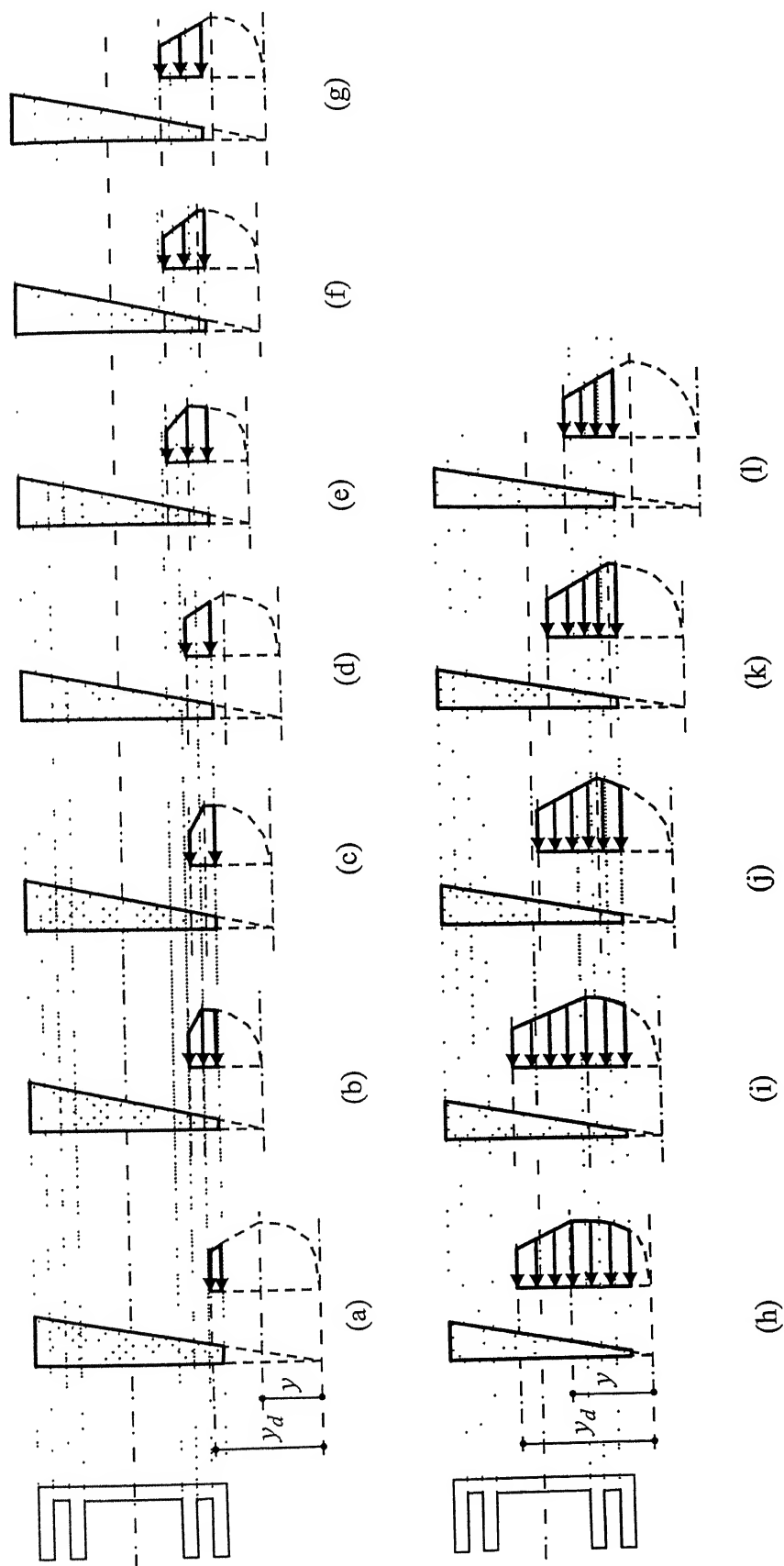


Figure A.2: Progressive movement of NA in the section, associated strain and stress variations in unconfined concrete

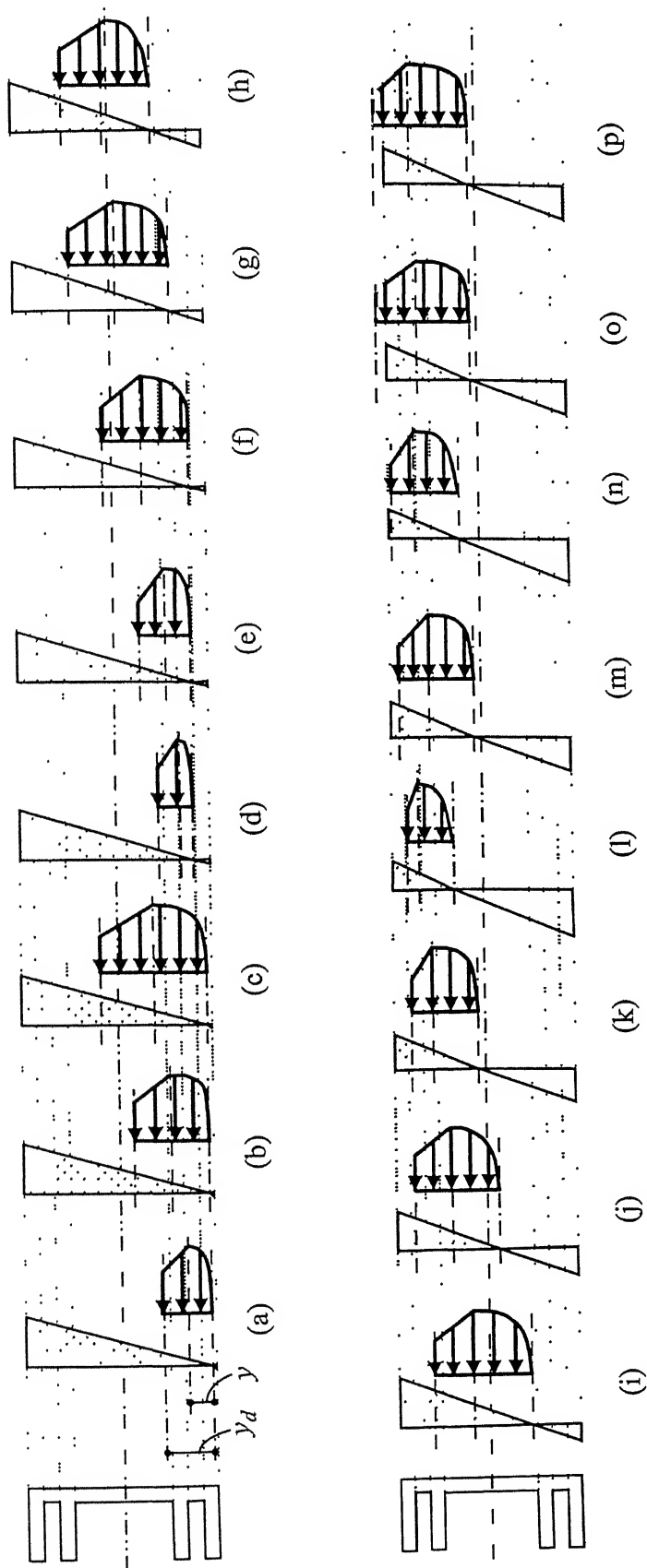


Figure A.3: Progressive movement of NA in the section with associated strain and stress variations in unconfined concrete.

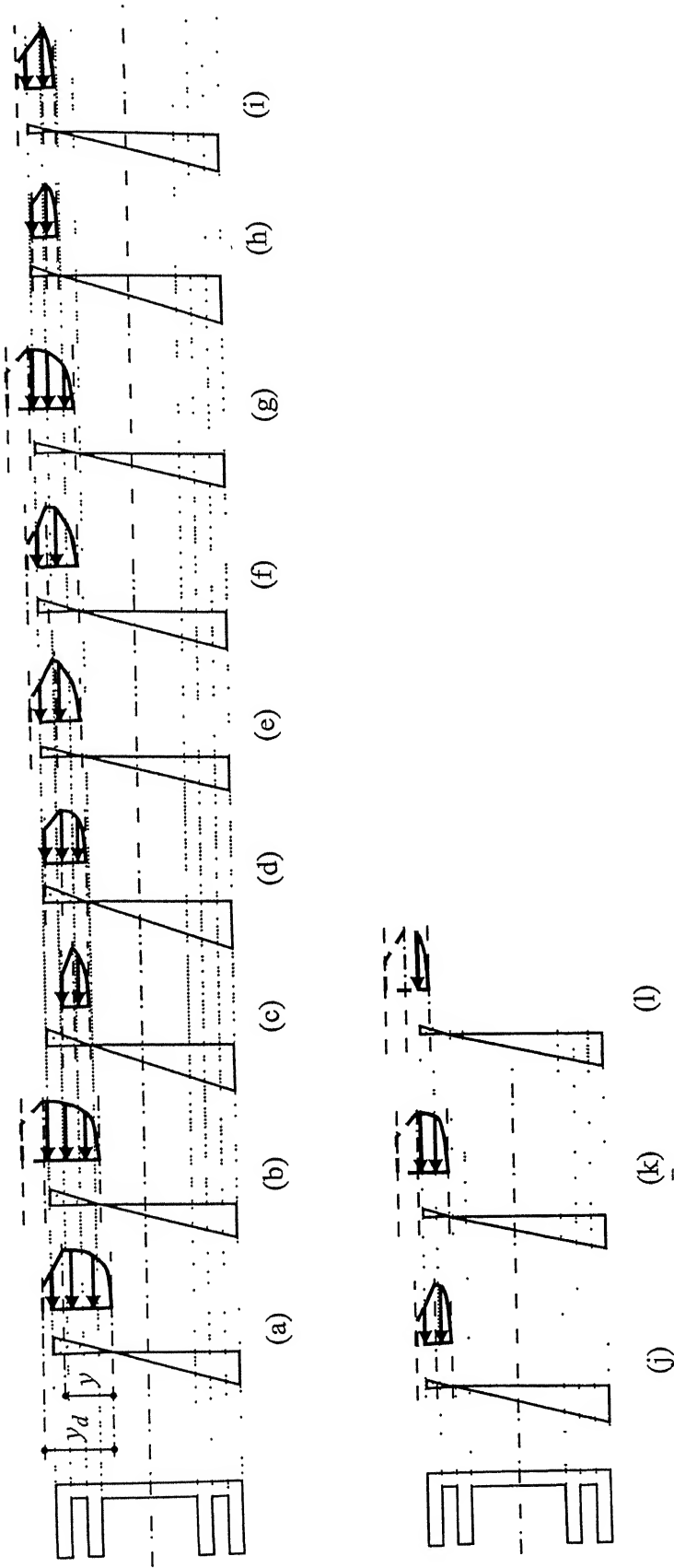


Figure A.4: Progressive movement of NA in the section with associated strain and stress variations in unconfined concrete.

Appendix B

Equations for Overstrength P-M Interaction Curve for Unconfined Web Concrete

The P-M interaction curve has been divided into three segments, namely AB, BC and CD, depending on the strain distribution across the section. The same figures are referred for the subcases as in Appendix A.

1.0 Segment AB

Total axial load and moment of resistance are given by

$$(P_{\Omega})_{AB} = 2(P_{cvt} + P_{crt}) + \sum_{i=1}^n A_{si} \sigma_{si}, \text{ and} \quad (\text{D.1})$$

$$(M_{\Omega})_{AB} = 2(M_{cvt} + M_{crt}) + \sum_{i=1}^n A_{si} \sigma_{si} (0.5l - y_{si}). \quad (\text{D.2})$$

1.1 Subcase 1

The strain condition for this case is, $\varepsilon_2 < \varepsilon_1$.

$$P_{crt} = f_{f1} + f_{f2}, \text{ and} \quad (\text{D.3})$$

$$M_{crt} = f_{f1} h_{f1} + f_{f2} h_{f2}. \quad (\text{D.4})$$

where

$$f_{f2} = 0.5(f_{6c} + f_{7c})(0.5a_o)s_o, \quad (\text{D.5})$$

$$h_{f2} = (0.5dl_o - a_o) + \frac{a_o}{3} \left(\frac{f_{6c} + 2f_{7c}}{f_{6c} + f_{7c}} \right), \quad (\text{D.6})$$

$$f_{f1} = 0.5(f_{2c} + f_{3c})(0.5c_o)r_o, \text{ and} \quad (\text{D.7})$$

$$h_{f1} = 0.5dl_o - \frac{c_o}{3} \left(\frac{f_{2c} + 2f_{3c}}{f_{2c} + f_{3c}} \right). \quad (\text{D.8})$$

1.1.1 Subcase 1.1

The strain condition for this case is, $\varepsilon_2 < -\varepsilon_{02}$.

$$P_{cvt} = 0, \text{ and} \quad (\text{D.9})$$

$$M_{cvt} = 0. \quad (\text{D.10})$$

1.2 Subcase 2

The strain condition for this case is, $\varepsilon_3 < \varepsilon_{lc} < \varepsilon_2$.

$$P_{crt} = f_{ftl} + f_{fp1} + f_{f2}, \text{ and} \quad (\text{D.11})$$

$$M_{crt} = -f_{ftl}h_{ftl} - f_{fp1}h_{fp1} + f_{f2}h_{f2}. \quad (\text{D.12})$$

where

$$f_{ftl} = 0.5(f_{3c} + f_{cc})(-x - y_c - 0.5dl_o + c_o)[0.5r_o], \quad (\text{D.13})$$

$$h_{ftl} = (-x - y_c) - \frac{(x + y_c - 0.5dl_o + c_o)}{3} \left(\frac{f_{cc} + 2f_{3c}}{f_{cc} + f_{3c}} \right), \quad (\text{D.14})$$

$$f_{fp1} = f_c(y_c + x + 0.5dl_o)[0.5r_o], \quad (\text{D.15})$$

$$h_{fp1} = -pl - x, \text{ and} \quad (\text{D.16})$$

$$y_c = \varepsilon_l \frac{(0.5l - x)}{\varepsilon_{8a}}. \quad (\text{D.17})$$

The expression for f_{f2} remains the same as in Eqs.(D.5) and (D.6).

1.2.1 Subcase 2.1

The strain condition for this case is, $\varepsilon_2 < (-\varepsilon_{02}) < \varepsilon_3$.

Axial load and moment of resistance are given by

$$P_{cvt} = f_w + f_l, \text{ and} \quad (\text{D.18})$$

$$M_{cvt} = -f_{mw} - f_l h_l, \quad (\text{D.19})$$

where

$$f_w = 0.5(-0.136f_{ck} + f_{la})(0.5l + x + y_d)0.5t, \quad (\text{D.20})$$

$$h_w = 0.5l - \frac{(0.5l + x + y_d)}{3} \left(\frac{f_{la} - 0.272f_{ck}}{f_{la} - 0.136f_{ck}} \right). \quad (\text{D.21})$$

$$f_l = 0.5(-0.136f_{ck} + f_{la})(0.5l + y_d + x)(0.5r), \quad (\text{D.22})$$

$$h_l = 0.5l - \frac{(0.5l + y_d + x)}{3} \left(\frac{-0.272f_{ck} + f_{la}}{-0.136f_{ck} + f_{la}} \right). \quad (\text{D.23})$$

$$y = -\varepsilon_{0l} \frac{(0.5l - x)}{\varepsilon_{8a}}, \text{ and} \quad (\text{D.24})$$

$$y_d = -0.0035 \frac{(0.5l - x)}{\varepsilon_{8a}}. \quad (\text{D.25})$$

1.2.2 Subcase 2.2

The strain condition for this case is, $\varepsilon_1 < -\varepsilon_{02}$.

$$P_{cvt} = 0, \text{ and} \quad (\text{D.26})$$

$$M_{cvt} = 0. \quad (\text{D.27})$$

1.3 Subcase 3

The strain condition for this case is, $\varepsilon_6 < \varepsilon_{1c} < \varepsilon_3$

$$P_{crt} = f_{f1} + f_{f2}, \text{ and} \quad (\text{D.28})$$

$$M_{crt} = f_{mwc} - f_{f1}h_{f1} + f_{f2}h_{f2}, \quad (\text{D.29})$$

where

$$f_{f2} = 0.5(f_{6c} + f_{7c})(0.5a_o)s_o, \text{ and} \quad (\text{D.30})$$

$$h_{f2} = 0.5dl_o - a_o + \frac{a_o}{3} \left(\frac{f_{6c} + 2f_{7c}}{f_{6c} + f_{7c}} \right). \quad (\text{D.31})$$

$$f_{f1} = f_c c_o 0.5r_o, \quad (\text{D.32})$$

$$h_{f1} = -p_l - x, \text{ and} \quad (\text{D.33})$$

$$y_c = \varepsilon_1 \frac{(0.5l - x)}{\varepsilon_{8a}}. \quad (\text{D.34})$$

1.3.1 Subcase 3.1

The strain condition for this case is, $\varepsilon_1 < -\varepsilon_{02}$

$$P_{cvt} = 0, \text{ and} \quad (\text{D.35})$$

$$M_{cvt} = 0. \quad (\text{D.36})$$

1.3.2 Subcase 3.2

The strain condition for this case is, $\varepsilon_2 < -\varepsilon_{02} < \varepsilon_1$.

The expressions are remain the same as given in Eqs. (D.18) and (D.25).

1.3.3 Subcase 3.3

The strain condition for this case is, $\varepsilon_3 < -\varepsilon_{02} < \varepsilon_2$.

1.3.3.1 Subcase 3.3.1

The strain condition for this case is, $\varepsilon_3 < -\varepsilon_{0l} < \varepsilon_2$.

$$P_{cvt} = f_w + f_l, \text{ and} \quad (\text{D.37})$$

$$M_{cvt} = -f_{mw} - f_l h_l. \quad (\text{D.38})$$

where

$$f_w = f_{wt} + f_{wp}, \quad (\text{D.39})$$

$$f_{mw} = f_{wt} h_{wt} + f_{wp} h_{wp}, \quad (\text{D.40})$$

$$f_{wt} = -0.408 f_{ck} (y_d - y) t, \quad (\text{D.41})$$

$$h_{wt} = -x - 0.389 y_d - 0.611 y; \quad (\text{D.42})$$

$$f_{wp} = f_c (0.5l + y + x) t, \quad (\text{D.43})$$

$$h_{wp} = x_p - x - y, \quad (\text{D.44})$$

$$f_l = f_c \text{cov}(0.5r), \text{ and} \quad (\text{D.45})$$

$$h_l = pl - x - y. \quad (\text{D.46})$$

1.3.3.2 Subcase 3.3.2

The strain condition for this case is, $\varepsilon_2 < -\varepsilon_{0l} < \varepsilon_1$.

$$P_{cvt} = f_w + f_{lt} + f_{lp}, \text{ and} \quad (\text{D.47})$$

$$M_{cvt} = -f_{mw} - f_{lt} h_{lt} - f_{lp} h_{lp}. \quad (\text{D.48})$$

where

$$f_{lt} = 0.5(-0.68 f_{ck} + f_{2a})(0.5r - t)(-x - y - 0.5l + \text{cov}), \quad (\text{D.49})$$

$$h_{lt} = (-x - y) - \frac{(-x - y - 0.5l + \text{cov})}{3} \left(\frac{-0.68 f_{ck} + 2f_{2a}}{-0.68 f_{ck} + f_{2a}} \right), \quad (\text{D.50})$$

$$f_{lp} = f_c (y + 0.5l + x)(0.5r - \text{cov}), \text{ and} \quad (\text{D.51})$$

$$h_{lp} = x_p - x - y. \quad (\text{D.52})$$

The expressions for the wall are the same as in Eqs.(D.39) to (D.44).

1.3.3.3 Subcase 3.3.3

The strain condition for this case is, $\varepsilon_1 < -\varepsilon_{0l}$.

$$P_{cvt} = f_w + f_l, \text{ and} \quad (\text{D.53})$$

$$M_{cvt} = -f_{mw} - f_l h_l, \quad (\text{D.54})$$

where

$$f_1 = 0.5(f_{1a} + f_{2a})(0.5r - t)cov, \text{ and} \quad (D.55)$$

$$h_1 = 0.5l - \frac{cov}{3} \left(\frac{f_{1a} + 2f_{2a}}{f_{1a} + f_{2a}} \right). \quad (D.56)$$

The expressions for force and moment in wall are same as in Eqs.(D.20) and (D.21).

1.3.4 Subcase 3.4

The strain condition for this case is, $\varepsilon_4 < -\varepsilon_{02} < \varepsilon_3$.

1.3.4.1 Subcase 3.4.1

The strain condition for this case is, $\varepsilon_3 < -\varepsilon_{01} < \varepsilon_2$.

$$P_{cvt} = f_w + f_1 + f_2, \text{ and} \quad (D.57)$$

$$M_{cvt} = -f_{mw} - f_1 h_1 - f_2 h_2, \quad (D.58)$$

where

$$f_2 = 0.5(-0.136f_{ck} + f_{3a})(0.5l - cov - c_o + x + y_d)(0.5r - t), \text{ and} \quad (D.59)$$

$$h_2 = 0.5l - \frac{(0.5l - cov - c_o + x + y_d)}{3} \left(\frac{f_{3a} - 0.272f_{ck}}{f_{3a} - 0.136f_{ck}} \right). \quad (D.60)$$

The values of the parameters for *zone 1* are the same as in Eqs.(D.45) and (D.46).

The values of the parameters for wall are same as in Eqs.(D.39) to (D.44).

1.3.4.2 Subcase 3.4.2

The strain condition for this case is, $\varepsilon_2 < -\varepsilon_{01} < \varepsilon_1$.

$$P_{cvt} = f_w + f_2 + f_{1t} + f_{1p}, \text{ and} \quad (D.61)$$

$$M_{cvt} = -f_{mw} - f_2 h_2 - f_{1t} h_{1t} - f_{1p} h_{1p}. \quad (D.62)$$

The values of the parameters for wall are the same as given in Eqs.(D.39) to (D.40).

The values of the parameters for *zone 1* are the same as given in Eqs.(D.49) to (D.52).

The values of the parameters for *zone 2* are the same as given in Eqs.(D.59) and (D.60).

1.3.4.3 Subcase 3.4.3

The strain condition for this case is, $\varepsilon_1 < -\varepsilon_{01}$.

$$P_{cvt} = f_w + f_1 + f_2, \text{ and} \quad (D.63)$$

$$M_{cvt} = -f_{mw} - f_1 h_1 - f_2 h_2. \quad (D.64)$$

The values of the parameters for wall are the same as in Eqs.(D.20) and (D.21).

The values of the parameters for *zone 1* are the same as in Eqs.(D.55) and (D.56).

The values of the parameters for *zone 2* are the same as in Eqs.(D.59) and (D.60).

1.3.5 Subcase 3.5

The strain condition for this case is, $\varepsilon_5 < -\varepsilon_{02} < \varepsilon_4$.

1.3.5.1 Subcase 3.5.1

The strain condition for this case is, $\varepsilon_5 < -\varepsilon_{01} < \varepsilon_4$.

$$P_{cvt} = f_w + f_1 + f_2, \text{ and} \quad (D.65)$$

$$M_{cvt} = -f_{mw} - f_1 h_1 - f_2 h_2, \quad (D.66)$$

where

$$f_2 = f_c \cos(0.5r - t), \text{ and} \quad (D.67)$$

$$h_2 = x_p - x - y. \quad (D.68)$$

The values of the parameters for wall are the same as in Eqs.(D.39) to (D.44).

The values of the parameters for *zone 1* are the same as in Eqs.(D.45) and (D.46).

1.3.5.2 Subcase 3.5.2

The strain condition for this case is, $\varepsilon_4 < -\varepsilon_{01} < \varepsilon_3$.

$$P_{cvt} = f_w + f_{2t} + f_{2p} + f_1, \text{ and} \quad (D.69)$$

$$M_{cvt} = -f_{mw} - f_{2t} h_{2t} - f_{2p} h_{2p} - f_1 h_1, \quad (D.70)$$

where

$$f_{2t} = 0.5(-0.68f_{ck} + f_{4a})(-0.5l - x - y + c)(0.5r - t), \quad (D.71)$$

$$h_{2t} = (-x - y) - \frac{(-0.5l - x - y + c)}{3} \left(\frac{-0.68f_{ck} + 2f_{4a}}{-0.68f_{ck} + f_{4a}} \right), \quad (D.72)$$

$$f_{2p} = f_c(y + 0.5l + x - c_o - \cos)(0.5r - t), \text{ and} \quad (D.73)$$

$$h_{2p} = x_p - x - y. \quad (D.74)$$

The values of the parameters for wall are the same as in Eqs.(D.39) to (D.44).

The values of the parameters for *zone 1* are the same as in Eqs.(D.45) and (D.46).

1.3.5.3 Subcase 3.5.3

The strain condition for this case is, $\varepsilon_3 < -\varepsilon_{02} < \varepsilon_2$.

$$P_{cvt} = f_w + f_1 + f_2, \text{ and} \quad (D.75)$$

$$M_{cvt} = -f_{mw} - f_1 h_1 - f_2 h_2, \quad (D.76)$$

where

$$f_2 = 0.5(f_{4a} + f_{3a})\text{cov}(0.5r - t), \text{ and} \quad (D.77)$$

$$h_2 = (0.5l - \text{cov} - c_o) - \frac{\text{cov}}{3} \left(\frac{f_{3a} + 2f_{4a}}{f_{3a} + f_{4a}} \right). \quad (D.78)$$

The values of the parameters for wall are the same as in Eqs.(D.39) to (D.44).

The values of the parameters for *zone 1* are the same as in Eqs.(D.45) and (D.46).

1.3.5.4 Subcase 3.5.4

The strain condition for this case is, $\varepsilon_2 < -\varepsilon_{0l} < \varepsilon_1$.

Axial load and moment of resistance are given by

$$P_{cvt} = f_w + f_{1t} + f_{1p} + f_2, \text{ and} \quad (D.79)$$

$$M_{cvt} = -f_{mw} - f_{1t} h_{1t} - f_{1p} h_{1p} - f_2 h_2. \quad (D.80)$$

The values of the parameters for wall are the same as in Eqs.(D.39) to (D.44).

The values of the parameters for *zone 1* are the same as in Eqs.(D.49) and (D.52).

The values of the parameters for *zone 2* are the same as in Eqs.(D.77) and (D.78).

1.3.5.5 Subcase 3.5.5

The strain condition for this case is, $\varepsilon_1 < -\varepsilon_{0l}$.

$$P_{cvt} = f_w + f_1 + f_2, \text{ and} \quad (D.81)$$

$$M_{cvt} = -f_{mw} - f_1 h_1 - f_2 h_2. \quad (D.82)$$

The values of the parameters for wall are the same as in Eqs.(D.20) and (D.21).

The values of the parameters for *zone 1* are the same as in Eqs.(D.55) and (D.56).

The values of the parameters for *zone 2* are the same as in Eqs.(D.77) and (D.78).

2.0 Segment BC

Total axial load and moment of resistance are given by

$$(P_\Omega)_{BC} = 2(P_{cvt} + P_{crt}) + \sum_{i=1}^n A_{si} \sigma_{si}, \text{ and} \quad (D.83)$$

$$(M_\Omega)_{BC} = 2(M_{cvt} + M_{crt}) + \sum_{i=1}^n A_{si} \sigma_{si} (0.5l - y_{si}). \quad (D.84)$$

2.1 Subcase 1

For this case, the neutral axis lies in *zone 1*.

2.1.1 Subcase 1.1

The strain condition for this case is, $\varepsilon_6 < \varepsilon_{1c} < \varepsilon_3$.

$$P_{crt} = f_{f1} + f_{f2}, \text{ and} \quad (D.85)$$

$$M_{crt} = -f_{f1}h_{f1} + f_{f2}h_{f2}. \quad (D.86)$$

where

$$f_{f2} = 0.5(f_{6c} + f_{7c})(0.5a_o)s_o, \quad (D.87)$$

$$h_{f2} = (0.5dl_o - a_o) + \frac{a_o}{3} \left(\frac{f_{6c} + 2f_{7c}}{f_{6c} + f_{7c}} \right), \quad (D.88)$$

$$f_{f1} = f_c(0.5r_o)c_o, \text{ and} \quad (D.89)$$

$$h_{f1} = -p_l - x. \quad (D.90)$$

2.1.1.1 Subcase 1.1.1

The strain condition for this case is, $\varepsilon_5 < \varepsilon_{1c} < \varepsilon_4$.

$$P_{cvt} = f_w + f_1 + f_2, \text{ and} \quad (D.91)$$

$$M_{cvt} = -f_{mw} - f_1h_1 - f_2h_2. \quad (D.92)$$

where

$$f_{mw} = f_w h_w, \quad (D.93)$$

$$f_w = -0.36f_{ck}y_d t, \text{ and} \quad (D.94)$$

$$h_w = -x - 0.58y_d \quad (D.95)$$

$$f_1 = f_c[y - cov + 0.5l + x](0.5r - t), \quad (D.96)$$

$$h_1 = x_p - x - y. \quad (D.97)$$

$$f_2 = 0.5[f_{4a} + f_{3a}](0.5r - t)cov, \text{ and} \quad (D.98)$$

$$h_2 = (0.5l - c) + \frac{cov}{3} \left(\frac{f_{3a} + 2f_{4a}}{f_{3a} + f_{4a}} \right). \quad (D.99)$$

2.1.1.2 Subcase 1.1.2

The strain condition for this case is, $\varepsilon_4 < -\varepsilon_{01} < \varepsilon_3$.

$$P_{cvt} = f_w + f_{2t} + f_{2p} + f_1, \text{ and} \quad (D.100)$$

$$M_{cvt} = -f_{mw} - f_{2t}h_{2t} - f_{2p}h_{2p} - f_1h_1, \quad (D.101)$$

The values of the parameters for wall are the same as in Eqs.(D.93) to (D.95).

The values of the parameters for *zone 1* are the same as in Eqs.(D.96) and (D.97).

The values of the parameters for *zone 2* are the same as in Eqs.(D.71) and (D.74).

2.1.1.3 Subcase 1.1.3

The strain condition for this case is, $\varepsilon_5 < -\varepsilon_{01} < \varepsilon_4$.

$$P_{cvt} = f_w + f_1 + f_2, \text{ and} \quad (D.102)$$

$$M_{cvt} = -f_{mw} - f_1h_1 - f_2h_2. \quad (D.103)$$

where

$$f_2 = f_c(0.5r - t)_{cov}, \text{ and} \quad (D.104)$$

$$h_2 = x_p - x - y. \quad (D.105)$$

The values of the parameters for wall are the same as in Eqs.(D.93) to (D.95).

The values of the parameters for *zone 1* are the same as in Eqs.(D.96) and (D.97).

2.2 Subcase 2

For this case, the neutral axis lies between *zones 1* and *2*.

2.2.1 Subcase 2.1

The strain condition for this case is, $\varepsilon_6 < \varepsilon_{1c} < \varepsilon_3$.

$$P_{crt} = f_{f1} + f_{f2}, \text{ and} \quad (D.106)$$

$$M_{crt} = -f_{f1}h_{f1} + f_{f2}h_{f2}. \quad (D.107)$$

where

$$f_{f1} = f_c(0.5r_o)(-x - 0.5dl_o + c_o), \text{ and} \quad (D.108)$$

$$h_{f1} = -p_l - x. \quad (D.109)$$

The values of the parameters for *zone 2con* are the same as in Eqs.(D.87) and (D.88).

2.2.1.1 Subcase 2.1.1

The strain condition for this case is, $\varepsilon_5 < -\varepsilon_{02} < \varepsilon_4$.

2.2.1.1.1 Subcase 2.1.1.1

The strain condition for this case is, $\varepsilon_3 < -\varepsilon_{01} < \varepsilon_2$.

$$P_{cvt} = f_w + f_2, \text{ and} \quad (D.110)$$

$$M_{cvt} = -f_{mw} - f_2 h_2. \quad (\text{D.111})$$

The values of the parameters for wall are the same as in Eqs.(D.93) to (D.95).

The values of the parameters for *zone 2* are the same as in Eqs.(D.98) and (D.99).

2.2.1.1.2 Subcase 2.1.1.2

The strain condition for this case is, $\varepsilon_4 < -\varepsilon_{0l} < \varepsilon_3$.

$$P_{cvt} = f_w + f_{2t} + f_{2p}, \text{ and} \quad (\text{D.112})$$

$$M_{cvt} = -f_{mw} - f_{2t} h_{2t} - f_{2p} h_{2p}. \quad (\text{D.113})$$

The values of the parameters for wall are the same as in Eqs.(D.93) to (D.95).

The values of the parameters for *zone 2* are the same as in Eqs.(D.71) and (D.74).

2.2.1.1.3 Subcase 2.1.1.3

The strain condition for this case is, $\varepsilon_5 < -\varepsilon_{0l} < \varepsilon_4$.

$$P_{cvt} = f_w + f_2, \text{ and} \quad (\text{D.114})$$

$$M_{cvt} = -f_{mw} - f_2 h_2. \quad (\text{D.115})$$

The values of the parameters for wall are the same as in Eqs.(D.93) to (D.95).

The values of the parameters for *zone 2* are the same as in Eqs.(D.98) and (D.99).

2.3 Subcase 3

For this case, the neutral axis lies in *zone 2*.

2.3.1 Subcase 3.1

The strain condition for this case is, $\varepsilon_6 < \varepsilon_{lc} < \varepsilon_3$.

$$P_{crt} = f_{f2}, \text{ and} \quad (\text{D.116})$$

$$M_{crt} = f_{f2} h_{f2}. \quad (\text{D.117})$$

The values of the parameters for *zone 2con* are the same as in Eqs.(D.87) and (D.88).

2.3.1.1 Subcase 3.1.1

The strain condition for this case is, $\varepsilon_5 < -\varepsilon_{02} < \varepsilon_4$.

2.3.1.1.1 Subcase 3.1.1.1

The strain condition for this case is, $\varepsilon_5 < -\varepsilon_{0l} < \varepsilon_4$.

$$P_{cvt} = f_w + f_2, \text{ and} \quad (\text{D.118})$$

$$M_{cvt} = -f_{mw} - f_2 h_2. \quad (\text{D.119})$$

where

$$f_2 = f_c(-0.5l - x + c)(0.5r - t), \text{ and} \quad (\text{D.120})$$

$$h_2 = x_p - x - y. \quad (\text{D.121})$$

The values of the parameters for wall are the same as in Eqs.(D.93) to (D.95).

2.4 Subcase 4

For this case, the neutral axis lies between *zones* 2 and 3.

2.4.1 Subcase 4.1

The strain condition for this case is, $\varepsilon_6 < \varepsilon_{1c} < \varepsilon_3$.

$$P_{crt} = f_{f2}, \text{ and} \quad (\text{D.122})$$

$$M_{crt} = f_{f2} h_{f2}. \quad (\text{D.123})$$

The values of the parameters for *zone 2con* are the same as in Eqs.(D.87) and (D.88).

2.4.1.1 Subcase 4.1.1

The strain condition for this case is, $\varepsilon_5 < -\varepsilon_{02} < \varepsilon_4$.

2.4.1.1.1 Subcase 4.1.1.1

The strain condition for this case is, $\varepsilon_5 < -\varepsilon_{01} < \varepsilon_4$.

$$P_{cvt} = f_w, \text{ and} \quad (\text{D.124})$$

$$M_{cvt} = -f_{mw}. \quad (\text{D.125})$$

The values of the parameters for wall are the same as in Eqs.(D.93) to (D.95).

2.4.2 Subcase 4.2

The strain condition for this case is, $\varepsilon_7 < \varepsilon_{1c} < \varepsilon_6$.

$$P_{crt} = f_{f12} + f_{fp2}, \text{ and} \quad (\text{D.126})$$

$$M_{crt} = f_{f12} h_{f12} + f_{fp2} h_{fp2}. \quad (\text{D.127})$$

where

$$f_{f12} = 0.5(f_{cc} + f_{7c})(0.5s_o)(0.5dl_o - y_c - x), \quad (\text{D.128})$$

$$h_{f12} = (y_c + x) - \frac{(0.5dl_o - y_c - x)}{3} \left(\frac{f_{cc} + 2f_{7c}}{f_{cc} + f_{7c}} \right), \quad (\text{D.129})$$

$$f_{fp2} = f_c(0.5s_o)(y_c + x + c_o - 0.5dl_o), \text{ and} \quad (\text{D.130})$$

$$h_{fp2} = -p_l - x. \quad (\text{D.131})$$

2.4.2.1 Subcase 4.2.1

The strain condition for this case is, $\varepsilon_5 < -\varepsilon_{02} < \varepsilon_4$.

2.4.2.1.1 Subcase 4.2.1.1

The strain condition for this case is, $\varepsilon_5 < -\varepsilon_{01} < \varepsilon_4$.

$$P_{cvt} = f_w, \text{ and} \quad (\text{D.132})$$

$$M_{cvt} = -f_{mw}. \quad (\text{D.133})$$

The values of the parameters for wall are the same as in Eqs.(D.93) to (D.95).

2.4.2.2 Subcase 4.2.2

The strain condition for this case is, $\varepsilon_6 < -\varepsilon_{02} < \varepsilon_5$.

2.4.2.2.1 Subcase 4.2.2.1

The strain condition for this case is, $\varepsilon_5 < -\varepsilon_{01} < \varepsilon_4$.

$$P_{cvt} = f_w + f_3, \text{ and} \quad (\text{D.134})$$

$$M_{cvt} = -f_{mw} + f_3 h_3. \quad (\text{D.135})$$

where

$$f_3 = 0.5[f_{5a} + f_{6a}](0.5s - t)(y_d + x - 0.5l + a), \text{ and} \quad (\text{D.136})$$

$$h_3 = (y_d - x) + \frac{cov}{3} \left(\frac{f_{3a} + 2f_{4a}}{f_{3a} + f_{4a}} \right). \quad (\text{D.137})$$

The values of the parameters for wall are the same as in Eqs.(D.93) to (D.95).

2.4.2.3 Subcase 4.2.3

The strain condition for this case is, $\varepsilon_7 < -\varepsilon_{02} < \varepsilon_6$.

2.4.2.3.1 Subcase 4.2.3.1

The strain condition for this case is, $\varepsilon_5 < -\varepsilon_{01} < \varepsilon_4$.

$$P_{cvt} = f_w + f_3, \text{ and} \quad (\text{D.138})$$

$$M_{cvt} = -f_{mw} + f_3 h_3. \quad (\text{D.139})$$

where

$$f_3 = 0.5[f_{5a} + f_{6a}](0.5s - t)cov, \text{ and} \quad (\text{D.140})$$

$$h_3 = (0.5l - a) + \frac{cov}{3} \left(\frac{f_{5a} + 2f_{6a}}{f_{5a} + f_{6a}} \right). \quad (D.141)$$

The values of the parameters for wall are the same as in Eqs.(D.93) to (D.95).

2.4.2.3.2 Subcase 4.2.3.2

The strain condition for this case is, $\varepsilon_6 < -\varepsilon_{0l} < \varepsilon_5$.

$$P_{cvt} = f_w + f_{3t} + f_{3p}, \text{ and} \quad (D.142)$$

$$M_{cvt} = -f_{mw} + f_{3t}h_{3t} + f_{3p}h_{3p}. \quad (D.143)$$

where

The values of the parameters for wall are the same as in Eqs.(D.93) to (D.95).

2.4.2.3.3 Subcase 4.2.3.3

The strain condition for this case is, $\varepsilon_7 < -\varepsilon_{0l} < \varepsilon_6$.

$$P_{cvt} = f_w + f_3, \text{ and} \quad (D.148)$$

$$M_{cvt} = -f_{mw} + f_3h_3. \quad (D.149)$$

where

$$f_3 = f_c cov(0.5s - t), \text{ and} \quad (D.150)$$

$$h_3 = -p_l + x + y. \quad (D.151)$$

The values of the parameters for wall are the same as in Eqs.(D.93) to (D.95).

2.4.3 Subcase 4.3

The strain condition for this case is, $\varepsilon_7 > \varepsilon_{lc}$.

$$P_{crt} = f_{f2}, \text{ and} \quad (D.152)$$

$$M_{crt} = f_{f2}h_{f2}. \quad (D.153)$$

where

$$f_{f2} = f_c a_o(0.5s_o), \text{ and} \quad (D.154)$$

$$h_{f2} = x + x_p. \quad (D.155)$$

2.4.3.1 Subcase 4.3.1

The strain condition for this case is, $\varepsilon_5 < -\varepsilon_{02} < \varepsilon_4$.

2.4.3.1.1 Subcase 4.3.1.1

The strain condition for this case is, $\varepsilon_5 < -\varepsilon_{01} < \varepsilon_4$.

$$P_{cvt} = f_w, \text{ and} \quad (\text{D.156})$$

$$M_{cvt} = -f_{mw}. \quad (\text{D.157})$$

The values of the parameters for wall are the same as in Eqs.(D.93) to (D.95).

2.4.3.2 Subcase 4.3.2

The strain condition for this case is, $\varepsilon_6 < -\varepsilon_{02} < \varepsilon_5$.

2.4.3.2.1 Subcase 4.3.2.1

The strain condition for this case is, $\varepsilon_5 < -\varepsilon_{01} < \varepsilon_4$.

$$P_{cvt} = f_w + f_3, \text{ and} \quad (\text{D.158})$$

$$M_{cvt} = -f_{mw} + f_3 h_3. \quad (\text{D.159})$$

where

$$f_3 = 0.5[f_{5a} - 0.136f_{ck}](0.5s - t)(y_d + x - 0.5l + a), \text{ and} \quad (\text{D.160})$$

$$h_3 = (y_d + x) + \frac{(y_d + x - 0.5l + a)}{3} \left(\frac{f_{5a} - 0.272f_{ck}}{f_{5a} - 0.136f_{ck}} \right). \quad (\text{D.161})$$

The values of the parameters for wall are the same as in Eqs.(D.93) to (D.95).

2.4.3.3 Subcase 4.3.3

The strain condition for this case is, $\varepsilon_7 < -\varepsilon_{02} < \varepsilon_6$.

2.4.3.3.1 Subcase 4.3.3.1

The strain condition for this case is, $\varepsilon_5 < -\varepsilon_{01} < \varepsilon_4$.

$$P_{cvt} = f_w + f_3, \text{ and} \quad (\text{D.162})$$

$$M_{cvt} = -f_{mw} + f_3 h_3. \quad (\text{D.163})$$

where

$$f_3 = 0.5[f_{5a} + f_{6a}](0.5s - t)cov, \text{ and} \quad (\text{D.164})$$

$$h_3 = (y_d + x) + \frac{cov}{3} \left(\frac{f_{5a} + 2f_{6a}}{f_{5a} + f_{6a}} \right). \quad (\text{D.165})$$

The values of the parameters for wall are the same as in Eqs.(D.93) to (D.95).

2.4.3.3.2 Subcase 4.3.3.2

The strain condition for this case is, $\varepsilon_6 < -\varepsilon_{0I} < \varepsilon_5$.

$$P_{cvt} = f_w + f_{3t} + f_{3p}, \text{ and} \quad (\text{D.166})$$

$$M_{cvt} = -f_{mw} + f_{3t}h_{3t} + f_{3p}h_{3p}. \quad (\text{D.167})$$

where

The values of the parameters for wall are the same as in Eqs.(D.93) to (D.95).

The values of the parameters for *zone 3* are the same as in Eqs.(D.144) to (D.147).

2.4.3.3.3 Subcase 4.3.3.3

The strain condition for this case is, $\varepsilon_7 < -\varepsilon_{0I} < \varepsilon_6$.

$$P_{cvt} = f_w + f_3, \text{ and} \quad (\text{D.168})$$

$$M_{cvt} = -f_{mw} + f_3h_3. \quad (\text{D.169})$$

where

The values of the parameters for wall are the same as in Eqs.(D.93) to (D.95).

The values of the parameters for *zone 3* are the same as in Eqs.(D.150) to (D.151).

2.4.3.4 Subcase 4.3.4

The strain condition for this case is, $\varepsilon_8 < -\varepsilon_{02} < \varepsilon_7$.

2.4.3.4.1 Subcase 4.3.4.1

The strain condition for this case is, $\varepsilon_6 < -\varepsilon_{0I} < \varepsilon_5$.

$$P_{cvt} = f_w + f_{3t} + f_{3p} + f_4, \text{ and} \quad (\text{D.170})$$

$$M_{cvt} = -f_{mw} + f_{3t}h_{3t} + f_{3p}h_{3p} + f_4h_4. \quad (\text{D.171})$$

where

$$f_4 = 0.5[-0.136f_{ck} + f_{7a}](0.5s - t)(y_d + x - 0.5l + cov), \text{ and} \quad (\text{D.172})$$

$$h_4 = (y_d + x) - \frac{(y_d + x - 0.5l + cov)}{3} \left(\frac{f_{7a} - 0.272f_{ck}}{f_{7a} - 0.136f_{ck}} \right). \quad (\text{D.173})$$

The values of the parameters for wall are the same as in Eqs.(D.93) to (D.95).

The values of the parameters for *zone 3* are the same as in Eqs.(D.144) to (D.147).

2.4.3.4.2 Subcase 4.3.4.2

The strain condition for this case is, $\varepsilon_7 < -\varepsilon_{0I} < \varepsilon_6$.

$$P_{cvt} = f_w + f_3 + f_4, \text{ and} \quad (\text{D.174})$$

$$M_{cvt} = -f_{mw} + f_3 h_3 + f_4 h_4. \quad (D.175)$$

The values of the parameters for wall are the same as in Eqs.(D.93) to (D.95).

The values of the parameters for *zone 3* are the same as in Eqs.(D.150) and (D.151).

The values of the parameters for *zone 4* are the same as in Eqs.(D.172) and (D.173).

2.4.3.5 Subcase 4.3.5

The strain condition for this case is, $\varepsilon_8 > -\varepsilon_{02}$.

2.4.3.5.1 Subcase 4.3.5.1

The strain condition for this case is, $\varepsilon_6 < -\varepsilon_{01} < \varepsilon_5$.

$$P_{cvt} = f_w + f_{3t} + f_{3p} + f_4, \text{ and} \quad (D.176)$$

$$M_{cvt} = -f_{mw} + f_{3t} h_{3t} + f_{3p} h_{3p} + f_4 h_4. \quad (D.177)$$

where

$$f_w = f_{wt} + f_{wp}, \quad (D.178)$$

$$f_{mw} = f_{wt} h_{wt} + f_{wp} h_{wp}, \quad (D.179)$$

$$f_{wt} = 0.5[-0.68f_{ck} + f_{8a}](0.5l - x - y), \quad (D.180)$$

$$h_{wt} = (x + y) + \frac{(0.5l - x - y)}{3} \left(\frac{-0.68f_{ck} + 2f_{8a}}{-0.68f_{ck} + f_{8a}} \right), \quad (D.181)$$

$$f_{wp} = f_c y t, \quad (D.182)$$

$$h_{wp} = -x_p + x + y, \quad (D.183)$$

$$f_4 = 0.5[f_{7a} + f_{8a}]cov(0.5s - t), \text{ and} \quad (D.184)$$

$$h_4 = (0.5l - cov) + \frac{cov}{3} \left(\frac{f_{7a} + 2f_{8a}}{f_{7a} + f_{8a}} \right). \quad (D.185)$$

The values of the parameters for *zone 3* are the same as in Eqs.(D.144) and (D.147).

2.4.3.5.2 Subcase 4.3.5.2

The strain condition for this case is, $\varepsilon_7 < -\varepsilon_{01} < \varepsilon_6$.

$$P_{cvt} = f_w + f_3 + f_4, \text{ and} \quad (D.186)$$

$$M_{cvt} = -f_{mw} + f_3 h_3 + f_4 h_4. \quad (D.187)$$

The values of the parameters for wall are the same as in Eqs.(D.178) to (D.183).

The values of the parameters for *zone 3* are the same as in Eqs.(D.150) and (D.151).

The values of the parameters for *zone 4* are the same as in Eqs.(D.184) and (D.185).

2.4.3.5.3 Subcase 4.3.5.3

The strain condition for this case is, $\varepsilon_8 < -\varepsilon_{0l} < \varepsilon_7$.

$$P_{cvt} = f_w + f_3 + f_{4t} + f_{4p}, \text{ and} \quad (\text{D.188})$$

$$M_{cvt} = -f_{mw} + f_3 h_3 + f_{4t} h_{4t} + f_{4p} h_{4p}. \quad (\text{D.189})$$

where

$$f_{4t} = 0.5[-0.68f_{ck} + f_{7a}](0.5s - t)(0.5l - x - y), \quad (\text{D.190})$$

$$h_{4t} = (x + y) + \frac{(0.5l - x - y)}{3} \left(\frac{-0.68f_{ck} + 2f_{7a}}{-0.68f_{ck} + f_{7a}} \right), \quad (\text{D.191})$$

$$f_{4p} = f_c(x + y + cov - 0.5l)(0.5s - t), \quad (\text{D.192})$$

$$h_{4p} = -x_p + x + y. \quad (\text{D.193})$$

The values of the parameters for wall are the same as in Eqs.(D.178) to (D.183).

The values of the parameters for *zone 3* are the same as in Eqs.(D.150) and (D.151).

2.4.3.5.4 Subcase 4.3.5.4

The strain condition for this case is, $\varepsilon_8 < -\varepsilon_{0l}$.

$$P_{cvt} = f_w + f_3 + f_4, \text{ and} \quad (\text{D.194})$$

$$M_{cvt} = -f_{mw} + f_3 h_3 + f_4 h_4. \quad (\text{D.195})$$

where

$$f_w = f_c(0.5l - x)t, \quad (\text{D.196})$$

$$h_w = -x_p + x + y, \quad (\text{D.197})$$

$$f_4 = f_c cov(0.5s - t), \text{ and} \quad (\text{D.198})$$

$$h_4 = -x_p + x + y. \quad (\text{D.199})$$

The values of the parameters for *zone 3* are the same as in Eqs.(D.150) and (D.151).

2.5 Subcase 5

For this case, the neutral axis lies in *zone 3*.

2.5.1 Subcase 5.1

The strain condition for this case is, $\varepsilon_7 < \varepsilon_{lc}$.

$$P_{crt} = f_{ft2} + f_{fp2}, \text{ and} \quad (\text{D.200})$$

$$M_{crt} = f_{ft2} h_{ft2} + f_{fp2} h_{fp2}. \quad (\text{D.201})$$

The values of the parameters for *zone 2con* are the same as in Eqs.(D.128) and (D.131).

2.5.1.1 Subcase 5.1.1

The strain condition for this case is, $\varepsilon_7 < -\varepsilon_{02} < \varepsilon_6$.

2.5.1.1.1 Subcase 5.1.1.1

The strain condition for this case is, $\varepsilon_7 < -\varepsilon_{01} < \varepsilon_6$.

$$P_{cvt} = f_w + f_3, \text{ and} \quad (\text{D.202})$$

$$M_{cvt} = -f_{mw} - f_3 h_3. \quad (\text{D.203})$$

where

$$f_3 = f_c(0.5l - x - a_o - cov)(0.5s - t), \text{ and} \quad (\text{D.204})$$

$$h_3 = -x_p + x + y. \quad (\text{D.205})$$

The values of the parameters for wall are the same as in Eqs.(D.93) to (D.95).

2.5.2 Subcase 5.2

The strain condition for this case is, $\varepsilon_7 > \varepsilon_{1c}$.

$$P_{crt} = f_{f2}, \text{ and} \quad (\text{D.206})$$

$$M_{crt} = f_{f2} h_{f2}. \quad (\text{D.207})$$

where

$$f_{f2} = f_c a_o(0.5s_o), \text{ and} \quad (\text{D.208})$$

$$h_{f2} = -x_p + x + y_c. \quad (\text{D.209})$$

2.5.2.1 Subcase 5.2.1

The strain condition for this case is, $\varepsilon_7 < -\varepsilon_{02} < \varepsilon_6$.

2.5.2.1.1 Subcase 5.2.1.1

The strain condition for this case is, $\varepsilon_7 < -\varepsilon_{01} < \varepsilon_6$.

$$P_{cvt} = f_w + f_3, \text{ and} \quad (\text{D.210})$$

$$M_{cvt} = -f_{mw} - f_3 h_3. \quad (\text{D.211})$$

The values of the parameters for wall are the same as in Eqs.(D.93) to (D.95).

The values of the parameters for *zone 3* are the same as in Eqs.(D.204) and (D.205).

2.5.2.2 Subcase 5.2.2

The strain condition for this case is, $\varepsilon_8 < -\varepsilon_{02} < \varepsilon_7$.

2.5.2.2.1 Subcase 5.2.2.1

The strain condition for this case is, $\varepsilon_6 < -\varepsilon_{01} < \varepsilon_5$.

$$P_{cvt} = f_w + f_3 + f_4, \text{ and} \quad (\text{D.212})$$

$$M_{cvt} = -f_{mw} + f_3 h_3 + f_4 h_4. \quad (\text{D.213})$$

where

$$f_3 = f_c (x + y - 0.5l + a_o + cov)(0.5s - t), \text{ and} \quad (\text{D.214})$$

$$h_3 = -x_p + x + y. \quad (\text{D.215})$$

The values of the parameters for wall are the same as in Eqs.(D.93) to (D.95).

The values of the parameters for *zone 4* are the same as in Eqs.(D.172) and (D.173).

2.5.2.3 Subcase 5.2.3

The strain condition for this case is, $\varepsilon_8 > -\varepsilon_{02}$.

2.5.2.3.1 Subcase 5.2.3.1

The strain condition for this case is, $\varepsilon_7 < -\varepsilon_{01} < \varepsilon_6$.

$$P_{cvt} = f_w + f_3 + f_4, \text{ and} \quad (\text{D.216})$$

$$M_{cvt} = -f_{mw} + f_3 h_3 + f_4 h_4. \quad (\text{D.217})$$

The values of the parameters for wall are the same as in Eqs.(D.178) to (D.183).

The values of the parameters for *zone 3* are the same as in Eqs.(D.214) and (D.215).

The values of the parameters for *zone 4* are the same as in Eqs.(D.184) and (D.185).

2.5.2.3.2 Subcase 5.2.3.2

The strain condition for this case is, $\varepsilon_8 < -\varepsilon_{01} < \varepsilon_7$.

$$P_{cvt} = f_w + f_3 + f_{4t} + f_{4p}, \text{ and} \quad (\text{D.218})$$

$$M_{cvt} = -f_{mw} + f_3 h_3 + f_{4t} h_{4t} + f_{4p} h_{4p}. \quad (\text{D.219})$$

The values of the parameters for wall are the same as in Eqs.(D.178) to (D.183).

The values of the parameters for *zone 3* are the same as in Eqs.(D.214) and (D.215).

The values of the parameters for *zone 4* are the same as in Eqs.(D.190) to (D.193).

2.5.2.3.3 Subcase 5.2.3.3

The strain condition for this case is, $\varepsilon_8 > -\varepsilon_{01}$.

$$P_{cvt} = f_w + f_3 + f_4, \text{ and} \quad (\text{D.220})$$

$$M_{cvt} = -f_{mw} + f_3 h_3 + f_4 h_4. \quad (\text{D.221})$$

The values of the parameters for wall are the same as in Eqs.(D.196) and (D.197).

The values of the parameters for *zone 3* are the same as in Eqs.(D.214) and (D.215).

The values of the parameters for *zone 4* are the same as in Eqs.(D.198) to (D.199).

2.6 Subcase 6

For this case, the neutral axis lies in *zone 3*.

2.6.1 Subcase 6.1

The strain condition for this case is, $\varepsilon_7 > \varepsilon_{1c}$.

$$P_{crt} = f_{f2}, \text{ and} \quad (\text{D.222})$$

$$M_{crt} = f_{f2} h_{f2}. \quad (\text{D.223})$$

where

$$f_{f2} = f_c (0.5l - x)(0.5s_o), \text{ and} \quad (\text{D.224})$$

$$h_{f2} = -x_p + x. \quad (\text{D.225})$$

2.6.1.1 Subcase 6.1.1

The strain condition for this case is, $\varepsilon_7 < -\varepsilon_{02} < \varepsilon_6$.

2.6.1.1.1 Subcase 6.1.1.1

The strain condition for this case is, $\varepsilon_7 < -\varepsilon_{01} < \varepsilon_6$.

$$P_{cvt} = f_w + f_4, \text{ and} \quad (\text{D.226})$$

$$M_{cvt} = -f_{mw} - f_4 h_4. \quad (\text{D.227})$$

The values of the parameters for wall are the same as in Eqs.(D.93) to (D.95).

The values of the parameters for *zone 4* are the same as in Eqs.(D.172) and (D.173).

2.6.1.2 Subcase 6.1.2

The strain condition for this case is, $\varepsilon_8 > -\varepsilon_{02}$.

2.6.1.2.1 Subcase 6.1.2.1

The strain condition for this case is, $\varepsilon_7 < -\varepsilon_{01} < \varepsilon_6$.

$$P_{cvt} = f_w + f_4, \text{ and} \quad (\text{D.228})$$

$$M_{cvt} = -f_{mw} - f_4 h_4. \quad (D.229)$$

The values of the parameters for wall and *zone 4* are the same as in Eqs.(D.178) to (D.185).

2.6.1.2.2 Subcase 6.1.2.2

The strain condition for this case is, $\varepsilon_8 < -\varepsilon_{01} < \varepsilon_7$.

$$P_{cvt} = f_w + f_4, \text{ and} \quad (D.230)$$

$$M_{cvt} = -f_{mw} - f_4 h_4. \quad (D.231)$$

The values of the parameters for wall are the same as in Eqs.(D.178) to (D.183).

The values of the parameters for *zone 4* are the same as in Eqs.(D.190) to (D.193).

2.6.1.2.3 Subcase 6.1.2.3

The strain condition for this case is, $\varepsilon_8 > -\varepsilon_{01}$.

$$P_{cvt} = f_w + f_4, \text{ and} \quad (D.232)$$

$$M_{cvt} = -f_{mw} - f_4 h_4. \quad (D.233)$$

The values of the parameters for wall and *zone 4* are the same as in Eqs.(D.196) to (D.199).

2.7 Subcase 7

For this case, the neutral axis lies in *zone 3*.

2.7.1 Subcase 7.1

The strain condition for this case is, $\varepsilon_7 > \varepsilon_{1c}$.

$$P_{crt} = 0, \text{ and} \quad (D.234)$$

$$M_{crt} = 0. \quad (D.235)$$

2.7.1.1 Subcase 7.1.1

The strain condition for this case is, $\varepsilon_8 > -\varepsilon_{02}$.

2.7.1.1.1 Subcase 7.1.1.1

The strain condition for this case is, $\varepsilon_8 > -\varepsilon_{01}$.

$$P_{cvt} = f_w + f_4, \text{ and} \quad (D.236)$$

$$M_{cvt} = -f_{mw} - f_4 h_4. \quad (D.237)$$

where

$$f_w = f_c(0.5l - x)t, \quad (\text{D.238})$$

$$h_w = -x_p + x + y, \quad (\text{D.239})$$

$$f_4 = f_c(0.5l - x)(0.5s - t), \text{ and} \quad (\text{D.240})$$

$$h_4 = -x_p + x + y. \quad (\text{D.241})$$